EVOLUTION OF EUKARYAL tRNA-GUANINE TRANSGLYCOSYLASE: INSIGHT GAINED FROM THE CHARACTERIZAION OF THE HUMAN AND *ESCHERICHIA COLI* tRNA-GUANINE TRANSGLYCOSYLASES

by

Yi-Chen Chen

A dissertation submitted in partial fulfillment
of the requirements for the degree of
Doctor of Philosophy
(Medicinal Chemistry)
in the University of Michigan
2011

Doctoral Committee:

Associate Professor George A. Garcia, Chair
Professor Ronald W. Woodard
Assistant Professor Jason E. Gestwicki
Assistant Professor Patrick J. O'Brien
Assistant Professor Oleg V. Tsodikov

2011

What I learned the most besides science throughout the years in the States

IT’S GREAT TO BE A MICHIGAN WOLVERINE.

For my parents,

Li-Man Lin and Keng-Chin Chen,

my brother,

Charles Chen,

and my beloved wife/best friend,

Dr. Eliza Tsou

ACKNOWLEDGEMENTS

It still feels surreal for me to finally write my acknowledgements in my dissertation since it means that I am about to end this enjoyable journey being a graduate student at the University of Michigan. To achieve this important milestone in my life, I would like to express my deep gratitude to my advisor, Dr. George Garcia, for his inspiring guidance. For the past five and a half years, he has been a great mentor and a wonderful friend, where the latter role of his has really meant a lot to me. In addition to all the science and knowledge I have learned from him, I cannot thank him enough for the friendship and the support he has offered me throughout the years. Also, I want to sincerely thank my committee members: Drs. Jason E. Gestwicki, Patrick J. O'Brien, Oleg V. Tsodikov and Ronald W. Woodard, for their helpful suggestions and scientific input on my project. Additionally, I gratefully thank our collaborators, Drs. Vincent Kelly and Hollis Showalter, as the completion of this research project would not have been possible without their assistance.

It has been a fantastic time working in the Garcia lab with a great group of people. Many thanks go to Dr. Julie Hurt and Suman Gill, who have been two very important friends of mine here in the United States. I will never forget the joyful moments we shared along with all of those scientific discussions and deep life-related conversations we had (and will have). Seriously Julie, you need to

come back for a No Thai trip! It is just different without you! In addition, I cannot forget to thank Dr. Jeffrey Kittendorf (especially for completing the evolution paper with us), Dr. Stephanie Chervin, Allen Brooks (especially for conducting queuine and $preQ_1$ syntheses), Frank Kwarcinski, Rebecca Lalani, Joslyn Neal, Anthony Emanuele and Chris Holt for their help and friendship along the way. Furthermore, I want to thank all of my friends who supported me continuously during my graduate study, and just to name a few: Drs. Parag Aggarwal, Fernanda Burke, Steve Kawamoto, Yasuhiro Tsume and Chen-Chung Lee (who flew in from sunny California to freezing Michigan for my defense). Thank you all for making this journey unforgettable.

From the bottom of my heart, I thank my families (my parents, my brother and my in-laws) for their consideration and tremendous encouragement over the past five years. Without them, I would not have been able to accomplish my degree and pursue my goals in the United States. Also, I am thankful for my beloved wife, Dr. Eliza Tsou. It has been more than 4,700 days (and still counting) we have been together, and I will never be able to thank her enough for the love and full support she has offered since Day 1.

This dissertation research was supported by the University of Michigan, College of Pharmacy, Vahlteich and UpJohn Research funds, Elizabeth Broomfield Scholarship Fund, Sheila B Cresswell Fellowship in Medicinal Chemistry, and Fred Lyons Fellowship.

TABLE OF CONTENTS

LIST OF FIGURES

Figure

Appendix Figure

LIST OF TABLES

Table

Appendix Table

ABSTRACT

EVOLUTION OF EUKARYAL tRNA-GUANINE TRANSGLYCOSYLASE: INSIGHT GAINED FROM THE CHARACTERIZAION OF THE HUMAN AND *ESCHERICHIA COLI* tRNA-GUANINE TRANSGLYCOSYLASES

by

Yi-Chen Chen

Chair: George A. Garcia

Of the approximately 100 tRNA modifications that have been identified thus far, queuine (Q, 7-((4, 5-cis-dihydroxy-2-cyclopenten-1-yl) amino) methyl-7-deazaguanine) is one of the most complicated. Although its physiological role is largely obscure, the Q modification of tRNA in eukarya has been suggested to be involved in cell differentiation, proliferation and response to oxidative stress. Additionally, the malfunction of Q modification has been correlated with several biological disorders. These observations have elicited an interest in acquiring a greater understanding of the physiological role(s) of the queuosine modification.

To explore the biological significance of queuosine modification in eukarya, this dissertation work studied the key human enzyme, tRNA-guanine transglycosylase (TGT), which catalyzes the exchange of queuine for guanine in its substrate tRNAs. The eukaryal TGT was previously proposed to be a heterodimeric protein composed of queuine tRNA-ribosyltransferase 1 (QTRT1)

and ubiquitin-specific protease 14 (USP14). However, physical and kinetic evidence that we have obtained make it clear that the human TGT consists of QTRT1 and its homologue, queuine tRNA-ribosyltransferase domain-containing 1 (QTRTD1). Additional mutagenesis studies reveal that QTRT1 is responsible for the transglycosylase activity. Our results along with previous observations by others also led us to propose that QTRTD1 not only assists in recognizing substrate tRNAs, but has also evolved into a queuine salvage enzyme that generates the heterocyclic substrate (queuine) for the transglycosylation. Future work is pending to validate the latter part of this hypothesis.

To the best of our knowledge, we have also provided the first report of the kinetics of the eukaryal TGT via direct incorporation assays. *In vitro* kinetic studies reported in this dissertation demonstrate preferential heterocyclic substrate recognition for the human TGT. Follow-up work of wild-type and mutant, human and *Escherichia coli* TGTs confirmed that active site residues of both enzymes evolved to selectively recognize their cognate heterocyclic substrates.

This work has provided a greater understanding of the eukaryal TGT via rigorous enzymatic characterization of the recombinant human and *E. coli* TGTs. Our results are consistent with the concept that the present forms of TGT have arisen via divergent evolution.

CHAPTER I

INTRODUCTION

It is well known that the primary role of transfer ribonucleic acid (tRNA) is to decode genetic messages by translating specific nucleotide triplets (codons) into amino acids during protein synthesis. What is less appreciated is that prior to that process, the nucleosides in a nascent tRNA molecule can undergo biochemical modifications via a variety of tRNA-modifying enzymes *in vivo*. Since the discovery of pseudouridine approximately half a century ago (1), over one hundred modified nucleosides have been identified in RNA, where the majority (>85%) are found in tRNA. All of the modified nucleosides are generated post-transcriptionally, and they can be relatively simple as methylations of canonical nucleosides (adenosine, guanosine, cytidine and uridine) or much more complicated such as formation of queuosine and pseudouridine. A few examples of modified nucleosides are shown in Figure I-1.

The modification of tRNA has been widely believed to modulate tRNA structure and function. For example, it has been observed in both *Escherichia coli* and *Saccharomyces cerevisiae* $tRNA^{Phe}$ that the unmodified tRNA (in contrast to the modified form) only forms the cloverleaf secondary structure but not the tertiary fold in the absence of Mg^{2+}, suggesting that modified nucleotides

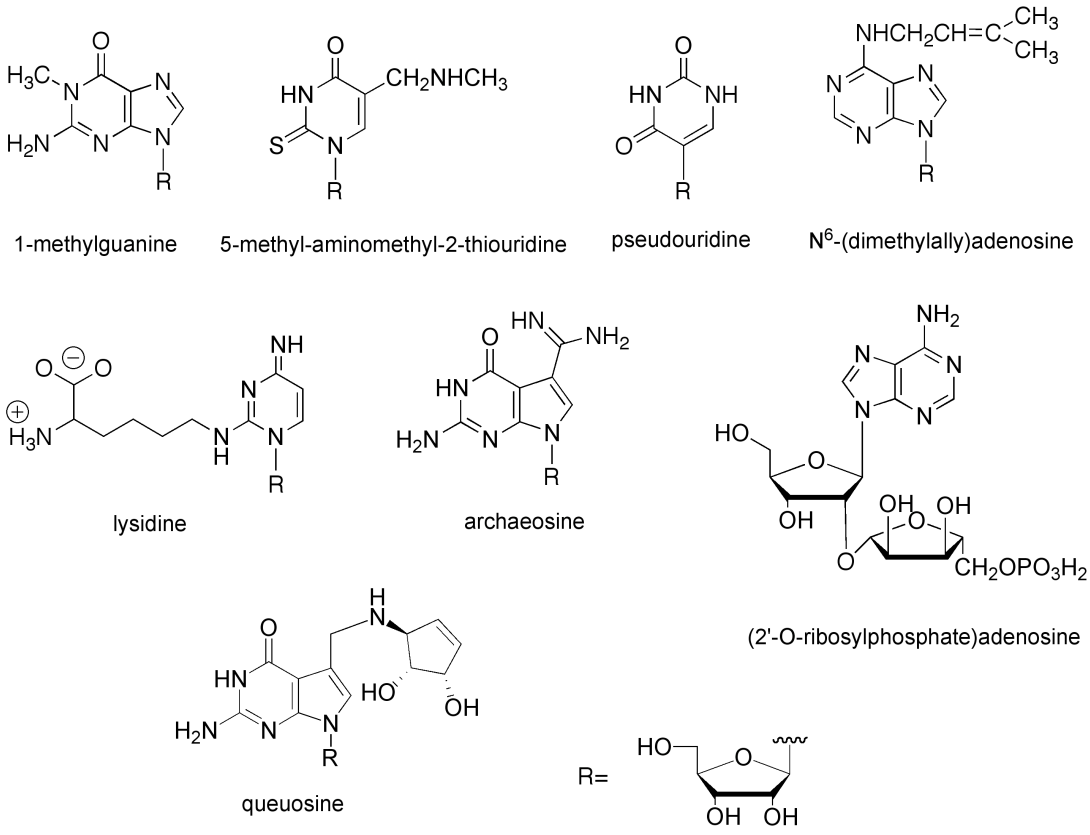

Figure I-1: Examples of Modified Nucleosides Found in RNA. Modifications are observed in a variety of positions of the canonical nucleosides, even at the 2'ribosyl hydroxyl.

stabilize tRNA tertiary interactions and facilitate correct folding (2,3). Studies have also indicated that the diverse extents of tRNA modification observed from psychrophilic bacteria and hyperthermophilic archaea result in the higher tRNA flexibility and greater tRNA structural stability, respectively, for adaptation to extreme temperatures (4,5). Lysine-modified cytidine (lysidine, Figure I-1) is an example of a modified nucleotide affecting the function of tRNA (6,7). Lysidine is found at the wobble position (C_{34}) of AUA codon-specific $tRNA^{Ile}$ in eubacteria. Instead of recognizing guanosine to form the normal Watson-Crick interactions,

lysidine actually pairs with adenosine. This converts the codon specificity of $tRNA^{Ile}$, with the genetically encoded anticodon $C_{34}A_{35}U_{36}$, from AUG (methionine) to AUA (Isoleucine). Interestingly, lysidine modification also alters the aminoacylation specificity between methionine and isoleucine (8). It was found that replacement of C_{34} of $tRNA^{Ile}$ with L_{34} leads to a significant switch from methionine-accepting activity to isoleucine-accepting activity. Another interesting example is the prevention of translational frameshifting by modified nucleosides at positions 34 and 37 (3'-adjacent to the anticodon) at the anticodon loop as those are two of the most commonly seen modification sites, which have been believed to maintain proper structure of the loop to ensure the correct codon binding (9,10).

In sum, although their functions have begun to be understood, very little is still known about the physiological roles of modified nucleosides in tRNA. As a result, there is much interest in understanding the biological significance of these modified nucleosides.

Queuosine Modification

Of the over 90 tRNA modifications, queuosine (Q, 7-((4, 5-cis-dihydroxy-2-cyclopenten-1-yl) amino) methyl-7-deazaguanosine, Figure I-1) is one of the most complicated forms that have been identified thus far. The incorporation of Q has been found extensively in eubacterial and eukaryal species except for *S. cerevisiae* and *mycoplasma* (11). In some cases, further modifications of

queuosine occur, as glycosylated (mannosylation and galactosylation on the 5-hydoxyl of the cyclopentenyl ring) and glutamylated forms of queuosine have been observed (12,13). The Q modification arises via a base exchange reaction mediated by the enzyme tRNA-guanine transglycosylase (TGT, E.C. 2.4.2.29), which catalyzes a direct replacement of a genetically encoded guanine. The process requires neither the cleavage of the phosphodiester backbone of tRNA nor the hydrolysis of ATP (14,15). The reaction takes place at the first anticodon position (G_{34}) of tRNAs coding for aspartic acid, asparagine, histidine and tyrosine (16,17). These tRNAs all possess a common $G_{34}U_{35}N_{36}$ anticodon sequence, where N represents any of the four canonical nucleosides. In spite of sharing the same outcome, eubacteria and eukarya utilize very different strategies to generate Q-tRNA. In contrast to eukarya being unable to synthesize queuosine *de novo* (18,19), there is a complete Q-tRNA biosynthetic pathway in eubacteria involving two levels: biosynthesis of a heterocyclic base, 7-aminomethyl-7-deazaguanine ($preQ_1$), the substrate for transglycosylation by TGT and further chemical modifications at the tRNA level (shown in Figure I-2).

Early on, Kuchino *et al.* demonstrated that the backbone structure of queuosine (pyrrolopyrimidine or 7-deazapurine) is derived from guanosine 5'-triphosphate (GTP) where the C^8 and N^7 atoms (purine numbering) of guanine both are replaced through the biotransformation (20). A very similar process was previously found in the biosyntheses of antibiotic toyocamycin (21) and cellular pteridines (22), providing insight into understanding the biosynthesis of 7-deazapurines. Later, 7-cyano-7-deazaguanine ($preQ_0$) was suggested to be the

intermediate precursor, as the compound was observed to accumulate in Q-deficient *E. coli* mutants (23). However, the details regarding the conversion of GTP to $preQ_0$ were not revealed until recent breakthroughs in the field. Comparative genomic analysis and biochemical re-examination first identified four genes (*queC, -D, -E, and -F*), which are essential for the formation of queuosine *in vivo* (24). More recently, the first step of the pathway has been confirmed to be mediated by GTP cyclohydrolase I (GCYH-I) to generate 7,8-dihydroneopterin triphosphate (H_2NTP) (25,26). Subsequently, H_2NTP is converted to 6-carboxy-5,6,7,8-tetrahydropterin (CPH_4) by QueD, a mammalian 6-pyruvoyltetrahydropterin synthase (PTPS) homologue (27). The most significant structural transformation takes place when QueE (a member of the radical SAM protein superfamily) catalyzes the conversion of CPH_4 to 7-carboxy-7-deazaguanine (CDG). Then a QueC-mediated reaction carries CDG further to form the product, $preQ_0$, in an ATP-dependent manner (28). A unique conversion of $preQ_0$ to $preQ_1$ has been elucidated by Iwata-Reuyl and coworkers (29,30). The key enzyme, QueF, is confirmed to be a NADPH-dependent nitrile oxidoreductase, and a GCYH-I homologue although it does not catalyze the initial step in the biosynthesis pathway (29). The base, $preQ_1$, is then incorporated into the polynucleotide chain by TGT (31) followed by at least two additional enzymatic transformations to yield the final product, Q-tRNA. QueA (AdoMet:tRNA ribosyltransferase-isomerase) catalyzes the first step that involves the transfer and isomerization of the ribose moiety of S-adenosylmethionine (AdoMet) to the aminomethyl side chain of $preQ_1$ to form epoxyqueuosine (oQ)

(32,33). The second step has yet to be identified; however, it is believed that cobalamin (Vitamin B_{12}) serves as a cofactor in the reduction of oQ to queuosine (34).

As mentioned previously, eukarya lack a queuosine biosynthetic pathway and have to obtain free queuine from diet and then directly incorporate it as a substrate (35). It was reported that germ-free mice could utilize dietary Q-tRNA to produce free base, suggesting a salvage system in eukarya to compensate for the inability to synthesize queuine (36). Subsequent studies showed that epithelial cells of monkey kidney are able to uptake queuine from degraded tRNA, and queuosine 5'-monophosphate (QMP) appears to be the substrate for this salvage activity (37,38). Interestingly enough, similar salvage activity has been observed in two eukaryal algae although queuosine (the nucleoside) rather than QMP was found to be the substrate in these plant cells (39). In addition to the salvage system, a specific queuine transport system was observed in human fibroblasts, and the process appears to be modulated by protein kinase C (PKC) phosphorylation (40,41).

Although the presence of queuosine has been known since the late 1960s (42), its physiological role is still largely unknown. The Q modification has been suggested to be involved in cell differentiation and proliferation while the level of Q-tRNA appears to correlate with the developmental state of the cells (43,44). Additionally, it has been proposed that the incorporation of Q may play a role in affecting translation efficiency *in vivo*, as Q-tRNA does not seem to show

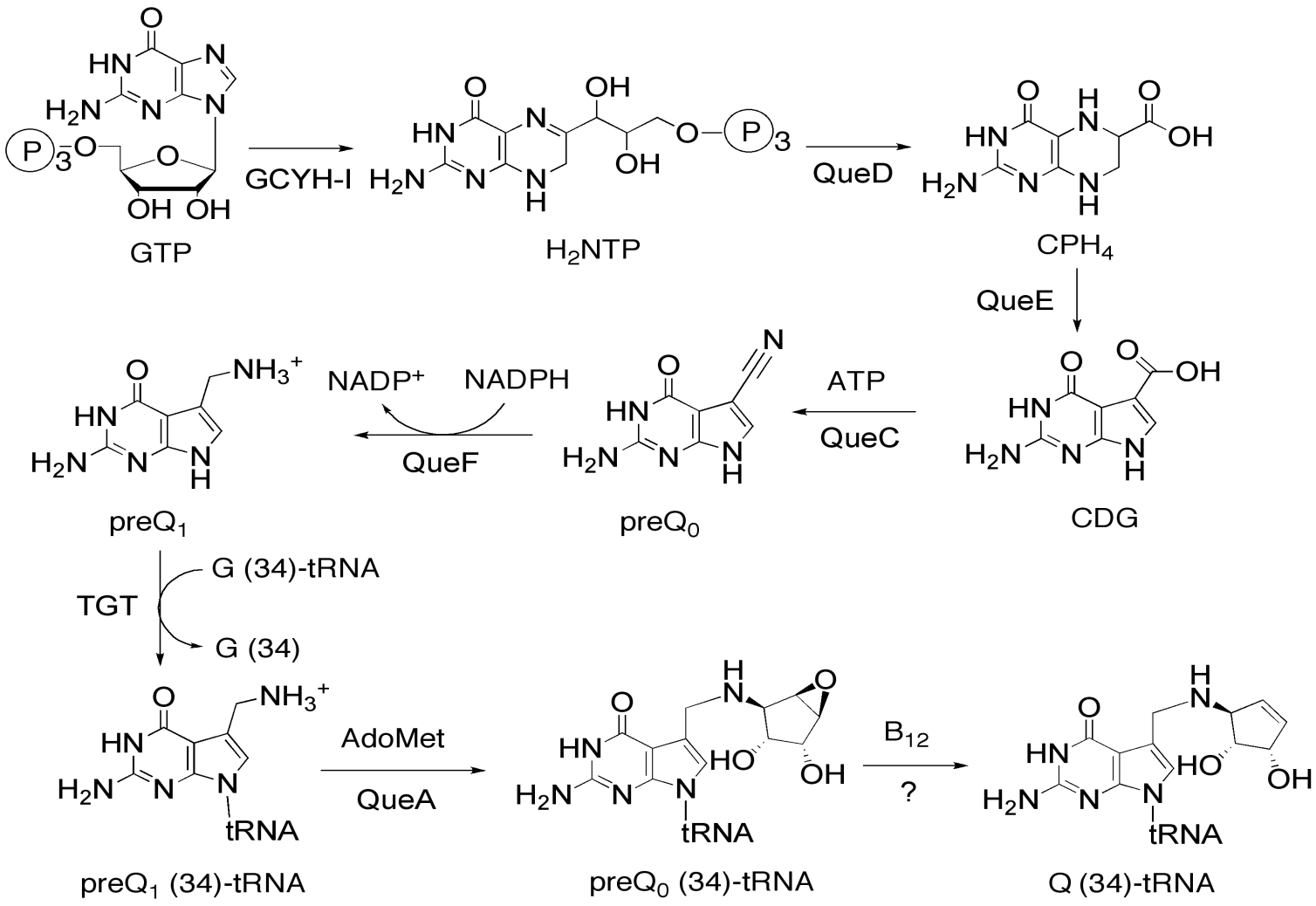

Figure I-2: Biosynthetic Pathway of Queuosine (34)-tRNA in Eubacteria.

preference for either NAU or NAC codons; whereas, unmodified G-tRNAs favorably recognize NAC (45). Later, this observation was further supported bycomputational work that predicted equal base-pairing interactions of Q-tRNA with uridine or cytidine (2 hydrogen bonds in either case) in comparison to the predominant Watson-Crick G-C pairing of G-tRNA (46). That being said, it should be noted that queuosine does not alter the amino acid composition in translation due to the degeneracy of codons.

In attempts to understand the physiological role of the Q modification, several basic and clinical studies have been performed to observe the biological relevance of the Q-deficiency. It has been found that there is no obvious phenotypic change in an *E. coli tgt* knockout strain except for lower viability in the stationary phase (47). However, Q-deficient *Shigella flexneri* shows significantly lower expression levels of virulence factors, leading to a decrease in cellular invasion (48,49). For eukaryotes, it was reported that long-term Q-deficient sterile mice appear normal (36). Even so, queuine- and tyrosine- deficient mice showed severe abnormalities (such as labored breathing, seizures etc.), and the adverse effect could even be lethal (50). Observed in Chinese hamster embryo cells, 7-methylguanine induced Q deficiency leads to cell transformation in terms of anchorage-independent growth, which has been related to the promotion of carcinogenesis (51). In addition, perhaps drawing the most attention, studies have shown a positive correlation between a low extent of Q-modified tRNA and the degree of malignancy of several cancer cells, including both solid and lymphoproliferative cancers (52-55).

Transfer RNA-Guanine Transglycosylase

The tRNA-modifying enzyme, tRNA-guanine transglycosylase (TGT), is the key enzyme responsible for the queuine modification of tRNA, one of the most intricate tRNA posttranscriptional modifications. Due to the sequence similarity and conserved key catalytic residues, TGT has been thought to constitute a family of homologous enzymes with differing substrate recognition across eukarya, eubacteria and archaea (56). As briefly described above, the eukaryal and eubacterial enzymes incorporate queuine and $preQ_1$, respectively, into the anticodon wobble position (G_{34}) of their cognate tRNAs through a direct replacement process (14,57). Interestingly, the incorporation of queuine and $preQ_1$ was proven to be irreversible due to the fact that TGT does not utilize fully modified tRNA as substrates (31). In addition to the interest in heterocyclic substrate recognition, studies have been done to gain insight into tRNA recognition by eubacterial TGT. *In vitro* experiments showed that *E. coli* TGT appears to modify a stem-loop structure, so-called “minihelix”, demonstrating that full length cognate tRNAs are not required for substrate recognition. It should be noted that eukaryal TGT has been reported only to utilize full-length tRNAs (58), and the preliminary studies with the human TGT seem to support this conclusion (Chen and Garcia, unpublished). Nevertheless, it was confirmed that the minimal recognition element for eubacterial TGT is $U_{33}G_{34}U_{35}$, in the loop of an RNA hairpin structure (59-61). These findings have raised an interesting question regarding whether TGT can modify other RNA species. Follow-up studies have indeed identified alternative TGT recognition sites, such as a UGU sequence

within an unmodified TψC loop of $tRNA^{Phe}$ or within the virF mRNA, which is a pathogenic virulence gene of *Shigella flexneri* (62,63). In fact, studies have also shown that TGT is capable of recognizing an artificial DNA minihelix, where the thymidines are replaced with 2'-deoxyuridines (64).

In contrast to queuosine modification in eubacteria and eukarya, the archaeal TGT replaces G_{15} at the D loop of tRNAs with the queuine/$preQ_1$/archaeosine precursor, $preQ_0$. Subsequently, an additional biotransformation occurs to generate the nucleoside archaeosine (G^+, 7-formamidino-7-deazaguanosine, Figure I-1) (65). It is interesting to note that the same position (G_{15}) in eukaryal and eubacterial tRNAs remains unmodified. Although the detailed chemical mechanism has yet to be revealed, Phillips *et al.* recently identified an amidinotransferase (named archaeosine synthase) that allows direct addition of an ammonia molecule to the nitrile side chain of $preQ_0$ in the absence of ATP (66). Although not completely understood, it has been suggested that the archaeosine modification helps stabilize tRNA tertiary structure in comparison to the anticodon loop queuosine modification that seems to modulate translation efficiency.

The biochemical characterization of a typical TGT-catalyzed reaction has been understood via extensive studies with the eubacterial enzyme (Figure I-3). The catalysis follows a ping-pong bi-substrate mechanism. During the first half of the reaction, TGT binds to any of its cognate tRNAs, attacks the glycosidic bond to liberate G_{34}, and spontaneously forms a covalent intermediate with RNA, consistent with an associative mechanism (67,68). The incoming heterocyclic

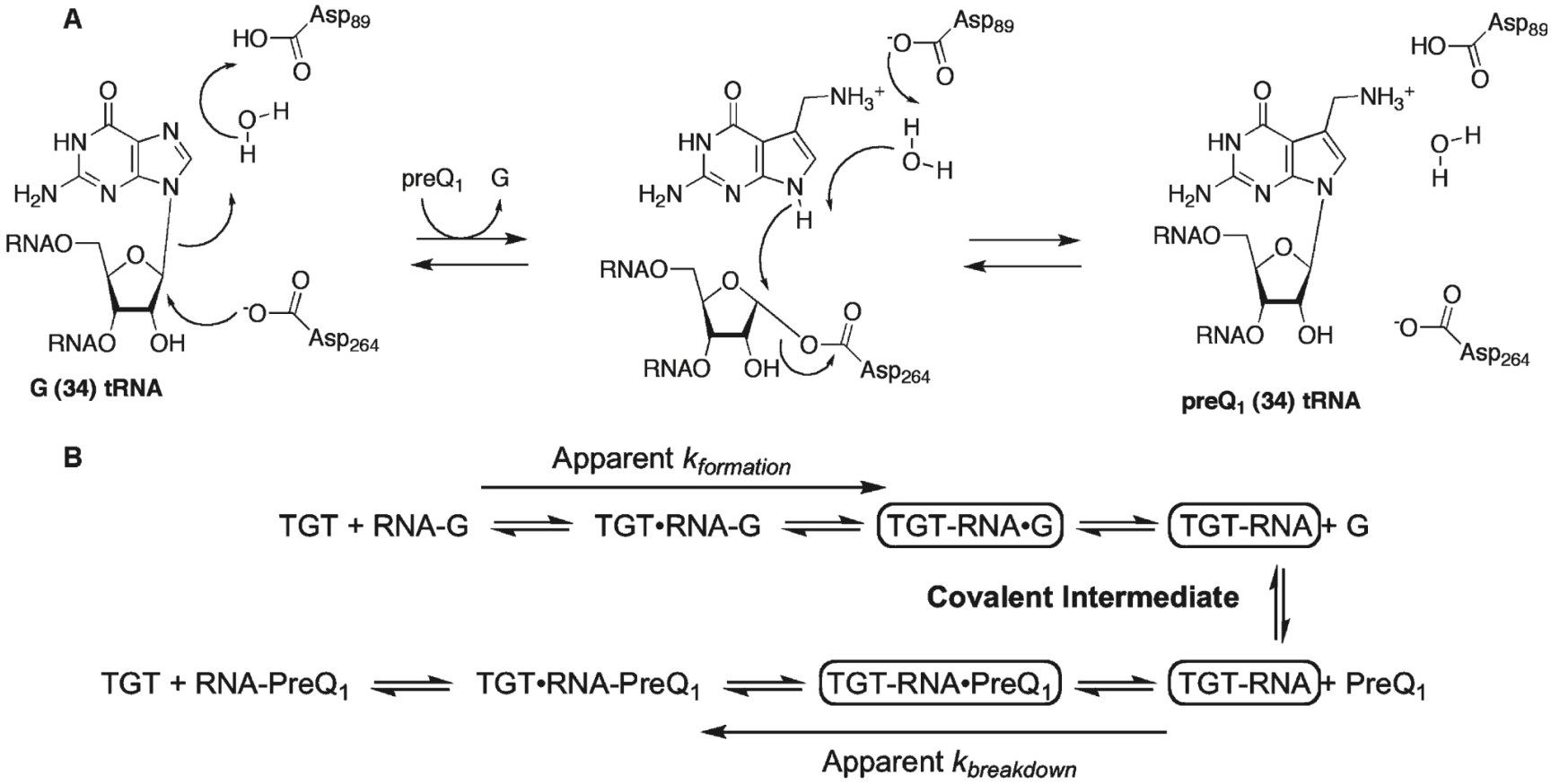

Figure I-3: Chemical and Kinetic Mechanism of a TGT-Catalyzed Reaction. (A) Associative mechanism involving nucleophilic catalysis by aspartate 264 (*E. coli* numbering). Aspartate 89 is proposed to serve as a general acid/base. (B) Ping-pong bi-substrate mechanism. Covalent Intermediates containing the TGT-RNA complex are circled. (Reprinted from Garcia *et al*., *Biochemistry*, 2009, **48**: 11243-11251.)

base is then recognized and serves as a nucleophile after being deprotonated at the N^9 position to reestablish the glycosidic bond. The last step of the reaction, product release, is now known to be rate-determining (69). The three active site aspartate residues (Asp89, Asp143 and Asp264, *E. coli* TGT numbering) that are conserved in TGTs across all three kingdoms are known or thought to be involved in catalysis. Mutagenesis and computational studies have shown that Asp143 is involved in hydrogen bonding with the aminopyrimidone portion of the base, maintaining the substrate specificity (70,71). More importantly, the X-ray co-crystal structure of the tRNA bound *Zymomonas mobilis* TGT confirmed that Asp264 is the enzymatic nucleophile (68). Although further evidence is pending, Asp89 is suggested to act as a general acid/general base assisting in protonating/deprotonating the leaving/incoming heterocyclic base, respectively (72).

The physical characterization of TGT has also been carried out mainly on the eubacterial and archaeal enzymes. The X-ray crystal structures revealed that both eubacterial and archaeal TGTs characteristically adopt a $(\beta/\alpha)_8$ TIM barrel fold and contain a zinc-binding motif, where TGT coordinates one zinc ion via the four ligands: Cys302, Cys304, Cys307 and His333 (*E. coli* TGT numbering) (73-75). It appears that the binding of zinc is important for maintaining TGT structure (75,76). Also based on the crystallographic evidence, the quaternary structure of the functional TGT is now considered to be dimeric. (However, previous cross-linking and band-shift experiments suggested a trimeric form in solution and a monomeric conformation upon substrate tRNA

binding (77,78)). The concept of a homodimeric TGT resulted from the observation of a potential dimer interface in the structure of *Z. mobilis* TGT (73). This was further confirmed by the co-crystallization of the enzyme with an anticodon stem loop, where the second TGT monomer has been proposed only to maintain a proper orientation of the bound tRNA and does not participate in actual catalysis (79). In addition, the archaeal TGT has also been shown to be homodimeric and the two subunits were suggested to interact tightly through the zinc-binding domain (74).

Due to the lack of crystal structures and previous misconceptions (thoroughly described in Chapter II), the characteristics of the eukaryal TGT are much less understood. Earlier, the reports of TGTs isolated from a number of sources exhibit inconclusive discrepancies in terms of the size and composition of the subunits (80-83). Nevertheless, the general perception was that the subunit structure of the eukaryal TGT is heterodimeric, consisting of 44- and 60-kDa subunits. The 44-kDa subunit of the eukaryal TGT, QTRT1 (queuine tRNA-ribosyltransferase 1), is believed to be the subunit responsible for the transglycosylase activity, as it shows a high degree of protein sequence homology (~40%) to the eubacterial TGT (84). On the other hand, the 60-kDa subunit has no TGT-like catalytic activity and was proposed to act as a regulatory subunit, modulating the activity of the eukaryal TGT in response to phosphorylation by protein kinase C (83). At that time, what also made this heterodimeric subunit structure very interesting is that the 60-kDa subunit, annotated as USP14, is functionally classified as a member of the ubiquitin-

specific protease family (85). The possibility of TGT activity being related to the ubiquitin-dependent proteolytic pathway (86) made us believe that there could be an intriguing linkage between RNA posttranscriptional and protein posttranslational modifications. However, not only is there little evidence to support the USP14 regulation model, but the QTRT1-USP14 subunit structure has now been proven to be incorrect. Very recently, Kelly and co-workers showed that a homologue of QTRT1, termed QTRTD1 (queuine tRNA-ribosyltransferase domain containing 1), associated with QTRT1 both *in vitro* and *in vivo* (87). Their observations indicate that QTRTD1 may also play a role in queuosine incorporation.

Research Objectives

As mentioned previously, the Q-deficiency appears to correlate well with several physiological abnormalities. As a result, our laboratory has been working to obtain a greater understanding of TGT, and ultimately hoping to identify this key enzyme as a potential target for therapeutic purposes. Although eubacterial TGTs have been extensively studied for the past two decades, very little work has been done to characterize the eukaryal TGTs. Due to previous success of our laboratory in constructing the recombinant human QTRT1 and USP14 clones, this dissertation was originally designed to investigate the substrate specificity of QTRT1, the potential interaction between QTRT1 and USP14, and the characteristics of USP14. Preliminary attempts in our laboratory have shown

that the recombinant human QTRT1 when expressed alone in various *E. coli* strains is either insoluble or catalytically inactive. Given the concept that one protein may require its protein partner during over-expression process to be fully functional, we then attempted to co-express human QTRT1 and USP14. However, no transglycoslase activity was observed, which led us to suspect either there was other unknown piece(s) missing in the puzzle or an incorrect model had been pursued. A breakthrough finally occurred when QTRTD1 was introduced to the system, inspired by the report of Kelly and colleagues (87). As a consequence, the objectives of this research project have been modified and three research chapters have been accomplished to address the following questions:

1. What is the actual subunit structure of the human TGT?

   Chapter II: Confirmation of the Heterodimeric Subunit Structure of the Human tRNA-Guanine Transglycosylase

2. What is the heterocyclic substrate specificity of the human TGT?

   Chapter III: Heterocyclic Substrate Specificity of the Human and *E. coli* tRNA-Guanine Transglycosylases

3. How are TGT across all three kingdoms of life evolutionarily related?

   Chapter IV: Divergent Evolution of Eukaryal TGT: Insight Gained from the Heterocyclic Substrate Specificity of the Human and *E. coli* tRNA-Guanine Transglycosylases

Notes to Chapter I

1. Davis, F.F. and Allen, F.W. (1957) Ribonucleic acids from yeast which contain a fifth nucleotide. *J. Biol. Chem.*, **227**, 907-915.

2. Maglott, E.J., Deo, S.S., Przykorska, A. and Glick, G.D. (1998) Conformational transitions of an unmodified tRNA: Implications for RNA folding. *Biochemistry*, **37**, 16349-16359.

3. Serebrov, V., Vassilenko, K., Kholod, N., Gross, H.J. and Kisselev, L. (1998) Mg2+ binding and structural stability of mature and in vitro synthesized unmodified Escherichia coli tRNA(Phe). *Nucleic Acids Res*, **26**, 2723-2728.

4. Kowalak, J.A., Dalluge, J.J., McCloskey, J.A. and Stetter, K.O. (1994) The role of posttranscriptional modification in stabilization of transfer RNA from hyperthermophiles. *Biochemistry*, **33**, 7869-7876.

5. Dalluge, J.J., Hamamoto, T., Horikoshi, K., Morita, R.Y., Stetter, K.O. and McCloskey, J.A. (1997) Posttranscriptional Modification of tRNA in Psychrophilic Bacteria. *J. Bacteriol.*, **179**, 1918-1923.

6. Muramatsu, T., Yokoyama, S., Horie, N., Matsuda, A., Ueda, T., Yamaizumi, Z., Kuchino, Y., Nishimura, S. and Miyazawa, T. (1988) A Novel Lysine-Substituted Nucleoside In The 1st Position Of The Anticodon Of Minor Isoleucine Transfer-Rna From Escherichia-Coli. *J. Biol. Chem.*, **263**, 9261.

7. Muramatsu, T., Nishikawa, K., Nemoto, F., Kuchino, Y., Nishimura, S., Miyazawa, T. and Yokoyama, S. (1988) Codon and Amino-acid Specificities of a Transfer RNA are Both Converted by a Single Post-transcriptional Modification. *Nature*, **336**, 179.

8. Soma, A., Ikeuchi, Y., Kanemasa, S., Kobayashi, K., Ogasawara, N., Ote, T., Kato, J., Watanabe, K., Sekine, Y. and Suzuki, T. (2003) An RNA-modifying enzyme that governs both the codon and amino acid specificities of isoleucine tRNA. *Molecular Cell*, **12**, 689-698.

9. Urbonavicius, J., Stahl, G., Durand, J.M.B., Ben Salem, S.N., Qian, Q., Farabaugh, P.J. and Bjork, G.R. (2003) Transfer RNA modifications that alter+1 frameshifting in general fail to affect-1 frameshifting. *Rna-A Publication of the Rna Society*, **9**, 760-768.

10. Gustilo, E.M., Franck, A.P.F. and Agris, P.F. (2008) tRNA's modifications bring order to gene expression. *Current Opinion in Microbiology*, **11**, 134-140.

11. Walden, T.M., Reyniers, J.P., Hiatt, V. and Farkas, W.R. (1982) Yeast Cells Cannot Incorporate Queuine into Their tRNA. *Proceedings of the Society for Experimental Biology and Medicine*, **170**, 328.

12. Kasai, H., Nakanishi, K., Macfarlane, R.D., Torgerson, D.F., Ohashi, Z., McCloskey, J.A., Gross, H.J. and Nishimura, S. (1976) The Structure of Q Nucleoside Isolated from Rabbit Liver Transfer Ribonucleic Acid. *J. Am. Chem. Soc.*, **98**, 5044.

13. Salazar, J.C., Ambrogelly, A., Crain, P.F., McCloskey, J.A. and Soll, D. (2004) A truncated aminoacyl-tRNA synthetase modifies RNA. *Proceedings of the National Academy of Sciences of the United States of America*, **101**, 7536-7541.

14. Okada, N. and Nishimura, S. (1979) Isolation and Characterization of a Guanine Insertion Enzyme, a Specific tRNA Transglycosylase, from *Escherichia coli*. *J. Biol. Chem.*, **254**, 3061-3066.

15. Singhal, R.P. (1983) Queuine: An Addendum. *Progress in Nucleic Acids Research and Molecular Biology*, **28**, 75-80.

16. Harada, F. and Nishimura, S. (1972) Possible Anticodon Sequences of $tRNA^{His}$, $tRNA^{Asn}$, and $tRNA^{Asp}$ from *Escherichia coli* B. Universal Presence of Nucleoside Q in the First Position of the Anticodons of These Transfer Ribonucleic Acids. *Biochemistry*, **11**, 301-308.

17. Tsang, T.H., Buck, M. and Ames, B.N. (1983) Sequence Specificity of tRNA-Modifying Enzymes. *Biochimica Biophysica Acta*, **741**, 180-196.

18. Katze, J.R., Gunduz, U., Smith, D.L., Cheng, C.S. and McCloskey, J.A. (1984) Evidence That the Nucleic Acid Base Queuine Is Incorporated Intact into tRNA by Animal Cells. *Biochemistry*, **23**, 1171-1176.

19. Pawelkiewicz, J., Sroga, G.E., Starzynska, E. and Zawielak, J. (1986) Formation of Queuine-Containing Transfer RNA(Tyr) in Higher Plants. *Plant Sci.*, **47**, 83-89.

20. Kuchino, Y., Kasai, H., Nihei, K. and Nishimura, S. (1976) Biosynthesis of the Modified Nucleoside Q in Transfer RNA. *Nucleic Acids Research*, **3**, 393-398.

21. Suhadoln.Rj and Uematsu, T. (1970) Biosynthesis Of Pyrrolopyrimidine Nucleoside Antibiotic, Toyocamycin .7. Origin Of Pyrrole Carbons And Cyano Carbon. *J. Biol. Chem.*, **245**, 4365.

22. Krumdieck, C.L., Shaw, E. and Baugh, C.M. (1966) The Biosynthesis of 2-Amino-4-hydroxy-6-substituted Pteridines. *J. Biol. Chem.*, **241**, 383-387.

23. Noguchi, S., Yamaizumi, Z., Ohgi, T., Goto, T., Nishimura, Y., Hirota, Y. and Nishimura, S. (1978) Isolation of Q Nucleoside Precursor Present in tRNA of an *E. coli* Mutant and Its Characterization as 7-(Cyano)-7-deazaguanine. *Nucleic Acids Research*, **5**, 4215-4223.

24. Reader, J.S., Metzgar, D., Schimmel, P. and de Crecy-Lagard, V. (2004) Identification of four genes necessary for biosynthesis of the modified nucleoside queuosine. *J. Biol. Chem.*, **279**, 6280-6285.

25. McCarty, R.M. and Bandarian, V. (2008) Deciphering deazapurine biosynthesis: Pathway for pyrrolopyrimidine nucleosides toyocamycin and sangivamycin. *Chemistry & Biology*, **15**, 790-798.

26. Phillips, G., El Yacoubi, B., Lyons, B., Alvarez, S., Iwata-Reuyl, D. and de Crecy-Lagard, V. (2008) Biosynthesis of 7-Deazaguanosine-Modified tRNA Nucleosides: a New Role for GTP Cyclohydrolase I. *J. Bacteriol.*, **190**, 7876-7884.

27. McCarty, R.M., Somogyi, A. and Bandarian, V. (2009) Escherichia coli QueD Is a 6-Carboxy-5,6,7,8-tetrahydropterin Synthase. *Biochemistry*, **48**, 2301-2303.

28. McCarty, R.M., Somogyi, A., Lin, G.X., Jacobsen, N.E. and Bandarian, V. (2009) The Deazapurine Biosynthetic Pathway Revealed: In Vitro Enzymatic Synthesis of PreQ(0) from Guanosine 5 '-Triphosphate in Four Steps. *Biochemistry*, **48**, 3847-3852.

29. Van Lanen, S.G., Reader, J.S., Swairjo, M.A., de Crecy-Lagard, V., Lee, B. and Iwata-Reuyl, D. (2005) From cyclohydrolase to oxidoreductase: discovery of nitrile reductase activity in a common fold. *Proceedings of the National Academy of Sciences of the United States of America*, **102**, 4264-4269.

30. Lee, B.W.K., Van Lanen, S.G. and Iwata-Reuyl, D. (2007) Mechanistic studies of bacillus subtilis QueF, the nitrile oxidoreductase involved in queuosine biosynthesis. *Biochemistry*, **46**, 12844.

31. Okada, N., Noguchi, S., Kasai, H., Shindo-Okada, N., Ohgi, T., Goto, T. and Nishimura, S. (1979) Novel Mechanism of Post-Transcriptional Modification of tRNA. *J. Biol. Chem.*, **254**, 3067-3073.

32. Slany, R.K., Bösl, M., Crain, P.F. and Kersten, H. (1993) A New Function of S-Adensoylmethionine: The Ribosyl Moiety of AdoMet is the Precursor of the Cyclopentenediol Moiety of the tRNA Wobble Base Queuine. *Biochemistry*, **32**, 7811-7817.

33. Slany, R.K., Bosl, M. and Kersten, H. (1994) Transfer and isomerization of the ribose moiety of AdoMet during the biosynthesis of queuosine tRNAs,

a new unique reaction catalyzed by the QueA protein from *Escherichia coli*. *Biochimie*, **76**, 389-393.

34. Frey, B., McCloskey, J., Kersten, W. and Kersten, H. (1988) New Function of Vitamin B_{12}: Cobamide-Dependent Reduction of Epoxyqueuosine to Queuosine in tRNAs of *Escherichia coli* and *Salmonella typhimurium*. *J. Bacteriol.*, **170**, 2078-2082.

35. Katze, J.R. and Farkas, W.R. (1979) A Factor in Serum and Amniotic Fluid is a Substrate for the tRNA-modifying Enzyme tRNA-guanine Transferase. *Proceedings of the National Academy of Sciences*, **76**, 3271-3275.

36. Reyniers, J.P., Pleasants, J.R., Wostmann, B.S., Katze, J.R. and Farkas, W.R. (1981) Administration of Exogenous Queuine Is Essential for the Biosynthesis of the Queuosine-containing Trnasfer RNAs in the Mouse. *J. Biol. Chem.*, **206**, 11591-11594.

37. Gunduz, U. and Katze, J.R. (1982) Salvage of the nucleic acid base queuine from queuine-containing tRNA by animal cells. *Biochem Biophys Res Commun*, **109**, 159-167.

38. Gunduz, U. and Katze, J.R. (1984) Queuine salvage in mammalian cells. Evidence that queuine is generated from queuosine 5'-phosphate. *J Biol Chem*, **259**, 1110-1113.

39. Kirtland, G.M., Morris, T.D., Moore, P.H., O'Brian, J.J., Edmonds, C.G., McCloskey, J.A. and Katze, J.R. (1988) Novel Salvage of Queuine from Queuosine and Absence of Queuine Synthesis in *Chlorella pyrenoidosa* and *Chlamydomonas reinhardii*. *J. Bacteriol.*, **170**, 5633.

40. Morris, R.C., Brooks, B.J., Hart, K.L. and Elliott, M.S. (1996) Modulation of queuine uptake and incorporation into tRNA by protein kinase C and protein phosphatase. *Biochimica et Biophysica Acta*, **1311**, 124-132.

41. Elliott, M.S. and Crane, D.L. (1990) Protein Kinase C Modulation of Queuine Uptake in Cultured Human Fibroblasts. *Biochem. Biophys. Res. Commun.*, **171**, 393-400.

42. Goodman, H.M., Abelson, J., Landy, A., Brenner, S. and Smith, J.D. (1968) Amber Suppression - A Nucleotide Change in Anticodon of A Tyrosine Transfer RNA. *Nature*, **217**, 1019-1024.

43. Nishimura, S. (1983) Structure, Biosynthesis, and Function of Queuosine in Transfer RNA. *Progress in Nucleic Acids Research*, **28**, 49-73.

44. Langgut, W. and Kersten, H. (1990) The Deazaguanine-derivative, Queuine, Affects Cell Proliferation, Protein Phosphorylation, and the

Expression of Proto Oncogenes *c-fos* and *c-myc* in HeLa Cells. *FEBS Letters*, **265**, 33.

45. Meier, F., Suter, B., Grosjean, H., Keith, G. and Kubli, E. (1985) Queuosine modification of the wobble base in $tRNA^{His}$ influences '*in vivo*' decoding properties. *EMBO J.*, **4**, 823-827.

46. Morris, R.C., Brown, K.G. and Elliott, M.S. (1999) The effect of queuosine on tRNA structure and function. *Journal of Biomolecular Structure & Dynamics*, **16**, 757-774.

47. Noguchi, S., Nishimura, Y., Hirota, Y. and Nishimura, S. (1982) Isolation and Characterization of an *Escherichia coli* Mutant Lacking tRNA-Guanine Transglycosylase. *J. Biol. Chem.*, **257**, 6544-6550.

48. Durand, J.M., Okada, N., Tobe, T., Watarai, M., Fukuda, I., Suzuki, T., Nakata, N., Komatsu, K., Yoshikawa, M. and Sasakawa, C. (1994) *vacC*, a Virulence-associated Chromosomal Locus of *Shigella flexneri*, is Homologous to *tgt*, a Gene Encoding tRNA-Guanine Transglycosylase (TGT) of *Escherichia coli* K-12. *J. Bacteriol.*, **176**, 4627-4634.

49. Durand, J.M., Dagberg, B., Uhlin, B.E. and Bjork, G.R. (2000) Transfer RNA modification, temperature and DNA superhelicity have a common target in the regulatory network of the virulence of Shigella flexneri: the expression of the virF gene. *Molecular Microbiology*, **35**, 924-935.

50. Marks, T. and Farkas, W.R. (1997) Effects of a diet deficient in tyrosine and queuine on germfree mice. *Biochem Biophys Res Commun*, **230**, 233-237.

51. Muralidhar, G., Ochieng, J. and Trewyn, R.W. (1989) Altered Queuine Modification of Transfer RNA Involved in the *in Vitro* Transformation of Chinese Hampster Embryo Cells. *Cancer Res.*, **49**, 7110.

52. Huang, B.-S., Wu, R.-T. and Chien, K.-Y. (1992) Relationship of the Queuine Content of Transfer Ribonucleic Acids to Histopathological Grading and Survival in Human Lung Cancer. *Cancer Research*, **52**, 4696-4700.

53. Baranowski, W., Dirheimer, G. and Jakowicki, J.A. (1994) Deficiency of Queuine, a Highly Modified Purine Base, in Transfer RNAs from Primary and Metastatic Ovarian Malignant Tumors in Women. *Cancer Research*, **54**, 4468-4471.

54. Emmerich, B., Zubrod, E., Weber, H., Maubach, P.A., Kersten, H. and Kersten, W. (1985) Relationship of Queuine-Lacking Transfer RNAs to the Grade of Malignancy in Human Leukemias and Lymphomas. *Cancer Res.*, **45**, 4308.

55. Pathak, C., Jaiswal, Y.K. and Vinayak, M. (2005) Hypomodification of transfer RNA in cancer with respect to queuosine. *RNA Biol*, **2**, 143-148.

56. Stengl, B., Reuter, K. and Klebe, G. (2005) Mechanism and substrate specificity of tRNA-guanine transglycosylases (TGTs): tRNA-modifying enzymes from the three different kingdoms of life share a common catalytic mechanism. *Chembiochem*, **6**, 1926-1939.

57. Shindo-Okada, N., Okada, N., Ohgi, T., Goto, T. and Nishimura, S. (1980) Transfer Ribonucleic Acid Guanine Transglycosylase Isolated from Rat Liver. *Biochemistry*, **19**, 395-400.

58. Grosjean, H., Edqvist, J., Straby, K.B. and Giege, R. (1996) Enzymatic formation of modified nucleosides in tRNA: Dependence on tRNA architecture. *J Mol Biol*, **255**, 67-85.

59. Curnow, A.W., Kung, F.L., Koch, K.A. and Garcia, G.A. (1993) tRNA-Guanine Transglycosylase from *Escherichia coli*: Gross tRNA Structural Requirements for Recognition. *Biochemistry*, **32**, 5239-5246.

60. Curnow, A.W. and Garcia, G.A. (1995) tRNA-Guanine Transglycosylase from *Escherichia coli* - Minimal tRNA Structure and Sequence Requirements for Recognition. *J. Biol. Chem.*, **270**, 17264-17267.

61. Nakanishi, S., Ueda, T., Hori, H., Yamazaki, N., Okada, N. and Watanabe, K. (1994) A UGU sequence in the anticodon loop is a minimum requirement for recognition by *Escherichia coli* tRNA-guanine transglycosylase. *J. Biol. Chem.*, **269**, 32221-32225.

62. Kung, F.L., Nonekowski, S. and Garcia, G.A. (2000) tRNA-Guanine Transglycosylase from *Escherichia coli*: Recognition of Noncognate-Cognate Chimeric tRNA and Discovery of a Novel Recognition Site Within the TΨC Arm of $tRNA^{Phe}$. *RNA*, **6**, 233-244.

63. Hurt, J.K., Olgen, S. and Garcia, G.A. (2007) Site-specific modification of Shigella flexneri virF mRNA by tRNA-guanine transglycosylase in vitro. *Nucleic Acids Research*, **35**, 4905-4913.

64. Nonekowski, S.T., Kung, F.L. and Garcia, G.A. (2002) The Escherichia coli tRNA-Guanine Transglycosylase Can Recognize and Modify DNA. *J. Biol. Chem.*, **277**, 7178-7182.

65. Watanabe, M., Matsuo, M., Tanaka, S., Akimoto, H., Asahi, S., Nishimura, S., Katze, J.R., Hashizume, T., Crain, P.F., McCloskey, J.A. *et al.* (1997) Biosynthesis of archaeosine, a novel derivative of 7-deazaguanosine specific to archaeal tRNA, proceeds *via* a pathway involving base replacement on the tRNA polynucleotide chain. *J. Biol. Chem.*, **272**, 20146-20151.

66. Phillips, G., Chikwana, V.M., Maxwell, A., El-Yacoubi, B., Swairjo, M.A., Iwata-Reuyl, D. and de Crecy-Lagard, V. (2010) Discovery and Characterization of an Amidinotransferase Involved in the Modification of Archaeal tRNA. *J. Biol. Chem.*, **285**, 12706-12713.

67. Goodenough-Lashua, D.M. and Garcia, G.A. (2003) tRNA-Guanine Transglycosylase from *Escherichia coli*: a Ping-Pong Kinetic Mechanism is Consistent with Nucleophilic Catalysis. *Bioorganic Chemistry*, **31**, 331-344.

68. Xie, W., Liu, X.J. and Huang, R.H. (2003) Chemical trapping and crystal structure of a catalytic tRNA guanine transglycosylase covalent intermediate. *Nature Structural Biology*, **10**, 781-788.

69. Garcia, G.A., Chervin, S.M. and Kittendorf, J.D. (2009) Identification of the Rate-Determining Step of tRNA-Guanine Transglycosylase from Escherichia coli. *Biochemistry*, **48**, 11243-11251.

70. Todorov, K.A., Tan, X.J., Nonekowski, S.T., Garcia, G.A. and Carlson, H.A. (2005) The Role of Aspartic Acid 143 in E. coli tRNA-Guanine Transglycosylase: Insights from Mutagenesis Studies and Computational Modeling. *Biophysical Journal*, **89**, 1965-1977.

71. Todorov, K.A. and Garcia, G.A. (2006) Role of aspartate 143 in Escherichia coli tRNA-guanine transglycosylase: Alteration of heterocyclic substrate specificity. *Biochemistry*, **45**, 617-625.

72. Garcia, G.A. and Kittendorf, J.D. (2005) Transglycosylation: A mechanism for RNA modification (and editing?). *Bioorganic Chemistry*, **33**, 229-251.

73. Romier, C., Reuter, K., Suck, D. and Ficner, R. (1996) Crystal structure of tRNA-guanine transglycosylase: RNA modification by base exchange. *EMBO Journal*, **15**, 2850-2857.

74. Ishitani, R., Nureki, O., Fukai, S., Kijimoto, T., Nameki, N., Watanabe, M., Kondo, H., Sekine, M., Okada, N., Nishimura, S. *et al.* (2002) Crystal structure of archaeosine tRNA-guanine transglycosylase. *Journal of Molecular Biology*, **318**, 665-677.

75. Chong, S., Curnow, A.W., Huston, T.J. and Garcia, G.A. (1995) tRNA-guanine transglycosylase from *Escherichia coli* is a zinc metalloprotein. Site-directed mutagenesis studies to identify the zinc ligands. *Biochemistry*, **34**, 3694-3701.

76. Garcia, G.A., Tierney, D.L., Chong, S., Clark, K. and Penner-Hahn, J.E. (1996) X-ray absorption spectroscopy of the zinc site in tRNA-guanine transglycosylase from Escherichia coli. *Biochemistry*, **35**, 3133-3139.

77. Garcia, G.A., Koch, K.A. and Chong, S. (1993) tRNA-Guanine Transglycosylase from *Escherichia coli*: Overexpression, Purification, and Quaternary Structure. *Journal of Molecular Biology*, **231**, 489-497.

78. Curnow, A.W. and Garcia, G.A. (1994) tRNA-Guanine Transglycosylase from *Escherichia coli*: Recognition of Dimeric, Unmodified $tRNA^{Tyr}$. *Biochimie*, **76**, 1183-1191.

79. Stengl, B., Meyer, E.A., Heine, A., Brenk, R., Diederich, F. and Klebe, G. (2007) Crystal structures of tRNA-guanine transglycosylase (TGT) in complex with novel and potent inhibitors unravel pronounced induced-fit adaptations and suggest dimer formation upon substrate binding. *Journal of Molecular Biology*, **370**, 492-511.

80. Howes, N.K. and Farkas, W.R. (1978) Studies with a Homogeneous Enzyme from Rabbit Erythrocytes Catalyzing the Insertion of Guanine into tRNA. *J. Biol. Chem.*, **253**, 9082-9087.

81. Walden, J., T. L. , Howes, N. and Farkas, W.R. (1982) Purification and properties of guanine, queuine-tRNA transglycosylase from wheat germ. *J. Biol. Chem.*, **257**, 13218-13222.

82. Slany, R.K. and Mueller, S.O. (1995) tRNA-guanine transglycosylase from bovine liver - Purification of the enzyme to homogeneity and biochemical characterization. *Eur J Biochem*, **230**, 221-228.

83. Morris, R.C., Brooks, B.J., Eriotou, P., Kelly, D.F., Sagar, S., Hart, K.L. and Elliott, M.S. (1995) Activation of transfer RNA-guanine ribosyltransferase by protein kinase C. *Nucleic Acids Res*, **23**, 2492-2498.

84. Deshpande, K.L. and Katze, J.R. (2001) Characterization of cDNA encoding the human tRNA-guanine transglycosylase (TGT) catalytic subunit. *Gene*, **265**, 205-212.

85. Deshpande, K.L., Seubert, P.H., Tillman, D.M., Farkas, W.R. and Katze, J.R. (1996) Cloning and characterization of cDNA encoding the rabbit tRNA-guanine transglycosylase 60-kilodalton subunit. *Arch Biochem Biophys*, **326**, 1-7.

86. Hochstrasser, M. (1996) Ubiquitin-dependent protein degradation. *Annu. Rev. Genet.*, **30**, 405-439.

87. Boland, C., Hayes, P., Santa-Maria, I., Nishimura, S. and Kelly, V.P. (2009) Queuosine Formation in Eukaryotic tRNA Occurs via a Mitochondria-localized Heteromeric Transglycosylase. *J. Biol. Chem.*, **284**, 18218-18227.

CHAPTER II

CONFIRMATION OF THE HETERODIMERIC SUBUNIT STRUCTURE OF THE HUMAN tRNA-GUANINE TRANSGLYCOSYLASE

Abstract

The eukaryal tRNA-guanine transglycosylase (TGT) has been reported to exist as a heterodimer, in contrast to the homodimeric eubacterial TGT. While ubiquitin-specific protease 14 (USP14) has been proposed to act as a regulatory subunit of the eukaryotic TGT, the mouse TGT has recently been shown to be a queuine tRNA-ribosyltransferase 1 (QTRT1, eubacterial TGT homologue) •queuine tRNA-ribosyltransferase domain-containing 1 (QTRTD1) heterodimer. We find that human QTRTD1 (hQTRTD1) co-purifies with polyhistidine-tagged human QTRT1 (ht-hQTRT1) via Ni^{+2} affinity chromatography. Cross-linking experiments, mass spectrometry and size exclusion chromatography results are consistent with the two proteins existing as a heterodimer. We have not been able to observe co-purification and/or association of hQTRT1 and USP14 when co-expressed in *E. coli*. More importantly, under our experimental conditions, the transglycosylase activity of hQTRT1 is only observed when hQTRT1 and hQTRTD1 have been co-expressed and co-purified. Kinetic characterization

of the human TGT (hQTRT1• hQTRTD1) using human $tRNA^{Tyr}$ and guanine shows catalytic efficiency (k_{cat}/K_M) similar to that of the *E. coli* TGT. Furthermore, site-directed mutagenesis confirms that the hQTRT1 subunit is responsible for the transglycosylase activity. Taken together, these results indicate that the human TGT is composed of a catalytic subunit, hQTRT1, and hQTRTD1 not USP14.

Introduction

The enzyme tRNA-guanine transglycosylase (TGT) is responsible for a post-transcriptional base-exchange reaction in tRNAs across three kingdoms of life, eukarya, eubacteria and archaea. Although eubacterial TGTs have been intensively studied over the past two decades, the physical and kinetic properties of eukaryal TGTs have yet to be fully understood. While the eukaryal enzyme has been proposed to be a heterodimeric protein, differences in terms of the size and composition of the subunits have been reported in at least four different eukaryotes. When TGT was isolated from rabbit erythrocytes, 60 and 43 kDa subunits were observed (1). However, another study reported that the TGT from wheat germ is a homodimeric protein consisting of two 68 kDa subunits (2). Subsequent reports suggested that TGT isolated from bovine liver contains 66 and 32 kDa subunits (3), while 60 and 34.5 kDa subunits were found in purified rat liver cell extract (4).

In spite of these discrepancies, the general perception has been that the eukaryal TGT exists as a heterodimer that is comprised of a 44 kDa catalytic subunit and a putative 60 kDa regulatory subunit. The *qtrt1* gene (queuine tRNA-ribosyltransferase 1) was identified as the catalytic subunit due to a high degree of protein sequence homology (~40%) to the eubacterial TGT. The 60 kDa subunit has no TGT-like catalytic activity and has been annotated as a member of the ubiquitin-specific protease family (USP14) (5,6). Morris *et al.* reported that the 60 kDa subunit of rat liver TGT (presumably USP14) is a protein kinase C (PKC) substrate and proposed that unphosphorylated TGT exists in a low activity, dimeric state. The affinity between the two subunits reduces when the PKC-catalyzed phosphorylation takes place, and that results in the release of a highly active catalytic subunit (4). There has yet to be any detailed *in vitro* evidence supporting the USP14 regulation model. Interestingly, a very recent study revealed that in mouse, another TGT homologue, QTRTD1 (queuine tRNA-ribosyltransferase domain-containing 1) associates with QTRT1 resulting in transglycosylase activity *in vitro* and mitochondrial localization *in vivo* (7), suggesting a new paradigm for the eukaryal TGT.

In this part of the study, molecular biology strategies were applied to generate recombinant human hQTRT1, hQTRTD1 and the heterodimeric hQTRT1•hQTRTD1 complex for detailed characterization. The physical and kinetic evidence obtained is consistent with a 1:1 heterodimeric complex for the human tRNA-guanine transglycosylase consisting of hQTRT1 and hQTRTD1. Further, we find no evidence for the involvement of USP14.

Materials and Methods

Reagents

Unless otherwise specified, all reagents were ordered from Sigma-Aldrich. DNA oligonucleotides, agarose, dithiothreitol (DTT), T4 DNA ligase and DNA ladders were ordered from Invitrogen. The human $tRNA^{Tyr}$ gene was synthesized by The Midland Certified Reagent Company. All restriction enzymes and Vent® DNA polymerase were ordered from New England Biolabs. The ribonucleic acid triphosphates (NTPs), pyrophosphatase and kanamycin sulfate were ordered from Roche Applied Sciences. The deoxyribonucleic acid triphosphates (dNTPs) were ordered from Promega. Low-melting Seaplaque agarose was ordered from Lonza. Gelase™ Enzyme Prep and Scriptguard™ RNase Inhibitor were ordered from Epicentre. Epicurian coli® XL2-Blue ultracompetent cells were ordered from Stratagene, TG2 cells were from a laboratory stock and BL21-CodonPlus (DE3)-RIPL cells were from Novagen. His•Bind resin and lysonase bioprocessing reagent were also purchased from Novagen. The QIAPrep® Spin Miniprep and Maxiprep Kits were ordered from Qiagen. Precast PhastGels and SDS buffer strips were from VWR. Bradford reagent was from Bio-Rad. Whatman GF/C Glass Microfibre Filters, Amicon Ultra Centrifugal Filter Devices, carbenicillin and all bacterial media components were ordered from Fisher. [8-^{14}C] Guanine (50-60 mCi/mmol) was ordered from Moravek Biochemicals. T7 RNA polymerase was isolated from *E. coli* BL21 (DE3) pLysS cells harboring the plasmid pRC9 via minor modifications of the procedure described in the literature (8).

Preparation and Purification of Human tRNA^{Tyr}

The commercially synthesized DNA oligomer containing the human tRNA^{Tyr} gene (5'-gagaagctttaatacgactcactataggccttcgatagctcagttggtagagcggagga ctgtagatccttaggtcgctggttcgaatccggctcgaaggaccaggaattcgag-3', where the tRNA^{Tyr} gene is underlined) was amplified by polymerase chain reaction (PCR) under the following conditions: primers (20 pmol each), tRNA^{Tyr} gene (500 ng), Mg^{+2} (2 mM), dNTPs (0.5 mM each), ThermolPol buffer (1X), Vent DNA polymerase (2 U), in a final volume of 50 µL. The sample was treated with 30 PCR cycles of the following sequence: 94°C (1 min), 60°C (30 s), and 72°C (2 min). Following a double restriction enzyme digestion with Eco RI and Hind III (20 U each, 20-µL reaction) for 1 h at 37°C, the PCR product and vector pTZ18U^{Amp} were gel-purified from Seaplaque agarose with Gelase™ according to the vendor's protocol. The tRNA^{Tyr} gene was then ligated into pTZ18U^{Amp} (5:1 volume ratio, 20-µL reaction) following overnight incubation with T4 DNA ligase (2 U) at 16-17°C. The ligated sample (10 µL) was transformed into 100 µL of Epicurian coli® XL2-Blue ultracompetent cells according to the Stratagene protocol. Cells were grown overnight at 37°C on L-Amp plates (50 µg/mL ampicillin). Individual colonies were isolated, and 3 mL 2xTY (16 g bactotryptone, 10 g yeast extract, 5 g NaCl/L of water) with 50 µg/mL ampicillin liquid cultures were inoculated and grown overnight at 37°C with shaking. The plasmids were isolated via miniprep, and the tRNA^{Tyr} gene sequence was confirmed with DNA sequencing (University of Michigan DNA Sequencing Core Facilities). A plasmid containing the tRNA^{Tyr}

gene was then re-transformed into TG2 competent cells for scaled-up plasmid preparation.

To obtain the human $tRNA^{Tyr}$ for kinetic characterization of the human TGT, the plasmid containing the $tRNA^{Tyr}$ gene ($ptRNA^{Tyr}$) was first linearized at the end of the $tRNA^{Tyr}$ sequence with the restriction enzyme Bst NI (50 U, 200-µL reaction) for at least 4 h. The digested $ptRNA^{Tyr}$ was ethanol precipitated at −20°C overnight and then pelleted by centrifugation (13,000 rpm, 15 min). The $tRNA^{Tyr}$ was subsequently generated by *in vitro* transcription. *In vitro* transcription conditions were as follows: $ptRNA^{Tyr}$ template (re-suspended in 325 µL de-ionized water), transcription buffer (4 mM Tris–HCl, pH 8.0; 2 mM $MgCl_2$, 0.5 mM DTT, 0.1 mM spermidine), NTPs (4 mM each), T7 RNA polymerase (250 nM) and RNase inhibitor (100 U) in a total volume of 0.5 mL. The reaction was incubated at 37°C for approximately 4 h, after which time white precipitates (magnesium pyrophosphate) were removed by centrifugation (13,000 rpm, 5 min). The tRNA transcript was ethanol precipitated at −20°C and then pelleted by centrifugation (20,000 x g, 30 min, 4°C). Purification of the tRNA transcript was achieved by size exclusion chromatography using two Superose® 12 HR 10/30 columns (GE Healthcare) connected in series. The running buffer, which is also used for tRNA storage, contains 10 mM HEPES, pH 7.3 and 1 mM $MgCl_2$. The concentration of the tRNA was determined from the extinction coefficient at 260 nm (ε_{260} = 0.660 $A_{260} \bullet cm^{-1} \bullet \mu M^{-1}$, corrected for hypochromicity) (9) using a Cary UV-Visible Spectrophotometer (Varian).

Construction and Cloning of Human TGT

To ensure a higher efficiency of heterologous expression in an *E. coli* host, we took advantage of codon degeneracy and chemically synthesized the first 104 bases of human *qtrt1* gene (*hqtrt1*) with codons optimized for expression in *E. coli*. The fragment was then appended to the PCR product from the EST clone BE797707 (Incyte Genomics) through Kpn I digestion and subsequent ligation. The *usp14* gene was acquired from the EST clone BC003556 (Incyte Genomics) and amplified by PCR. The human *qtrtd1* gene (*hqtrtd1*, cloned in pET28a) was kindly provided by Dr. Jon Katze from the University of Tennessee, Memphis.

The *hqtrt1* and *usp14* genes were subcloned into a dual protein expression vector, pRSF-2 Ek/LIC (Ligation-Independent Cloning) following the vendor's protocol (Novagen) to obtain the construct of pht-hQTRT1-USP14. The construct of pht-hQTRT1•hQTRTD1 was generated by replacing *usp14* with *hqtrtd1* through double restriction enzyme digestion with Nde I and Hind III followed by the general laboratory ligation protocol described previously. The constructs of pht-hQTRT1(Asp279Asn)•hQTRTD1 and pht-hQTRT1 •hQTRTD1(Glu272Gln) mutants were generated from the wild-type pht-hQTRT1•hQTRTD1 using QuikChange™ site-directed mutagenesis (Stratagene). Briefly, 30 µL reactions containing 500 ng of plasmid pht-hQTRT1 •hQTRTD1, 333 nmol of each of the respective mutagenic primers synthesized by Invitrogen (for pht-hQTRT1(Asp279Asn)•hQTRTD1, fwd: 5'-gctcttggatgtgac atgttcaactgcgtcttccccacacggacag-3'; rev: 5'-ctgtccgtgtggggaagacgcagttgaacatgtc

acatccaagagc-3' and for pht-hQTRT1•hQTRTD1(Glu272Gln), fwd:5'-gaaag aggagtggacttatttcagagtttttttcccttatcaagtaac-3'; rev: 5'-gttacttgataagggaaaaaa ctctgaaataagtccactcctctttc), Mg^{+2} (2 mM), dNTPs (0.25 mM each), ThermoIPol buffer (1X) and 2 units of Vent DNA polymerase were subjected to 30 PCR cycles of the following temperature sequence: 94°C (30 s), 50°C (1 min), and 72°C (6.5 min). Following digestion with 20 units of Dpn I for 1 h, 10 µL of the PCR product was transformed into 100 µL of Epicurian coli® XL2-Blue ultracompetent cells according to the vendor's protocol (Stratagene). Cells were grown overnight at 37°C on L-Agar plates containing 50 µg/mL kanamycin and 30 µg/mL chloramphenicol. Individual colonies were isolated, and 3 mL 2xTY (with 50 µg/mL kanamycin and 30 µg/mL chloramphenicol) liquid cultures were inoculated at 37°C with shaking. The plasmids were isolated via miniprep, and the *tgt* mutant genes were confirmed with DNA sequencing.

Preparation and Purification of Human TGT

Plasmids containing the ht-hQTRT1•hQTRTD1 and ht-hQTRT1 (Asp279Asn)•hQTRTD1 genes were transformed into 200 µL of *E. coli* K12 (DE3, Δ*tgt*)-pRIPL competent cells for expression trials. In brief, cells were grown in 1-2 L of 2xTY liquid cultures containing 100 µM $ZnSO_4$ at 37°C with vigorous shaking until the OD_{600} value reached approximately 0.6. The cultures were transferred to 19°C for a 30-min incubation, and the protein was then induced by the addition of IPTG to a final concentration of 1 mM. The cultures were allowed to incubate at 19°C for additional 24-30 h, after which time the cells

were harvested by centrifugation (6,000 x g, 15 min, 4°C). The cell pellets from each 500 mL culture were re-suspended in 10 mL of Ni^{+2}-NTA bind buffer (300 mM NaCl, 50 mM NaH_2PO_4, 10 mM imidazole, pH 8.0) containing 100 µM phenylmethylsulfonyl fluoride (PMSF) and 10 µL lysonase. The cell suspensions were incubated at room temperature for 20 minutes and subjected to sonication (7 x 15 s pulses) on ice. The cellular debris was pelleted by centrifugation (13,000 x g, 30 min, 4°C).

All further purification steps were performed at 4°C. The supernatants were filtered through 0.22 µm syringe filters (Millipore) and incubated with 1 mL His•Bind resin slurry with gentle shaking for 1 h. Each supernatant-resin mixture was then applied to a column. Following loading, the columns were washed twice with 4 mL of Ni^{+2}-NTA wash buffer (300 mM NaCl, 50 mM NaH_2PO_4, 20 mM imidazole, pH 8.0). The amino-terminal polyhistidine-tagged proteins were eluted from each column with 2 mL of elute buffer (300 mM NaCl, 50 mM NaH_2PO_4, 250 mM imidazole, pH 8.0) and collected in 0.5 mL fractions. The eluates were examined by SDS-PAGE and fractions containing ht-hQTRT1•hQTRTD1 were combined. The enzyme samples were further applied to a HiPrep 16/60 Sephacryl S-200 HR (GE Healthcare) column. The running buffer was 25 mM HEPES (pH 7.3) with 300 mM NaCl and 2 mM DTT. Following verification by SDS-PAGE, fractions containing our proteins of interest were combined and concentrated. Subsequently, the proteins were exchanged into the hTGT storage buffer, 25 mM HEPES (pH 7.3), 2 mM DTT, 100 mM NaCl and 20% (w/v) glycerol, using Amicon Ultra Centrifugal Filter Devices (10,000

MWCO) following vendor protocols (the glycerol content was brought to 50% (w/v) immediately after buffer exchange for storage). The final concentrations of ht-hQTRT1•hQTRTD1 and ht-hQTRT1(Asp279Asn)•hQTRTD1 were determined with the Bio-Rad Protein Assay Kit based on the Bradford assay using BSA as the standard. The proteins were stored in liquid N_2 until needed. The ht-QTRT1 monomer was expressed in the same *E. coli* strain harboring plasmid pht-QTRT1-USP14, and then purified in the same fashion.

The ht-QTRTD1 monomer was expressed in an *E. coli* strain harboring a chaperone-containing plasmid, pGro7 (a pACYC derivative that contains two chaperones, groES and groEL; purchased from Takara Bio Inc.). Initially, pht-QTRTD1 was transformed into pGro7-containing BL21 (DE3) cells (from a laboratory stock). Subsequently, ht-QTRTD1 was expressed from the clone containing pht-QTRTD1 and pGro7 following the commercial protocol (Takara Bio Inc.). Briefly, in a 1 L culture containing 100 μM $ZnSO_4$, chaperones (groES-groEL) were first induced by the addition of $_L$-arabinose (2 mg/mL) at 37°C for approximately 2 h, until the culture reached an OD_{600} value of 0.4 to 0.6. Subsequently, the culture was transferred to 19°C for 30 min, followed by the addition of IPTG (0.5 mM) to induce the expression of ht-QTRTD1. The induction was then carried out at 19°C for approximately 24 h, after which time the cells were harvested by centrifugation (6,000 x g, 15 min, 4°C). The cell pellet from each 500 mL culture was lysed as described previously followed by Ni^{+2} affinity purification with some modifications. The filtered supernatant obtained from cell lysates was incubated with 1 mL His•Bind resin slurry and 10

mM ATP with gentle shaking for 1 h. The mixture was then applied to a column. Following loading, the column was washed with 2 x 4 mL of Ni^{+2}-NTA wash buffer (300 mM NaCl, 50 mM NaH_2PO_4, 20 mM imidazole, pH 8.0) containing 10 mM ATP. Subsequently, ht-QTRTD1 was eluted from the column with 2 mL of elute buffer (300 mM NaCl, 50 mM NaH_2PO_4, 250 mM imidazole, pH 8.0) and collected in 0.5 mL fractions. The eluates were verified by SDS-PAGE and fractions containing ht-hQTRTD1 were combined. Further purification of ht-QTRTD1 was achieved by anion exchange chromatography (MonoQ® HR 10/10 column, Pharmacia) with a binary elution gradient program. The two eluents were: (A) 25 mM HEPES (pH 7.3), 2 mM DTT and 300 mM NaCl; and (B) 25 mM HEPES (pH 7.3), 2 mM DTT and 1 M NaCl. Following the verification by SDS-PAGE, fractions containing ht-QTRTD1 were combined and concentrated. Subsequently, the protein was exchanged into the hTGT storage buffer and stored in liquid N_2 for further use as described above.

Examination of the Identity and Integrity of Human TGT

The identity and integrity of the human TGT samples were examined by the Michigan Proteome Consortium (University of Michigan). The proteins ht-hQTRT1 and QTRTD1 were separated and stained on a denaturing SDS-PAGE gel. Following the excision of the protein bands, the in-gel samples were digested with trypsin and analyzed by matrix-assisted laser desorption/Ionization (MALDI) time-of-flight (TOF) tandem mass spectrometry. The observed peptide fragments were then compared to IPI human database, and the data were

analyzed by Mascot and Protein Pilot to determine protein identity. Additionally, intact mass analyses were performed to confirm protein integrity, where the solution form of purified ht-hQTRT1 and ht-hQTRT1•QTRTD1 were subjected to MALDI-TOF mass spectrometry.

Chemical Cross-linking of ht-hQTRT1•hQTRTD1

Bisimidoester cross-linking was performed essentially as previously described (10). Briefly, purified ht-hQTRT1•hQTRTD1 in 0.2 M triethanolamine (TEA) buffer (pH 8.0) was mixed with a fresh preparation of dimethylsuberimidate (in 0.2 M TEA, pH 8.0) to give a final concentration of 14 μM ht-hQTRT1•hQTRTD1 and 20 mM dimethylsuberimidate in a 10-μL reaction. The reaction mixtures were incubated at a 25°C for 2 h, and the cross-linking products were then analyzed and visualized by SDS-PAGE. Additionally, the cross-linked protein band was excised and submitted to the Michigan Proteome Consortium for mass spectrometric analysis of protein identity.

Activity Screen and Kinetic Analyses

Guanine exchange assays were conducted by monitoring the incorporation of radiolabeled substrate, [8-^{14}C] guanine, into the human tRNA^{Tyr} using various human TGT samples (e.g., heterodimer, mutant and individual monomers). In brief, kinetic assays were set up under the following conditions: tRNA^{Tyr} (various concentrations but fixed at 10 μM for guanine kinetics), [8-^{14}C] guanine (57 mCi/mmol, various concentrations but fixed at 20 μM for tRNA

kinetics), human TGT (100 nM), and HEPES reaction buffer (100 mM HEPES, pH 7.3; 20 mM $MgCl_2$; 5 mM DTT) to a final volume of 400 µL. The studies were performed in triplicate at saturating concentration of the other substrate (10 µM for tRNA and for guanine). All samples were incubated at 37°C for purposes of equilibration before initiating the reaction with the addition of TGT. Aliquots (70 µL) were removed every 2 min throughout the 10-min time course and immediately quenched in 2.5 mL of 5% trichloroacetic acid (TCA) for 1 h before filtering on glass-fiber filters. Each filter was washed with three volumes of 5% TCA and a final wash of ethanol to dry the filter. The samples were analyzed in a scintillation counter (Beckman) for radioactive decay, where counts were reported in DPM and later converted to picomoles [8-^{14}C] guanine by the following conversion: pmol = DPM × 0.0079, for the [8-^{14}C] guanine stock with a specific activity of 57 mCi/mmol. To obtain steady-state kinetic parameters for the wild-type ht-hQTRT1•QTRTD1, initial velocities of guanine incorporation were determined by converting the slopes of these plots (pmol/min) to units of second^{-1}, taking into account the concentration of the enzyme and aliquot size. The individual data points from each trial were averaged, and the standard deviation was determined for each concentration of either tRNA^{Tyr} or guanine. The average data points (with error bars representing their standard deviations) were plotted. However, all of the individual data points were fit via non-linear regression to the Michaelis–Menten equation using Kaleidagraph (Abelbeck Software).

Results

Eubacterial TGT Homologues in H. sapiens

To investigate the subunit structure of the human TGT, we have cloned and expressed the genes for hQTRT1 and hQTRTD1. Figure II-1 shows the protein sequence alignment of *E. coli* TGT (ecTGT), hQTRT1 and hQTRTD1. Both human proteins share a high degree of homology to the *E. coli* enzyme (39.1% and 20.1% sequence identities, respectively). ecTGT has been shown to be a zinc-binding protein (11,12). In both hQTRT1 and hQTRTD1, the four key residues responsible for Zn^{+2} binding (Cys302, Cys304, Cys307 and His333; *E. coli* numbering) are conserved. While three TGT active site residues (Asp89, Asp143 and Asp264) are also conserved between ecTGT and hQTRT1, Cys, Ser and Glu are found at the corresponding positions in hQTRTD1. Interestingly, each of these aspartates is conserved across all known TGT sequences among eubacteria, archaea and eukarya. hQTRTD1 has been proposed to be a queuine salvage enzyme that catalyzes the hydrolysis of queuosine rather than transglycosylation (Katze, JR, personal communication).

Construction, Over-expression, and Purification of Human TGT

Polyhistidine-tagged *hqtrt1* and unaltered *hqtrtd1* genes were subcloned into a dual protein expression vector (pRSF-2 Ek/LIC) for co-expression trials. To eliminate any concerns regarding residual transglycosylase activity from the host cells and to enhance heterologous expression (i.e., rare codon usage), a *tgt* (-) *E. coli* strain containing a rare codon tRNA expression plasmid (*E. coli* K12

(DE3, Δ*tgt*)-pRIPL) was utilized. During the expression trials, the addition of Zn^{+2} (100 μM) and low temperature induction (19ºC) were found to be crucial for obtaining optimal yield of active protein. hQTRTD1 co-purifies with polyhistidine-tagged hQTRT1 (ht-hQTRT1) via Ni^{+2} affinity chromatography. We also

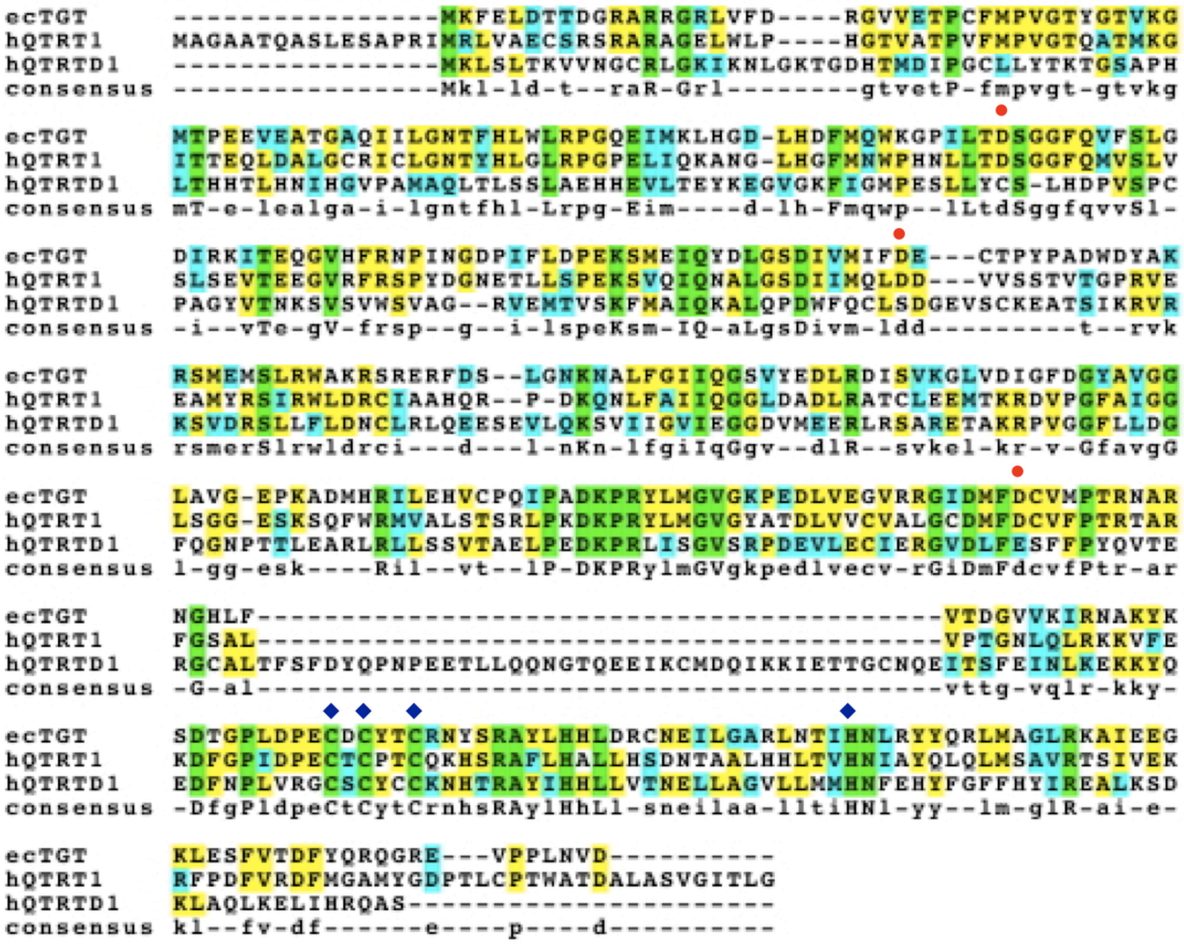

Figure II-1: Protein Sequence Alignment of *E. coli* TGT (ecTGT), Human QTRT1 (hQTRT1) and Human QTRTD1 (hQTRTD1), Conducted by CLUSTALW, Biology WorkBench 3.2. Completely conserved residues are highlighted in green while identical and similar residues are highlighted in yellow and cyan, respectively. The red dots indicate the three active site aspartates (Asp 89, Asp 143 and Asp 264; *E. coli* numbering), and the blue diamonds represent the four key residues (Cys302, Cys304, Cys307 and His333) responsible for Zn^{+2} binding.

attempted to co-express ht-hQTRT1 and USP14, which was previously proposed to be a regulatory subunit of human TGT (i.e., an hQTRT1•USP14 heterodimer); however, we did not observe any co-purification between ht-hQTRT1 and USP14. The ht-hQTRT1•hQTRTD1 complex was further purified by size-exclusion chromatography. The size-exclusion chromatography also separated ht-hQTRT1•hQTRTD1 from "free" ht-hQTRT1 monomer (data not shown), which was also confirmed by SDS-PAGE analysis.

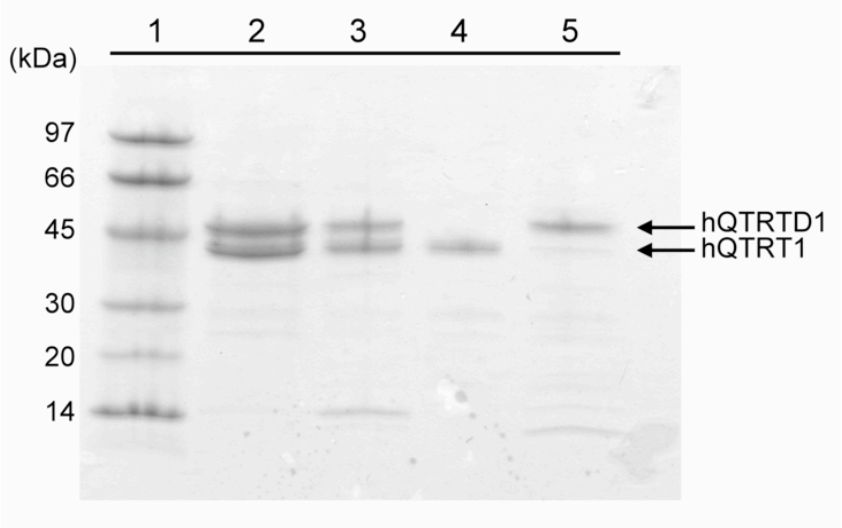

Figure II-2: SDS-PAGE of Various Human TGT Samples and Subunits. 1. Low molecular weight standards (GE Healthcare), 2. Wild-type ht-hQTRT1•hQTRTD1, 3. ht-hQTRT1(Asp279Asn)•hQTRTD1, 4. ht-hQTRT1 monomer, 5. ht-hQTRTD1 monomer. The molecular weight of ht-hQTRT1 is predicted to be ca. 45.7 kDa, while those of hQTRTD1 and ht-hQTRTD1 are approximately 46.7 kDa and 48.9 kDa, respectively.

The purified human TGT (ht-hQTRT1•hQTRTD1) tends to precipitate from the storage buffer that we typically use for the *E. coli* enzyme (25 mM HEPES (pH 7.3) and 2 mM DTT). We found that the addition of excipients (100 mM NaCl

and 50% (w/v) glycerol) stabilize the heterodimeric protein for storage. Densitometry analysis (data not shown) of denaturing SDS-PAGE (Figure II-2, lane 2) reveals that the ratio of ht-hQTRT1 to hQTRTD1 is approximately 1:1.

Unexpectedly, of the two protein bands detected, one (presumably ht-hQTRT1) migrates to a lower apparent molecular weight (< 45 kDa) than predicted from the amino acid sequence (45.7 kDa). To confirm the identity of both bands, we performed mass spectrometry analyses on peptides from tryptic digests of the bands excised from a denaturing gel (Michigan Proteome Core Facility). After mapping the observed peptide fragments against two protein databases, IPI Human and NCBI *E. coli*, our samples were confirmed to be hQTRT1 and hQTRTD1 (Appendix Figures II-1 & II-2 and Tables II-1 & II-2). Although the apparent molecular weight of ht-hQTRT1 on SDS-PAGE was less than the expected molecular weight, intact mass analysis reveled a molecular weight of 45.5 kDa (Figure II-3A), confirming that the protein was intact. Interestingly, a small peak corresponding to a dimeric form of hQTRT1 (90,931 kDa) was also seen in the mass spectrum (Figure II-3A), suggesting the formation of some amount of a homodimeric hQTRT1 under these conditions. The intact mass analysis of the purified ht-hQTRT1•hQTRTD1 complex further revealed that both ht-hQTRT1 and hQTRTD1 are able to form some smaller amount of homodimeric species as well as the predominant heterodimer. As shown in Figure II-3B, the peak at 91,290 kDa appears to be due to a homodimer of the protein giving rise to the peak at 45,510 kDa (ht-hQTRT1) and the peak at 94,724 kDa seems to represent a homodimer of the monomer with a molecular

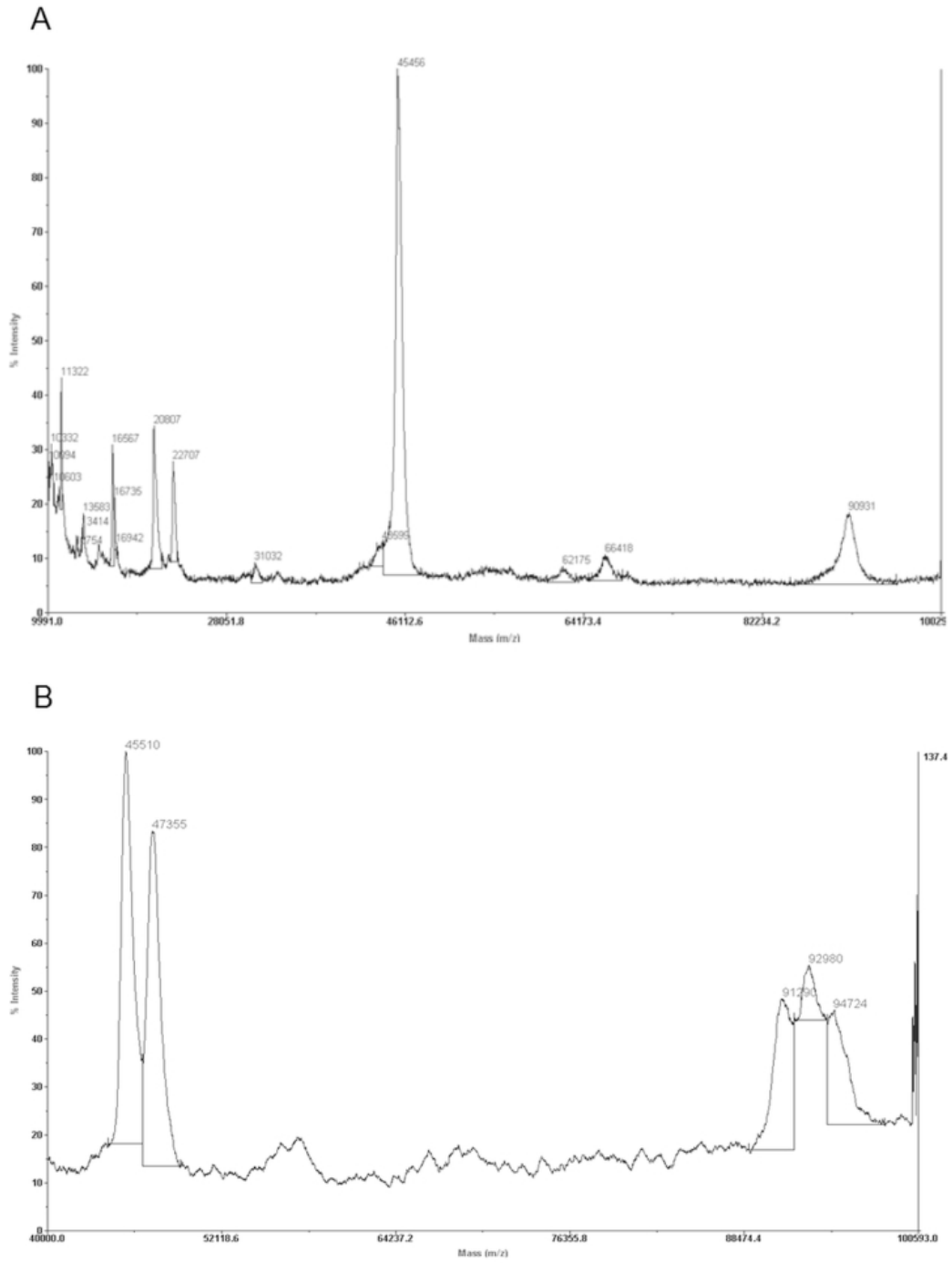

Figure II-3: Intact Mass Analysis of (A) ht-hQTRT1 and (B) ht-hQTRT1•hQTRTD1

weight of 47,355 kDa (hQTRTD1). Our observation of a peak corresponding to the hQTRTD1 homodimer is consistent with the report that the mouse QTRTD1 can self-associate weakly *in vivo* (7). Given that the hQTRTD1 homodimer is observed after Ni^{+2} affinity purification and that only ht-hQTRT1 is His-tagged, this suggests that there must be some form of a dynamic equilibrium existing between the dimeric forms, at least under these conditions. The most intense peak at 92,980 kDa matches the molecular weight of a heterodimeric ht-hQTRT1•hQTRTD1, confirming that these two proteins associate in a 1:1 complex.

Additionally, ht-hQTRT1 and ht-hQTRTD1 were also expressed and purified individually (as shown in Figure II-2, lanes 4 and 5). The recombinant ht-hQTRTD1 shows extremely low solubility during purification, most likely due to protein aggregation and/or misfolding. Using a chaperone-containing strain (*E. coli* BL21 (DE3)-pGro7), significantly higher amounts of soluble ht-hQTRTD1, compared to several other expression systems, were obtained. However, the chaperones groES and groEL co-purified with ht-hQTRTD1 upon Ni^{+2} affinity chromatography. Anion-exchange chromatography was subsequently utilized to separate ht-hQTRTD1 from the chaperones.

Chemical Cross-linking of ht-hQTRT1•hQTRTD1

To probe the nature of the human TGT subunit association, chemical cross-linking was performed using a bisimidoester cross-linker, dimethyl

suberimidate (DMS). As shown in Figure II-4, in addition to the two individual subunits of the human TGT, a higher molecular weight protein band is indeed observed on SDS-PAGE (Lane 3), and it migrates to a position near the 97 kDa marker (similar to the predicted molecular weight for the heterodimer), which suggests a 1:1 stoichiometry for the complex. While compelling, the SDS-PAGE analysis is only suggestive due to the low efficiency of cross-linking and the relatively low molecular weight resolution of the SDS-PAGE. Therefore, the cross-linked protein band was excised and subjected to trypsin digestion and mass spectrometry to confirm the protein identities. Peptide fragments corresponding to both ht-hQTRT1 and hQTRTD1 were both identified (Appendix Figure II-3 and Table II-3), consistent with a cross-linked TGT heterodimer.

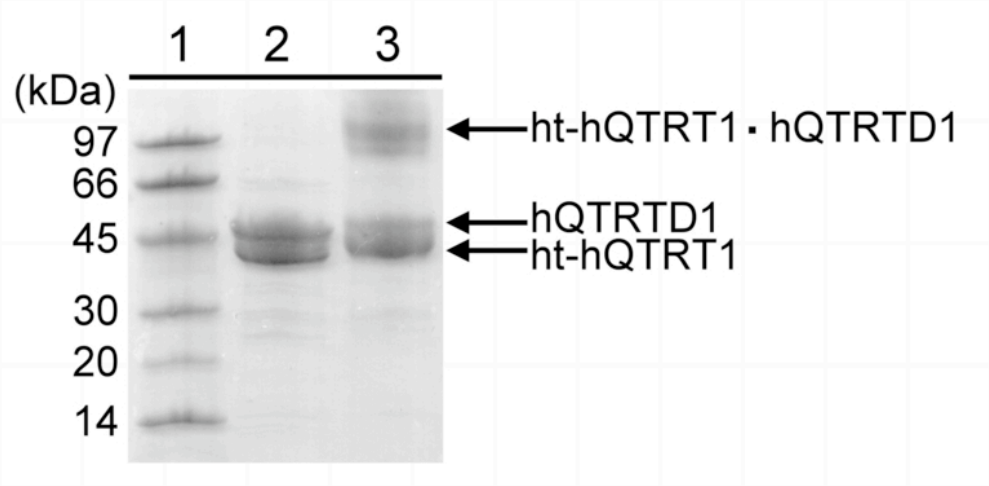

Figure II-4: SDS-PAGE of ht-hQTRT1•hQTRTD1 Cross-linking. 1. Low molecular weight standards (GE Healthcare), 2. ht-hQTRT1•hQTRTD1 control, 3. DMS treated ht-hQTRT1•hQTRTD1. The expected molecular weight for a heterodimeric form of ht-hQTRT1 and hQTRTD1 is approximately 93 kDa.

Kinetic Analyses of Human TGT with respect to Human tRNA^{Tyr} and Guanine

To kinetically characterize the human TGT transglycosylase activity, its cognate human tRNA^{Tyr} was first generated from *in vitro* transcription, purified via size-exclusion chromatography and verified by 2% agarose-TAE gels. The transglycosylase activity of the human TGT was examined by monitoring [^{14}C]-guanine incorporation into the human tRNA^{Tyr}, and kinetic parameters were determined by non-linear fits to the Michaelis–Menten equation (Figure II-5). As shown in Table II-1, tRNA^{Tyr} and guanine exhibit very similar K_M values (0.34 μM, 0.41 μM respectively) and, reassuringly, essentially identical (within experimental error) k_{cat} values (5.60 x 10^{-3} s^{-1}, 5.86 x 10^{-3} s^{-1} respectively). The catalytic efficiencies (as defined by k_{cat} / K_M) of the human TGT with respect to tRNA^{Tyr} and guanine are very similar to those for the *E. coli* enzyme (Table II-1).

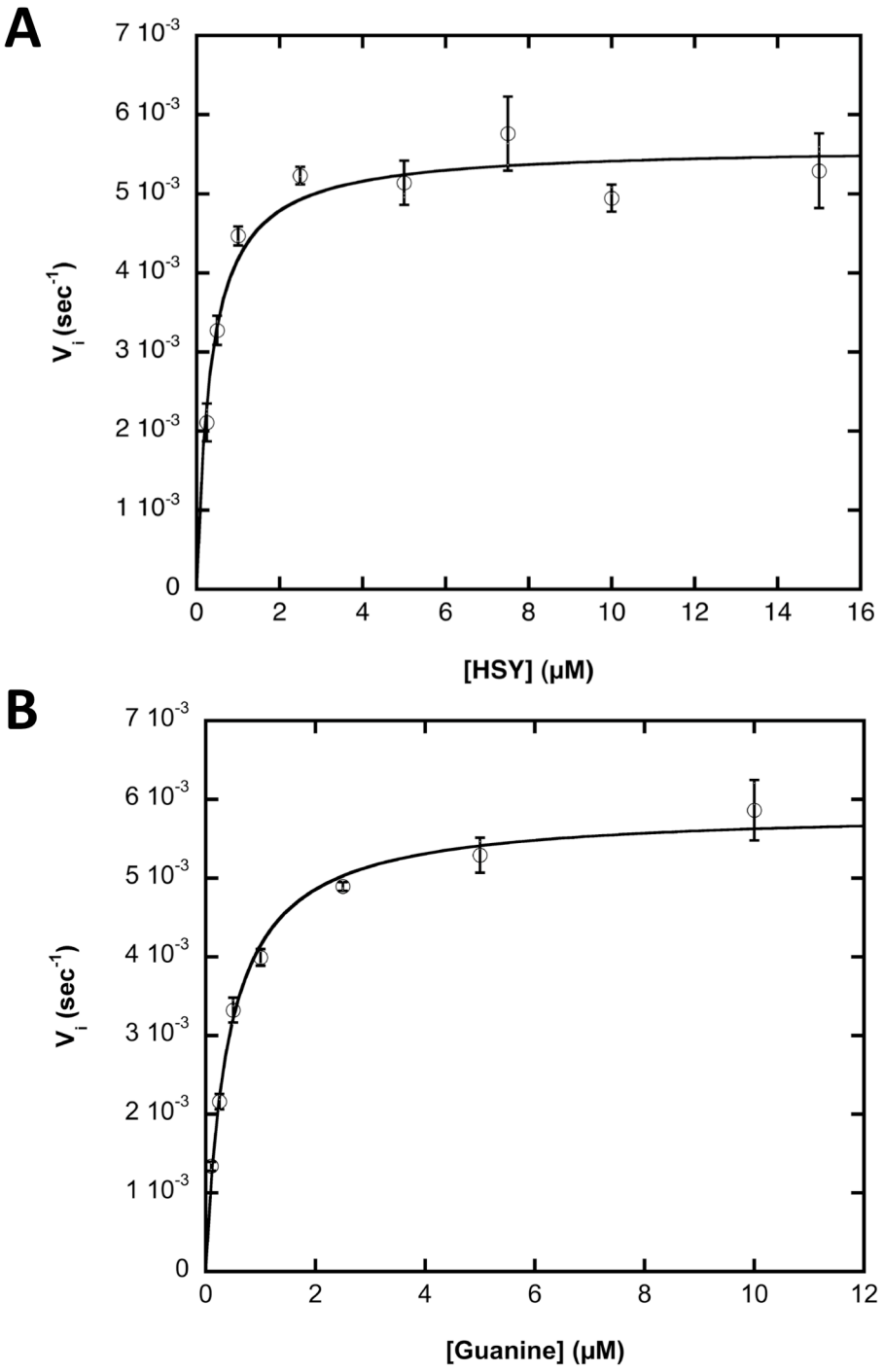

Figure II-5: Kinetic Characterization of (A) Human $tRNA^{Tyr}$ and (B) Guanine with Human TGT (co-expressed, co-purified ht-hQTRT1•hQTRTD1)

Table II-1. Kinetic Parameters for Human TGT and *E. coli* TGT with respect to their Cognate $tRNA^{Tyr}$ and Guanine

	K_M [a] (μM)	k_{cat} [a] (10^{-3}•s^{-1})	k_{cat}/K_M [a, b] (10^{-3}•s^{-1}•μM^{-1})
tRNA Kinetics			
Human TGT	0.34 (±0.04)	5.60 (±0.13)	16.5 (±1.9)
E. coli TGT[c]	0.12 (±0.04)	1.21 (±0.07)	10.1 (±3.4)
Guanine Kinetics			
Human TGT	0.41 (±0.03)	5.86 (±0.10)	14.2 (±0.9)
E. coli TGT[c]	0.10 (±0.03)	1.21 (±0.07)	12.1 (±3.7)

[a]Standard errors are in parentheses.

[b]Derived from fit to the following equation: $v_i = \dfrac{\frac{k_{cat}}{K_M}[S]}{1+\frac{[S]}{K_M}}$

[c]From Kittendorf *et al*., (2001) *Biochemistry* 40 (11), 14123-14133.

In attempts to reconstitute ht-hQTRT1•hQTRTD1 from individually prepared ht-hQTRT1 and ht-hQTRTD1, we observed only very low levels of transglycosylase activity. Unfortunately, the magnitude of the activity was significantly less than that for the co-expressed and purified ht-hQTRT1•hQTRTD1 complex and the data did not exhibit linearity over time. Neither ht-hQTRT1 nor ht-hQTRTD1 monomers are able to incorporate [^{14}C]-

guanine into the human $tRNA^{Tyr}$ (Figure II-6). Kinetic assays also showed that the ht-hQTRT1(Asp279Asn)•hQTRTD1 mutant exhibits no detectable transglycosylase activity (Figure II-6).

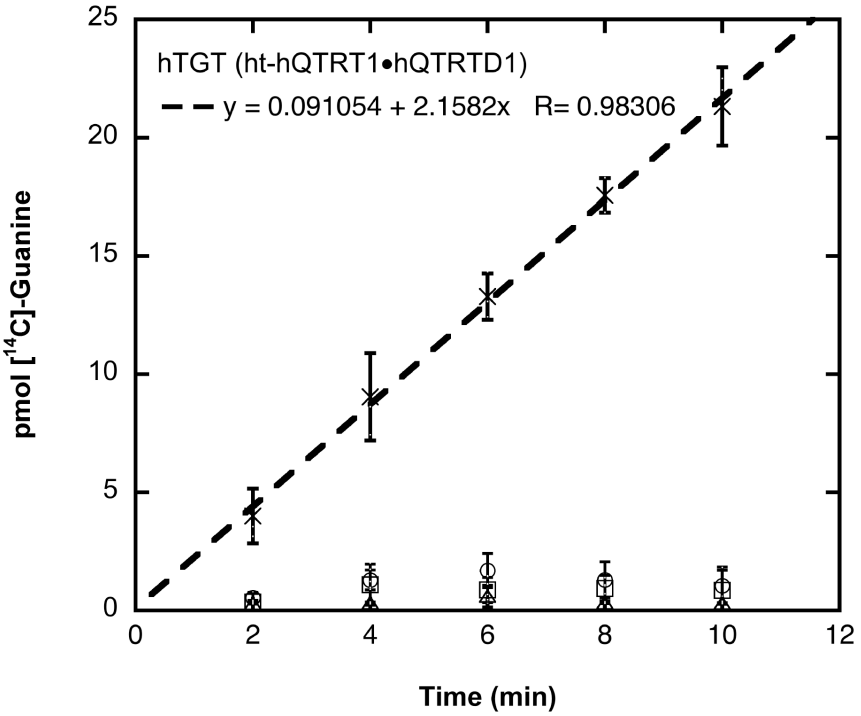

Figure II-6: [^{14}C]-Guanine Incorporated Over Time in Human $tRNA^{Tyr}$ in the presence of Wild-type Human TGT (ht-hQTRT1•hQTRTD1, crosses), Mutant TGT (ht-hQTRT1(Asp279Asn)•hQTRTD1, circles), QTRT1 monomer (triangles) and hQTRTD1 monomers (squares). Only the wild-type human TGT heterodimer shows an initial velocity (2.16 pmol/min, R=0.9831). The mutant heterodimer and hQTRT1 and hQTRTD1 monomers did not exhibit any incorporation of [^{14}C]-guanine into $tRNA^{Tyr}$.

Discussion

The general perception that eukaryal tRNA-guanine transglycosylases (TGTs) exist as dimeric proteins has been based on observations of TGTs

isolated from at least four different eukaryotes (rabbit erythrocytes, wheat germ, bovine liver and rat liver) (1-4). Protein sequence homology of QTRT1 (queuine tRNA-ribosyltransferase 1) to the eubacterial TGT, along with studies that indicated co-purification with USP14, led to the proposal that the eukaryal TGT was a heterodimer of QTRT1 and USP14 (ubiquitin-specific protease 14). It was hypothesized that QTRT1 was responsible for the transglycosylase activity whereas USP14 regulated the activity of QTRT1 in response to phosphorylation by protein kinase C (PKC) (4,5,14). Other than the reported co-purification of QTRT1 and USP14, there has not been any rigorous *in vitro* experiments to support this hypothesis.

To elucidate the subunit structure of the human TGT, significant efforts have been made to obtain soluble and active hQTRT1 in our laboratory. However, transglycosylase activity has not been observed, even when the protein was co-expressed in a construct containing both hQTRT1 and its proposed protein partner, USP14. A recent study revealed that the mouse QTRT1 and QTRTD1 (queuine tRNA-ribosyltransferase domain-containing 1) co-localize in mitochondria, suggesting the formation of a heterodimeric TGT complex between these two proteins (7). Additionally, they reported that transglycosylase activity was observed *in vitro* only when both subunits were present. Sequence analysis shows the high homology between hQTRT1 and hQTRTD1, especially in the C-terminal domain. Based upon the conservation of amino acid residues and tertiary structure prediction, both proteins most likely share the same $(\beta/\alpha)_8$ TIM barrel scaffold with the eubacterial TGT, revealed by

the crystal structure of *Z. mobilis* TGT (7,15). Therefore, we elected to attempt co-expression of the human counterparts of these two proteins. Co-expression was successful and all of the physical evidence (co-purification, chemical cross-linking, mass spectrometry) that we have obtained is consistent with the human TGT not only existing as a heterodimer of hQTRT1•hQTRTD1, but that the heterodimer is a 1:1 complex.

Our kinetic studies confirm that the transglycosylase activity of the human TGT comes from the hQTRT1•hQTRTD1 heterodimer and that neither hQTRT1 nor hQTRTD1 monomers exhibit any transglycosylase activity. The absence of any activity for the individual subunits also supports the idea that the homodimers we observed in the mass spectrometry studies likely have no physiological relevance as they would not have any activity even if they do exist *in vivo*. The human TGT exhibits kinetic parameters with respect to guanine and its cognate human $tRNA^{Tyr}$ that are essentially identical to those of the *E. coli* TGT. The sub-micromolar K_M for guanine that we have observed suggests that the natural substrate, queuine, would likely have an even smaller K_M (due to the likely additional binding interactions with the dihydroxycyclopentenylamine moiety). In various eukaryal tissues, the physiological queuine content is generally estimated to be in the low nM range (e.g., about 3.6 nM in human milk (16)). Given the low concentration of free queuine *in vivo*, this postulated high affinity of the human TGT for queuine seems reasonable. Kinetic studies of the human TGT and queuine are reported and discussed in Chapter III in this dissertation.

Our initial observations do not necessarily conflict with the previous proposal that USP14 regulates the transglycosylase activity of hQTRT1 in a protein kinase C (PKC)-dependent manner (4). Since hQTRT1 and hQTRTD1 are very similar in size, it is possible that in those previous studies they were not resolved as two distinct bands on SDS-PAGE. If so, USP14 could possibly bind to and regulate the heterodimer, consistent with their observation of 43 kDa (presumably unresolved TGT subunits) and 60 kDa bands on SDS-PAGE. However, we have seen no association of hQTRT1 and USP14 and in preliminary studies, we observed that the transglycosylase activity of ht-hQTRT1•hQTRTD1 is essentially unaffected by the presence of USP14, protein kinase C/ATP or alkaline phosphatase (data not shown). Further studies need to be conducted to absolutely confirm these observations, but at present we have no evidence supporting the USP14 regulation model.

To determine which subunit (hQTRT1 or hQTRTD1) is actually responsible for the transglycosylase activity, two human TGT mutants, ht-hQTRT1(Asp279Asn) •hQTRTD1 and ht-hQTRT1•hQTRTD1(Glu272Gln) were expressed and purified. The corresponding residue, aspartate 264, in the *E. coli* TGT is the nucleophilic catalyst that forms the covalent RNA-TGT intermediate (12,13,17). Mutation to anything other than glutamate yields catalytically inactive protein that is structurally unaltered (i.e., it folds correctly and binds, non-covalently to tRNA). As mentioned previously, in contrast to active site aspartate 279 in hQTRT1, glutamate 272 is found at the corresponding position in hQTRTD1. Unexpectedly, when purifying the ht-hQTRT1•hQTRTD1

(Glu272Gln) mutant via Ni^{+2} affinity chromatography, we experienced a significant loss of the hQTRTD1 subunit, which resulted in a mixture of heterodimer and monomeric ht-hQTRT1. Evidently, the mutation somehow reduces the affinity of the subunits in the heterodimer. The consequence is that we were unable to test the transglycosylase activity of the QTRTD1 mutant heterodimer.

Our attempts to reconstitute the wild-type heterodimer from individually expressed and purified subunits gave inconclusive results. It is possible that the N-terminal His-tag on hQTRTD1 (used for purification and not present in the co-expressed protein) may impair the interaction with ht-hQTRT1. The His-tag on hQTRT1 does not appear to affect the association between ht-hQTRT1 and hQTRTD1, as both physical and kinetic evidence supports the formation of the heterodimer. An N-terminal His-tag has previously been shown to have no affect on the activity of the eubacterial TGT (18). Our observation of an active dimeric human TGT is consistent with the crystallographic evidence derived from *Z. mobilis* TGT (12,19), which indicates that the eubacterial TGT forms a homodimer. While one subunit is capable of recognizing tRNA anticodon loop and performs the transglycosylase reaction, the other one assists in maintaining the proper orientation of bound tRNA.

Unlike eubacteria, which biosynthesize queuine from its precursor $preQ_1$, eukaryotes are incapable of synthesizing queuine *de novo* and have to obtain free queuine from diet. Almost three decades ago, Reyniers *et al.*, reported that germ-free mice could utilize dietary queuosine-containing tRNA (Q-tRNA) to

produce free queuine, suggesting that there is a salvage system existing in eukarya to compensate for the inability to synthesize queuine (20). Subsequent studies showed that monkey kidney epithelial cells are able to uptake queuine from degraded Q-tRNA and that the substrate for this salvage activity is queuosine 5'-monophosphate (QMP) (21,22). By studying partially purified extracts from two eukaryal algae, *Chlorella pyrenoidosa* and *Chlamydomonas reinhardtii*, the same group later reported similar observations with the exception that the nucleoside queuosine seems to be the substrate in these plant cells rather than QMP (23). Due to its high homology to QTRT1, QTRTD1 has been suggested to be involved in this salvage pathway (24), although *in vitro* evidence supporting this hypothesis has not yet been reported. It was observed that in every eukaryote that contains the *qtrt1* gene, a corresponding *qtrtd1* gene is found (Katze, JR, personal communication). Assuming that QTRTD1 is confirmed to be the queuine salvage enzyme, the fact that it forms the heterodimer with QTRT1, which catalyzes queuine transglycosylation, is evolutionarily intriguing. As mentioned previously, eukarya lack a queuine biosynthesis pathway. To insure a consistent supply of queuine *in vivo*, it seems reasonable for the eukaryal TGT to evolve into a heterodimer, where QTRTD1 is capable of assisting in tRNA binding and more importantly, generating the heterocyclic substrate, queuine, for QTRT1.

Conclusions

In summary, all of the physical and kinetic evidence in this study is most consistent with a new paradigm for the human TGT. Co-purification through two different chromatographic methods, mass spectrometry, and chemical cross-linking confirm a 1:1 association between ht-hQTRT1 and hQTRTD1. Transglycosylation activity was only seen for the ht-hQTRT1•hQTRTD1 heterodimer and hQTRT1 was shown to be responsible for this activity via specific mutagenesis of a key catalytic residue. Based on these results, we conclude that the functional human TGT is a heterodimeric protein, which consists of a transglycosylase subunit, hQTRT1, and hQTRTD1 (with the likely role of queuine salvage from QMP) and no evidence supporting the previous proposed involvement of USP14 was found.

Notes to Chapter II

This chapter has been published in, Chen, Y.-C., Kelly, V.P., Stachura, S.V., and Garcia, G.A. (2010) Characterization of the human tRNA-guanine transglycosylase: Confirmation of the heterodimeric subunit structure, *RNA*, 16 (5): 958-968. We thank Prof. Jon Katze (University of Tennessee, Memphis) for generously providing the human QTRTD1 clone and also wish to acknowledge Dr. Angela Walker and the Michigan Proteome Consortium for assistance with mass spectrometry analysis.

Abbreviations used: Q, queuine; $preQ_1$, 7-aminomethyl-7-deazaguanine; $preQ_0$, 7-cyano-7-deazaguanine; TGT, tRNA-guanine transglycosylase; QTRT1, queuine tRNA-ribosyltransferase 1; USP14, ubiquitin-specific protease 14; QTRTD1, queuine tRNA-ribosyltransferase domain-containing 1; DTT, dithiothreitiol; TAE, Tris-acetate-EDTA; HEPES, hydroxyethylpiperazine-ethylsulfonate; Tris–HCl, tris(hydroxymethyl) aminomethane hydrochloride; DMS, dimethyl suberimidate; PMSF, phenylmethylsulfonyl fluoride; SDS, sodium dodecyl sulfate; PAGE, polyacrylamide gel electrophoresis; TCA, trichloroacetic acid; TEA, triethanolamine; MALDI, matrix-assisted laser desorption/ionization; TOF, time-of-flight.

1. Howes, N.K. and Farkas, W.R. (1978) Studies with a Homogeneous Enzyme from Rabbit Erythrocytes Catalyzing the Insertion of Guanine into tRNA. *J. Biol. Chem.*, **253**, 9082-9087.

2. Walden, J., T. L. , Howes, N. and Farkas, W.R. (1982) Purification and properties of guanine, queuine-tRNA transglycosylase from wheat germ. *J. Biol. Chem.*, **257**, 13218-13222.

3. Slany, R.K. and Mueller, S.O. (1995) tRNA-guanine transglycosylase from bovine liver - Purification of the enzyme to homogeneity and biochemical characterization. *Eur J Biochem*, **230**, 221-228.

4. Morris, R.C., Brooks, B.J., Eriotou, P., Kelly, D.F., Sagar, S., Hart, K.L. and Elliott, M.S. (1995) Activation of transfer RNA-guanine ribosyltransferase by protein kinase C. *Nucleic Acids Res*, **23**, 2492-2498.

5. Deshpande, K.L., Seubert, P.H., Tillman, D.M., Farkas, W.R. and Katze, J.R. (1996) Cloning and characterization of cDNA encoding the rabbit tRNA-guanine transglycosylase 60-kilodalton subunit. *Arch Biochem Biophys*, **326**, 1-7.

6. Deshpande, K.L. and Katze, J.R. (2001) Characterization of cDNA encoding the human tRNA-guanine transglycosylase (TGT) catalytic subunit. *Gene*, **265**, 205-212.

7. Boland, C., Hayes, P., Santa-Maria, I., Nishimura, S. and Kelly, V.P. (2009) Queuosine Formation in Eukaryotic tRNA Occurs via a Mitochondria-localized Heteromeric Transglycosylase. *J. Biol. Chem.*, **284**, 18218-18227.

8. He, B., Rong, M.Q., Lyakhov, D., Gartenstein, H., Diaz, G., Castagna, R., McAllister, W.T. and Durbin, R.K. (1997) Rapid mutagenesis and purification of phage RNA polymerases. *Protein Expr. Purif.*, **9**, 142-151.

9. Curnow, A.W., Kung, F.L., Koch, K.A. and Garcia, G.A. (1993) tRNA-Guanine Transglycosylase from *Escherichia coli*: Gross tRNA Structural Requirements for Recognition. *Biochemistry*, **32**, 5239-5246.

10. Garcia, G.A., Koch, K.A. and Chong, S. (1993) tRNA-Guanine Transglycosylase from *Escherichia coli*: Overexpression, Purification, and Quaternary Structure. *Journal of Molecular Biology*, **231**, 489-497.

11. Chong, S., Curnow, A.W., Huston, T.J. and Garcia, G.A. (1995) tRNA-guanine transglycosylase from *Escherichia coli* is a zinc metalloprotein. Site-directed mutagenesis studies to identify the zinc ligands. *Biochemistry*, **34**, 3694-3701.

12. Xie, W., Liu, X.J. and Huang, R.H. (2003) Chemical trapping and crystal structure of a catalytic tRNA guanine transglycosylase covalent intermediate. *Nature Structural Biology*, **10**, 781-788.

13. Kittendorf, J.D., Sgraja, T., Reuter, K., Klebe, G. and Garcia, G.A. (2003) An essential role for aspartate 264 in catalysis by tRNA-guanine transglycosylase from *Escherichia coli*. *J. Biol. Chem.*, **278**, 42369-42376.

14. Langgut, W. and Reisser, T. (1995) Involvement of protein kinase C in the control of tRNA modification with queuine in HeLa cells. *Nucleic Acids Res*, **23**, 2488-2491.

15. Romier, C., Reuter, K., Suck, D. and Ficner, R. (1996) Crystal structure of tRNA-guanine transglycosylase: RNA modification by base exchange. *EMBO Journal*, **15**, 2850-2857.

16. Katze, J.R., Basile, B. and McClosky, J.A. (1982) Queuine, a Modified Base Incorporated Posttranscriptionally into Transfer RNA: Wide Distribution in Nature. *Science*, **216**, 55-56.

17. Garcia, G.A., Chervin, S.M. and Kittendorf, J.D. (2009) Identification of the Rate-Determining Step of tRNA-Guanine Transglycosylase from Escherichia coli. *Biochemistry*, **48**, 11243-11251.

18. Todorov, K.A., Tan, X.J., Nonekowski, S.T., Garcia, G.A. and Carlson, H.A. (2005) The Role of Aspartic Acid 143 in E. coli tRNA-Guanine Transglycosylase: Insights from Mutagenesis Studies and Computational Modeling. *Biophysical Journal*, **89**, 1965-1977.

19. Stengl, B., Meyer, E.A., Heine, A., Brenk, R., Diederich, F. and Klebe, G. (2007) Crystal structures of tRNA-guanine transglycosylase (TGT) in complex with novel and potent inhibitors unravel pronounced induced-fit adaptations and suggest dimer formation upon substrate binding. *J Mol Biol*, **370**, 492-511.

20. Reyniers, J.P., Pleasants, J.R., Wostmann, B.S., Katze, J.R. and Farkas, W.R. (1981) Administration of Exogenous Queuine Is Essential for the Biosynthesis of the Queuosine-containing Trnasfer RNAs in the Mouse. *J. Biol. Chem.*, **206**, 11591-11594.

21. Gunduz, U. and Katze, J.R. (1982) Salvage of the nucleic acid base queuine from queuine-containing tRNA by animal cells. *Biochem Biophys Res Commun*, **109**, 159-167.

22. Gunduz, U. and Katze, J.R. (1984) Queuine salvage in mammalian cells. Evidence that queuine is generated from queuosine 5'-phosphate. *J Biol Chem*, **259**, 1110-1113.

23. Kirtland, G.M., Morris, T.D., Moore, P.H., O'Brian, J.J., Edmonds, C.G., McCloskey, J.A. and Katze, J.R. (1988) Novel Salvage of Queuine from Queuosine and Absence of Queuine Synthesis in *Chlorella pyrenoidosa* and *Chlamydomonas reinhardii*. *J. Bacteriol.*, **170**, 5633.

24. Vandenbergh, D.J., Grant, M.D. and Severns, V. (2003) A simple tandem repeat polymorphism is present in the eighth intron of FLJ12960, a possible queuine salvage enzyme gene. *Molecular and Cellular Probes*, **17**, 319-320.

Appendix II

Mass spectra were acquired on an Applied Biosystems 4800 Maldi TOF/TOF Analyzer (TOF/TOF) using 4000 Series Explorer. MS spectra from 800-4000 Da were acquired from each well. The twelve most intense peaks in each MS spectrum were selected for MS/MS analysis. Peptide fragmentation is induced by the use of atmosphere as a collision gas with a pressure of ~ 1 $x10^{-7}$ torr and a collision energy of 2 kV.

Peptide identifications were performed using Mascot (v2.1 MatrixScience, London UK) and Protein Pilot (v3.0, Applied Biosystems). Mascot was used to perform PMF searches on the samples. Protein Pilot was used to perform searches on the MS/MS spectra. The spectra were searched against the IPI human database (v.3.63, 84,118 entries). In the Mascot PMF searches, trypsin specificity was selected. Carbamidomethyl cysteine was defined as a fixed modification and oxidized methionine was considered as a variable modification. The peptide tolerance was set to 75 ppm. The Mascot search engine returned a set of protein matches with protein scores and a significance level. Protein scores above the significance threshold were considered to be significant hits with a >95% probability of being correct. For the Protein Pilot MS/MS searches, cysteine alkylation was conducted by iodoacetamide, digestion was performed by trypsin, instrument was 4800, and search effort was thorough. Other parameters, such as mass tolerance were defined in the instrument type. Protein pilot automatically looked for missed and non-specific cleavages so they were not defined in the search parameters. Protein Pilot returned a list of proteins

along with a total score and the number of peptides identified above 95%. The total protein score was calculated from the scores of the individual peptides where the peptide score = -log(1-condfidence) (i.e. a peptide with a 95% confidence would have a score of 1.3 and a peptide with 99% confidence would have a score of 2.0).

Intact protein analysis was performed in the 4800 in linear mode. Two Invitrogen calibration standards with theoretical m/z 69205 and 89713 Da were spotted in wells adjacent to the sample. The spectra of the standards were internally calibrated and used to update the default calibration of the instrument. Spectra of the samples were acquired using the default calibration. Applied Biosystems Data Explorer was used for peak-picking after a 21-pt Gaussian smooth was applied to sample peaks. Mass error was determined by calculating the mass error of the standards using default calibration.

Appendix Table II-1. Mass Spectrometric Analysis of ht-hQTRT1 via Protein Pilot

N[a]	%Cov[b]	Conf[c]	Prec m/z[d]	Accessions[e]	Names[f]	Sequence[g]
1	19.60	99.00	1241.67	IPI:IPI00215974.2	Gene_Symbol=QTRT1 Queuine tRNA-ribosyltransferase	AIIQGGLDADLR
1	19.60	99.00	1924.73	IPI:IPI00215974.2	Gene_Symbol=QTRT1 Queuine tRNA-ribosyltransferase	DFGPIDPECTCPTCQK
1	19.60	99.00	1472.81	IPI:IPI00215974.2	Gene_Symbol=QTRT1 Queuine tRNA-ribosyltransferase	FGSALVPTGNLQLR
1	19.60	99.00	1433.69	IPI:IPI00215974.2	Gene_Symbol=QTRT1 Queuine tRNA-ribosyltransferase	GITTEQLDALGCR
1	19.60	99.00	1416.72	IPI:IPI00215974.2	Gene_Symbol=QTRT1 Queuine tRNA-ribosyltransferase	ICLGNTYHLGLR
1	19.60	99.00	1320.78	IPI:IPI00215974.2	Gene_Symbol=QTRT1 Queuine tRNA-ribosyltransferase	LGLRPGPELIQK
1	19.60	99.00	1743.91	IPI:IPI00215974.2	Gene_Symbol=QTRT1 Queuine tRNA-ribosyltransferase	QNLFAIIQGGLDADLR
1	19.60	99.00	1726.91	IPI:IPI00215974.2	Gene_Symbol=QTRT1 Queuine tRNA-ribosyltransferase	QNLFAIIQGGLDADLR

[a]The rank of the specified protein relative to all other proteins in the list of detected proteins

[b]The number of matching amino acids (from peptides) divided by the total number of amino acids in the sequence, express as a percentage

[c]The confidence for the peptide identification, expressed as a percentage

[d]The monoisotopic m/z for the ion fragmented in this cycle and experiment, as determined by the instrument

[e]The accession number of the detected protein

[f]The name of the detected protein

[g]The sequence of the peptide with the highest confidence that was identified by the search

Appendix Table II-2. Mass Spectrometric Analysis of hQTRTD1 via Protein Pilot

N	%Cov	Conf	Prec m/z	Accessions	Names	Sequence
1	26.51	99.00	1933.91	IPI:IPI00783033.2; IPI:IPI00074010.4	Gene_Symbol=QTRTD1 Queuine tRNA-ribosyltransferase domain-containing protein 1; Gene_Symbol=QTRTD1 48 kDa protein	GVDLFESFFPYQVTER
1	26.51	99.00	1408.70	IPI:IPI00783033.2; IPI:IPI00074010.4	Gene_Symbol=QTRTD1 Queuine tRNA-ribosyltransferase domain-containing protein 1; Gene_Symbol=QTRTD1 48 kDa protein	KYQEDFNPLVR
1	26.51	99.00	1971.97	IPI:IPI00783033.2; IPI:IPI00074010.4	Gene_Symbol=QTRTD1 Queuine tRNA-ribosyltransferase domain-containing protein 1; Gene_Symbol=QTRTD1 48 kDa protein	LISGVSRPDEVLECIER
1	26.51	99.00	1631.81	IPI:IPI00783033.2; IPI:IPI00074010.4	Gene_Symbol=QTRTD1 Queuine tRNA-ribosyltransferase domain-containing protein 1; Gene_Symbol=QTRTD1 48 kDa protein	LLDGFQGNPTTLEAR
1	26.51	99.00	1654.87	IPI:IPI00783033.2; IPI:IPI00074010.4	Gene_Symbol=QTRTD1 Queuine tRNA-ribosyltransferase domain-containing protein 1; Gene_Symbol=QTRTD1 48 kDa protein	LLSSVTAELPEDKPR
1	26.51	99.00	1250.64	IPI:IPI00783033.2; IPI:IPI00074010.4	Gene_Symbol=QTRTD1 Queuine tRNA-ribosyltransferase domain-containing protein 1; Gene_Symbol=QTRTD1 48 kDa protein	SLLFLDNCLR
1	26.51	99.00	1702.83	IPI:IPI00783033.2; IPI:IPI00074010.4	Gene_Symbol=QTRTD1 Queuine tRNA-ribosyltransferase domain-containing protein 1; Gene_Symbol=QTRTD1 48 kDa protein	SVIIGVIEGGDVMEER
1	26.51	99.00	1047.56	IPI:IPI00783033.2; IPI:IPI00074010.4	Gene_Symbol=QTRTD1 Queuine tRNA-ribosyltransferase domain-containing protein 1; Gene_Symbol=QTRTD1 48 kDa protein	SVSVWSVAGR
1	26.51	99.00	1280.61	IPI:IPI00783033.2; IPI:IPI00074010.4	Gene_Symbol=QTRTD1 Queuine tRNA-ribosyltransferase domain-containing protein 1; Gene_Symbol=QTRTD1 48 kDa protein	YQEDFNPLVR
1	26.51	92.00	1718.79	IPI:IPI00783033.2; IPI:IPI00074010.4	Gene_Symbol=QTRTD1 Queuine tRNA-ribosyltransferase domain-containing protein 1; Gene_Symbol=QTRTD1 48 kDa protein	SVIIGVIEGGDVMEER
2	6.22	99.00	1472.79	IPI:IPI00435964.3; IPI:IPI00215974.2	Gene_Symbol=QTRT1 Queuine tRNA-ribosyltransferase 1 (tRNA-guanine transglycosylase), isoform CRA_b; Gene_Symbol=QTRT1 Queuine tRNA-ribosyltransferase	FGSALVPTGNLQLR

Appendix Table II-3. Mass Spectrometric Analysis of Cross-linked ht-hQTRT1•hQTRTD1 via Protein Pilot

N	%Cov	Conf	Prec m/z	Accessions	Names	Sequence
1	16.39	99.00	1934.26	IPI:IPI00783033.2; IPI:IPI00074010.4	Gene_Symbol=QTRTD1 Queuine tRNA-ribosyltransferase domain-containing protein 1; Gene_Symbol=QTRTD1 48 kDa protein	GVDLFESFFPYQVTER
1	16.39	99.00	1972.35	IPI:IPI00783033.2; IPI:IPI00074010.4	Gene_Symbol=QTRTD1 Queuine tRNA-ribosyltransferase domain-containing protein 1; Gene_Symbol=QTRTD1 48 kDa protein	LISGVSRPDEVLECIER
1	16.39	99.00	1655.17	IPI:IPI00783033.2; IPI:IPI00074010.4	Gene_Symbol=QTRTD1 Queuine tRNA-ribosyltransferase domain-containing protein 1; Gene_Symbol=QTRTD1 48 kDa protein	LLSSVTAELPEDKPR
1	16.39	99.00	1250.86	IPI:IPI00783033.2; IPI:IPI00074010.4	Gene_Symbol=QTRTD1 Queuine tRNA-ribosyltransferase domain-containing protein 1; Gene_Symbol=QTRTD1 48 kDa protein	SLLFLDNCLR
1	16.39	99.00	1280.83	IPI:IPI00783033.2; IPI:IPI00074010.4	Gene_Symbol=QTRTD1 Queuine tRNA-ribosyltransferase domain-containing protein 1; Gene_Symbol=QTRTD1 48 kDa protein	YQEDFNPLVR
2	6.70	99.00	1473.06	IPI:IPI00215974.2	Gene_Symbol=QTRT1 Queuine tRNA-ribosyltransferase	FGSALVPTGNLQLR
2	6.70	99.00	1433.93	IPI:IPI00215974.2	Gene_Symbol=QTRT1 Queuine tRNA-ribosyltransferase	GITTEQLDALGCR
3	0.00	86.00	1377.93	IPI:IPI00938390.1; IPI:IPI00937646.1	Gene_Symbol=LOC100289012 hypothetical protein XP_002343616; Gene_Symbol=LOC100291040 hypothetical protein XP_002347839	EAVVLVPGQPVPR

```
  1 MAGAATQASL ESAPRIMRLV AECSRSRARA GELWLPHGTV ATPVFMPVGT
 51 QATMKGITTE QLDALGCRIC LGNTYHLGLR PGPELIQKAN GLHGFMNWPH
101 NLLTDSGGFQ MVSLVSLSEV TEEGVRFRSP YDGNETLLSP EKSVQIQNAL
151 GSDIIMQLDD VVSSTVTGPR VEEAMYRSIR WLDRCIAAHQ RPDKQNLFAI
201 IQGGLDADLR ATCLEEMTKR DVPGFAIGGL SGGESKSQFW RMVALSTSRL
251 PKDKPRYLMG VGYATDLVVC VALGCDMFDC VFPTRTARFG SALVPTGNLQ
301 LRKKVFEKDF GPIDPECTCP TCQKHSRAFL HALLHSDNTA ALHHLTVHNI
351 AYQLQLMSAV RTSIVEKRFP DFVRDFMGAM YGDPTLCPTW ATDALASVGI
401 TLG
```

Appendix Figure II-1: Mass Spectrometric Analysis of ht-hQTRT1 via Mascot. Shown is the sequence of hQTRT1, where the sequences highlighted in red and bold are protein fragments (processed by trypsin digestion) that were determined by MALDI-TOF analysis and analyzed by Mascot. Mascot confirmed that hQTRT1 was the only significant hit found with a Protein Score of 90 (Score < 62, p = 0.05) and an Expect value of 8.2E-5, where confident matches typically have Expect values < 0.1.

A

```
  1 MKLSLTKVVN GCRLGKIKNL GKTGDHTMDI PGCLLYTKTG SAPHLTHHTL
 51 HNIHGVPAMA QLTLSSLAEH HEVLTEYKEG VGKFIGMPES LLYCSLHDPV
101 SPCPAGYVTN KSVSVWSVAG RVEMTVSKFM AIQKALQPDW FQCLSDGEVS
151 CKEATSIKRV RKSVDRSLLF LDNCLRLQEE SEVLQKSVII GVIEGGDVME
201 ERLRSARETA KRPVGGFLLD GFQGNPTTLE ARLRLLSSVT AELPEDKPRL
251 ISGVSRPDEV LECIERGVDL FESFFPYQVT ERGCALTFSF DYQPNPEETL
301 LQQNGTQEEI KCMDQIKKIE TTGCNQEITS FEINLKEKKY QEDFNPLVRG
351 CSCYCCKNHT RAYIHHLLVT NELLAGVLLM MHNFEHYFGF FHYIREALKS
401 DKLAQLKELI HRQAS
```

B

```
  1 MVCWQDLEES LRMKLSLTKV VNGCRLGKIK NLGKTGDHTM DIPGCLLYTK
 51 TGSAPHLTHH TLHNIHGVPA MAQLTLSSLA EHHEVLTEYK EGVGKFIGMP
101 ESLLYCSLHD PVSPCPAGYV TNKSVSVWSV AGRVEMTVSK FMAIQKALQP
151 DWFQCLSDGE VSCKEATSIK RVRKSVDRSL LFLDNCLRLQ EESEVLQKSV
201 IIGVIEGGDV MEERLRSARE TAKRPVGGFL LDGFQGNPTT LEARLRLLSS
251 VTAELPEDKP RLISGVSRPD EVLECIERGV DLFESFFPYQ VTERGCALTF
301 SFDYQPNPEE TLLQQNGTQE EIKCMDQIKK IETTGCNQEI TSFEINLKEK
351 KYQEDFNPLV RGCSCYCCKN HTRAYIHHLL VTNELLAGVL LMMHNFEHYF
401 GFFHYIREAL KSDKLAQLKE LIHRQAS
```

Appendix Figure II-2: Mass Spectrometric Analysis of hQTRTD1 via Mascot (A) Sequence of hQTRTD1, where the sequences highlighted in red and bold represent the protein fragments that were determined by MALDI-TOF analysis and analyzed by Mascot. The Protein Score of 85 (Score < 62, p = 0.05) and an Expect value of 2.4E-4 were determined. (B) Sequence of hQTRTD1 - 48 kDa (containing twelve more amino acids on the N-terminus), where the sequences highlighted in red and bold are the same as described above. The Protein Score and Expect value are 84 and 3.5E-4, respectively. There has yet to be any reports supporting this 48 kDa hQTRTD1 as an expressed or functional protein. Since proteins A and B are identical, with the exception of the appending amino acids on the N-terminus of B, it is possible that protein B is an artifact found in the databases, where another start codon coincidentally exists at the upstream gene sequence of hQTRTD1.

A

```
  1 MAGAATQASL ESAPRIMRLV AECSRSRARA GELWLPHGTV ATPVFMPVGT
 51 QATMKGITTE QLDALGCRIC LGNTYHLGLR PGPELIQKAN GLHGFMNWPH
101 NLLTDSGGFQ MVSLVSLSEV TEEGVRFRSP YDGNETLLSP EKSVQIQNAL
151 GSDIIMQLDD VVSSTVTGPR VEEAMYRSIR WLDRCIAAHQ RPDKQNLFAI
201 IQGGLDADLR ATCLEEMTKR DVPGFAIGGL SGGESKSQFW RMVALSTSRL
251 PKDKPRYLMG VGYATDLVVC VALGCDMFDC VFPTRTARFG SALVPTGNLQ
301 LRKKVFEKDF GPIDPECTCP TCQKHSRAFL HALLHSDNTA ALHHLTVHNI
351 AYQLQLMSAV RTSIVEKRFP DFVRDFMGAM YGDPTLCPTW ATDALASVGI
401 TLG
```

B

```
  1 MKLSLTKVVN GCRLGKIKNL GKTGDHTMDI PGCLLYTKTG SAPHLTHHTL
 51 HNIHGVPAMA QLTLSSLAEH HEVLTEYKEG VGKFIGMPES LLYCSLHDPV
101 SPCPAGYVTN KSVSVWSVAG RVEMTVSKFM AIQKALQPDW FQCLSDGEVS
151 CKEATSIKRV RKSVDRSLLF LDNCLRLQEE SEVLQKSVII GVIEGGDVME
201 ERLRSARETA KRPVGGFLLD GFQGNPTTLE ARLRLLSSVT AELPEDKPRL
251 ISGVSRPDEV LECIERGVDL FESFFPYQVT ERGCALTFSF DYQPNPEETL
301 LQQNGTQEEI KCMDQIKKIE TTGCNQEITS FEINLKEKKY QEDFNPLVRG
351 CSCYCCKNHT RAYIHHLLVT NELLAGVLLM MHNFEHYFGF FHYIREALKS
401 DKLAQLKELI HRQAS
```

Appendix Figure II-3: Mass spectrometric analysis of cross-linked ht-hQTRT1 •hQTRTD1 via Mascot (A) Sequence of hQTRT1, where the sequences highlighted in red and bold represent the protein fragments that were determined by MALDI-TOF analysis and analyzed by Mascot. The Protein Score of 68 (Score < 62, p = 0.05) and an Expect value of 1.3E-2 were determined. (B) Sequence of hQTRTD1, where the sequences highlighted in red and bold are the same as above. The Protein Score and Expect value are 95 and 2.6E-5, respectively.

CHAPTER III

HETEROCYCLIC SUBSTRATE SPECIFICITY OF THE HUMAN AND *ESCHERICHIA COLI* tRNA-GUANINE TRANSGLYCOSYLASES

Abstract

In this study, tritium-labeled queuine and $preQ_1$ (accessed via the previously reported, efficient synthetic route for queuine, Brooks, et al. (2010) *Tetrahedron Letters*, **51**, 4163-4165) were used to investigate the heterocyclic substrate recognition of the human and *E. coli* tRNA-guanine transglycosylases. To the best of our knowledge, this is the first report that reveals the kinetics of the eukaryal TGT with respect to queuine and $preQ_1$ via direct incorporation assays. Our results show that the human TGT preferentially recognizes its natural heterocyclic substrate, queuine, with a sub-micromolar K_M while a k_{cat}/K_M approximately 500-fold greater than that for $preQ_1$ was observed. Along with the previous observation that the incorporation of queuine or $preQ_1$ is irreversible, this preferential heterocyclic substrate recognition demonstrates that the eukaryal TGT discriminates against $preQ_1$ to prevent the formation of the incompletely modified tRNA ($preQ_1$-tRNA). Additionally, the substantially lower k_{cat}/K_M for

preQ$_1$ compared to that for guanine led us to further investigate the role of a cysteine residue in the eubacterial TGT active site. The kinetic data are consistent with the crystallographic evidence that this cysteine residue appears to form a hydrophobic interaction with the side chain of preQ$_1$. Furthermore, our success in preparation of the human TGT and radiolabeled queuine/preQ$_1$ has provided a more rigorous approach to examine the heterocyclic substrate specificity of the eukaryal TGT.

Introduction

The tRNA-modifying enzyme TGT is found to be utilized across all three kingdoms of life, eukarya, eubacteria and archaea, with differing heterocyclic substrate and tRNA recognition (1). In eukarya and eubacteria, the corresponding enzyme incorporates queuine or preQ$_1$ (7-aminomethyl-7-deazaguanine), respectively, into the anticodon wobble position (position 34) of tRNAs (2,3), while the archaeal TGT places another 7-deazaguanine analogue, preQ$_0$ (7-cyano-7-deazaguanine), into the position 15 (D loop) of tRNAs (4). In all cases, the heterocyclic substrate is exchanged for a guanine at the third position of an RNA hairpin loop.

Although the crystal structure of the eukaryal TGT has yet to be solved, the determination of the *Zymomonas mobilis* TGT structure along with sequence homology analysis have provided insight into the major structural characteristics of all TGTs, including a $(\beta/\alpha)_8$ TIM barrel and a zinc-binding motif (5). A follow-up

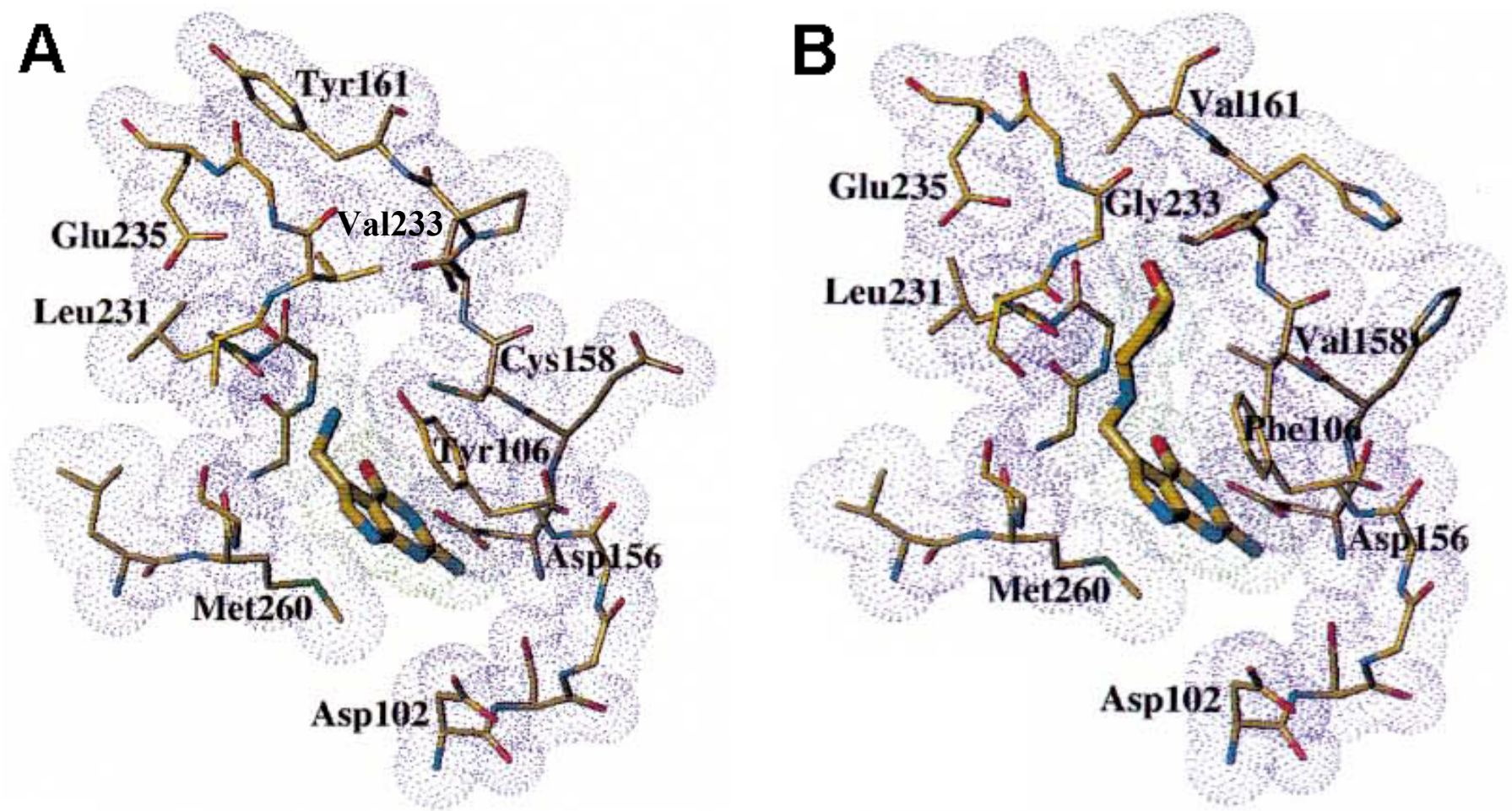

Figure III-1: (A) $PreQ_1$-Bound *Z. mobilis* TGT Active Site (Crystal Structure) and (B) Predicted Queuine-Bound *C. elegans* QTRT1 Active Site (Homology Model). The depictions are adopted from Romier *et al*., (1997) *FEBS Letters* 416, 93-98. Amino acids are labeled based on *Z. mobilis* TGT numberings. The residue 158 corresponds to residue 145 in *E. coli* and 161 in human, respectively. The residue 233 corresponds to residue 217 in *E. coli* and 232 in human.

study reports a comparison of the active sites of eubacterial and eukaryal TGTs based on the structure of *Z. mobilis* TGT and a homology model of the *C. elegans* enzyme (6) (Figure III-1). Interestingly, only a few differences in amino acid composition were observed in the active sites of those two enzymes. For instance, valine 233 (corresponding to Val217 in *E. coli*), which is replaced by a glycine in the eukaryal QTRT1 (corresponding to Gly232 in human), is thought to form the ceiling of the heterocyclic binding pocket and sterically prevent the enzyme from accommodating queuine, due to the larger cyclopentenediol side chain that $preQ_1$ lacks. However, since it has not been possible to obtain radiolabeled $preQ_1$ or queuine, previous studies have been generally performed via a "wash out" assay to probe the heterocyclic substrate specificity of the eukaryal enzyme. Radiolabeled *G-tRNA was used as a substrate for the enzyme, and the incorporation of non-radiolabeled $preQ_1$ or queuine was then measured by monitoring the loss of radioactivity (*G released) during the base replacement to determine the production of $preQ_1$- or queuine-tRNA. One of the major drawbacks of this approach is that the wash out assay monitors small changes in a large number (loss of radioactivity), which often results in significant experimental errors.

In addition to $preQ_1$ and queuine, a variety of guanine/$preQ_1$/queuine structural analogues were also previously utilized to study the substrate specificity of the eukaryal TGT (3,7). Of all the derivatives, pteridines are particularly interesting as they are not only involved in several enzymatic reactions (serve as cofactors), but also serve as precursors to other biological

molecules (such as folates). Although not substrates for TGT, pteridines have been shown to reduce/block formation of Q-tRNA *in vivo* and this seems to be due to the inhibition of TGT, based on *in vitro* studies with guanine. (7,8). In addition, in murine erythroleukemia cells, the cellular tetrahydrobiopterin level exhibits a positive correlation with the level of unmodified G-tRNA (9). Early studies have suggested that the queuosine biosynthesis pathway utilizes the same precursor (GTP) as the tetrahydrobiopterin (BH_4) and tetrahydrofolate (THF) biosynthesis pathways (10). More recently, it has been shown that those biosynthesis pathways appear to share the same first enzymatic step, which is mediated by GTP cyclohydrolase I (11,12). All of these observations suggest a physiological link between cellular pteridines and queuine modification *in vivo*.

Reported herein, we were able to directly investigate and obtain a greater understanding of the heterocyclic substrate specificity of the eukaryal TGT due to the success in preparing the recombinant human TGT and synthesizing radiolabeled $preQ_1$ and queuine. Also, inhibition studies were conducted to determine the inhibition constant (K_i) of biopterin with the human TGT, providing a pilot approach to gain further insight into how pteridines may regulate queuine modification.

Materials and Methods

Reagents

Unless otherwise specified, all reagents were ordered from Sigma-Aldrich. DNA oligonucleotides, agarose, dithiothreitol (DTT), isopropyl β-D-thiogalactopyranoside (IPTG) and DNA ladders were ordered from Invitrogen. All restriction enzymes and Vent® DNA polymerase were ordered from New England Biolabs. The ribonucleic acid triphosphates (NTPs), pyrophosphatase and kanamycin sulfate were ordered from Roche Applied Sciences. The deoxyribonucleic acid triphosphates (dNTPs) were ordered from Promega. Scriptguard™ RNase Inhibitor was ordered from Epicentre. Epicurian coli® XL2-Blue ultracompetent cells were ordered from Stratagene. TG2 cells, K12 (DE3, Δ*tgt*) cells and K12 (DE3, Δ*tgt*)-pRIPL cells were from laboratory stocks. His•Bind resin and lysonase bioprocessing reagent were also purchased from Novagen. The QIAPrep® Spin Miniprep and Maxiprep Kits were ordered from Qiagen. Precast PhastGels and SDS buffer strips were from VWR. Bradford reagent was from Bio-Rad. Whatman GF/C Glass Microfibre Filters, Amicon Ultra Centrifugal Filter Devices, carbenicillin and all bacterial media components were ordered from Fisher. $preQ_1$ and queuine precursors were synthesized by Allen Brooks (13) in the Showalter lab (Department of Medicinal Chemistry, University of Michigan), and the tritiations of [^{3}H]-$preQ_1$ (7 or 4.9 Ci/mmol) and [^{3}H]-queuine (7.3 Ci/mmol) were performed by Moravek Biochemicals (Figure III-2, the synthetic schemes of $preQ_1$ and queuine can be seen in Appendix Figure III-1). Biopterin was purchased from Schircks Laboratories. T7 RNA polymerase

was isolated from *E. coli* BL21 (DE3) pLysS cells harboring the plasmid pRC9 via minor modifications of the procedure described in the literature (14). The human $tRNA^{Tyr}$ was generated as described in Chapter II (this dissertation).

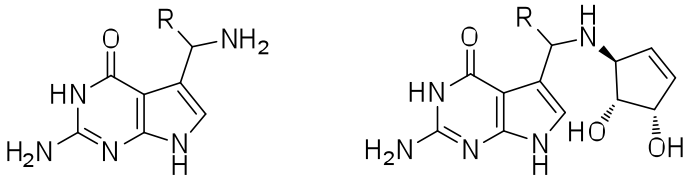

1: R = ^{1}H ($PreQ_1$)
2: R = ^{3}H

3: R = ^{1}H (Queuine)
4: R = ^{3}H

Figure III-2: Structures of [^{1}H]- and [^{3}H]-Labeled $PreQ_1$ and Queuine.

Expression and Purification of Human TGT

The plasmids of the polyhistidine-tagged wild-type human TGT and mutants were expressed in *E. coli* K12 (DE3, Δ*tgt*)-pRIPL competent cells and purified via Ni^{+2}-NTA affinity chromatography followed by size exclusion chromatography, essentially as described in Chapter II (this dissertation). The final concentrations of each of the TGT samples were determined with the Bio-Rad Protein Assay Kit based on the Bradford assay using BSA standards. The purified proteins were stored in liquid N_2 until needed.

Construction of E. coli TGT Cys145 Mutants

The Cys145Ala, Cys145Ser and Cys145Asp plasmids were previously generated via either a combined polymerase chain reaction-ligase chain reaction (15) or site-directed mutagenesis using pTGT5 as a template (16) by one of the lab former members, Dr. DeeAnne M. Goodenough-Lashua. To generate the plasmids of polyhistidine-tagged *E. coli* mutants, the *tgt* mutant genes were subcloned into vector pET-28a^{Kan} following general laboratory protocols. Briefly, the desired genes and pET-28a^{Kan} were digested with Nde I and Hind III (20 U each, 20-µL reaction) for 2 h at 37°C. Subsequently, the resulting fragments were gel-purified from Seaplaque agarose with Gelase™ according to the vendor's protocol, followed by overnight incubation with T4 DNA ligase (2 U) at 16-17°C for ligation. The ligated sample (10 µL) was transformed into 100 µL of Epicurian coli® XL2-Blue ultracompetent cells according to the Stratagene protocol. Cells were grown overnight at 37°C on L-Amp plates (50 µg/mL kanamycin). Individual colonies were isolated, and 3 mL 2xTY (16 g bactotryptone, 10 g yeast extract, 5 g NaCl/L of water) with 50 µg/mL kanamycin liquid cultures were inoculated and grown overnight at 37°C with shaking. The plasmids were isolated via miniprep, and the tRNA^{Tyr} gene sequence was confirmed with DNA sequencing (University of Michigan DNA Sequencing Core Facilities).

Expression and Purification of E. coli TGT and Cys145 Mutants

The wild-type polyhistidine-tagged *E. coli* TGT was prepared as described previously (17), and the polyhistidine-tagged *E. coli* TGT mutants were

expressed following an auto-induction procedure (18). In brief, plasmids containing polyhistidine-tagged *E. coli* TGT mutant genes were transformed into either *E. coli* K12 (DE3, Δ*tgt*) (for Cys145Ala and Cys145Ser) or BL21 (DE3) (for Cys145Asp) cells for expression. Cells were grown in 0.5 L of Zyp-5052 (10 g bactotryptone, 5 g yeast extract, 3.3 g $(NH_4)_2SO_4$, 6.8 g KH_2PO_4, 7.1 g Na_2HPO_4, 5 g glycerol, 0.5 g glucose, 2 g α-lactose, 0.12 g $MgSO_4$/L of water) with 50 μg/mL kanamycin liquid cultures containing 100 μM $ZnSO_4$ at 37°C overnight. The cells were then harvested by centrifugation (6,000 x g, 15 min, 4°C). The cell pellets from each 500 mL culture were re-suspended in 10 mL of Ni^{2+}-NTA bind buffer (300 mM NaCl, 50 mM NaH_2PO_4, 10 mM imidazole, pH 8.0) containing 100 μM PMSF and 10 μL lysonase. The cell suspensions were incubated at room temperature for 20 minutes and subjected to sonication (7 x 15 sec pulses) on ice. The cellular debris was pelleted by centrifugation (20,000 x g, 30 min, 4°C). All further purification steps were performed at 4°C. The supernatants were filtered through 0.22 μm syringe filters (Millipore) and incubated with 2 mL His•Bind resin slurry with gentle shaking for 1 h. Each supernatant-resin mixture was then applied to a column. Following loading, the columns were washed twice with 7 mL of Ni^{2+}-NTA wash buffer (300 mM NaCl, 50 mM NaH_2PO_4, 20 mM imidazole, pH 8.0). The amino-terminal polyhistidine-tagged proteins were eluted from each column with 7 mL of elute buffer (300 mM NaCl, 50 mM NaH_2PO_4, 250 mM imidazole, pH 8.0) and collected in 1 mL fractions. The eluates were examined by SDS-PAGE and fractions containing our proteins of interest were combined and concentrated. Subsequently, the

proteins were exchanged into the TGT storage buffer, 25 mM HEPES (pH 7.3), 2 mM DTT, 100 mM NaCl and 20% (w/v) glycerol, using Amicon Ultra Centrifugal Filter Devices (10,000 MWCO) following vendor protocols (the glycerol content was brought to 50% (w/v) immediately after buffer exchange). The final concentration of each protein was determined as described above. The proteins were stored in liquid N_2 and utilized to perform $preQ_1$ exchange assays.

Preparation and Purification of E. coli tRNA^{Tyr}

The *E. coli* $tRNA^{Tyr}$ was generated by run-off *in vitro* transcription, essentially the same fashion as human $tRNA^{Tyr}$, described in Chapter II (this dissertation). Purification of the tRNA transcript was also achieved by size exclusion chromatography using two Superose® 12 HR 10/30 columns (GE Healthcare) connected in tandem. The running buffer, which is also used for tRNA storage, contains 10 mM HEPES, pH 7.3 and 1 mM $MgCl_2$. However, due to the tendency of *E. coli tRNA^{Tyr}* transcript to dimerize during the preparation or/and purification, the purified tRNA was subjected to a denaturation-renaturation process that promotes monomerization (19). In brief, the tRNA was resuspended in 10 mM HEPES (pH 7.3) to a concentration less than 20 μM. Subsequently, the tRNA samples were slowly heated to 70°C and maintained at that temperature for 30 minutes. After the addition of $MgCl_2$ to a final concentration of 1 mM, the tRNA samples were immediately cooled on ice for 3 hours to allow renaturation. The tRNA was ethanol precipitated at −20°C overnight and then pelleted by centrifugation (13,000 rpm, 15 min). Finally, the

E. coli $tRNA^{Tyr}$ was resuspended in an appropriate volume of tRNA storage buffer to generate a stock concentration of 200 μM. The exact concentration of the tRNA was determined from the extinction coefficient at 260 nm (ε_{260} = 0.703 A_{260}•cm^{-1}•μM^{-1}, corrected for hypochromicity) (20) using a Cary UV-VisibleSpectrophotometer (Varian).

Activity Screen and Kinetic Analyses

Heterocyclic base exchange assays were conducted by monitoring the incorporation of radiolabeled substrates, [^{3}H]-$preQ_1$ and [^{3}H]-queuine into either the human or *E. coli* $tRNA^{Tyr}$ using various TGT samples. In general, kinetic assays were set up under the following conditions: $tRNA^{Tyr}$ (saturating concentrations depending on the K_M for each individual enzyme), individual radiolabeled base (various concentrations), TGT (25, 50 or 100 nM depending on the concentration of heterocyclic base used), and HEPES reaction buffer (100 mM HEPES, pH 7.3; 20 mM $MgCl_2$; 5 mM DTT) to a final volume of 400 μL. The studies were generally performed in triplicate. All samples were incubated at 37°C for purposes of equilibration before initiating the reaction with the addition of TGT. Aliquots were removed at specified time points throughout the 10- or 20-min time course and immediately quenched in 2.5 mL of 5% trichloroacetic acid (TCA) for 1 h before collection on glass-fiber filters. Each filter was washed with three volumes of 5% TCA and a final wash of ethanol to dry the filter. The samples were analyzed in a scintillation counter (Beckman) for radioactive decay, where counts were reported in DPM and later converted to picomoles

[^{3}H]-preQ$_1$ or [^{3}H]-queuine by following the general conversion between DPM and specific activity (e.g., pmol = DPM × 0.000617, for the [^{3}H]-queuine stock with a specific activity of 730 mCi/mmol). To obtain steady-state kinetic parameters, initial velocities of guanine/preQ$_1$/queuine incorporation were determined by converting the slopes of these plots (pmol/min) to units of 1/second (s^{-1}), taking into account the concentration of the enzyme and aliquot size. The individual data points from each trial were averaged, and the standard deviation was determined for each concentration of either tRNA^{Tyr} or heterocyclic base. The average data points (with error bars representing their standard deviations) were plotted. However, all of the individual data points were fit via non-linear regression to the Michaelis–Menten equation using KaleidaGraph (Abelbeck Software).

Biopterin Inhibition of the Human TGT

The biopterin stock solution (10 mM) was dissolved in water with the addition of 1% (v/v) 14.8 N ammonium hydroxide. Due to the light sensitivity of biopterin, the diluted biopterin solutions were prepared without direct light exposure and protected from light while stored. The queuine exchange assays were performed by varying the concentrations of queuine (1, 2.5 and 5 μM) and biopterin (10-500 μM), while holding tRNA concentrations at 10 μM (saturating condition). All reaction mixtures were incubated at 37°C for purposes of equilibration before initiating the reaction with the addition of the human TGT

(100 nM), and the studies were performed in duplicate. The initial velocities of queuine incorporation were determined by converting the slopes of these plots (pmol/min) to units of sec^{-1}, taking into account the concentration of the enzyme and aliquot size. The data were then analyzed graphically by plotting either (A) $1/V_{ini}$ vs. [Inhibitor] or (B) [queuine]/V_{ini} vs. [Inhibitor] to obtain Dixon plot or Cornish-Bowden plot. The average data points (with error bars representing their standard deviations) were plotted. However, all of the individual data points were fit via linear regression using Kaleidagraph (Abelbeck Software). To obtain the K_i for the inhibitor, the following equation was used: slope (obtained from the Dixon plot) = K_M / (k_{cat})(K_i)[S], where K_M and k_{cat} with respect to queuine have been determined previously.

Results

Kinetics Analysis of Human TGT with respect to Queuine and $PreQ_1$

To investigate the heterocyclic substrate specificity of the human TGT (Figure III-3, lane 2), the transglycosylase activity was measured via monitoring [^{3}H]-queuine and [^{3}H]-$preQ_1$ incorporation into human $tRNA^{Tyr}$. The concentration of tRNA was fixed at saturation (10 μM), as the K_M value was previously determined to be 0.34 ± 0.04 μM (21). The kinetic parameters were then determined by non-linear fits to the Michaelis-Menten equation (Figure III-4, A and B, Table III-1). The results show that the k_{cat} values for both substrates are essentially identical (approximately 8 x 10^{-3} s^{-1}); however, the human TGT

incorporates its natural heterocyclic substrate, queuine, with a sub-micromolar K_M (0.26 ± 0.03 μM), while a 500-fold larger K_M for preQ$_1$ (132.33 ± 27.6 μM) was observed. Due to the indistinguishable k_{cat} values, the difference in K_M also leads to a significantly higher catalytic efficiency (as defined by k_{cat}/K_M) toward queuine, clearly indicating the preferential recognition of queuine by the human TGT.

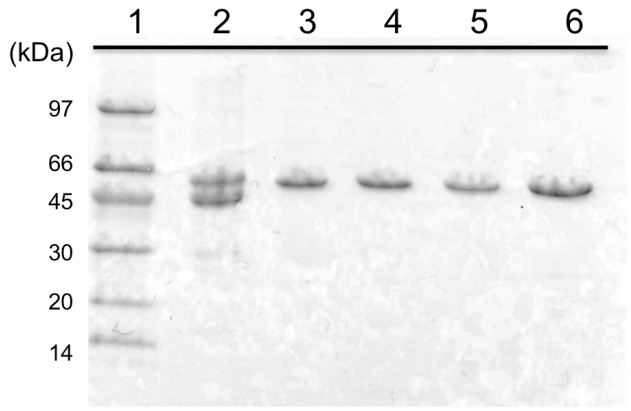

Figure III-3: SDS-PAGE of Various Human and *E. coli* TGT Samples. 1. Low molecular weight standards (GE Healthcare), 2. Wild-type human TGT, 3. Wild-type *E. coli* TGT, 4. *E. coli* TGT Cys145Ala mutant, 5. *E. coli* TGT Cys145Ser mutant, 6. *E. coli* TGT Cys145Asp mutant. Note: These proteins are all polyhistidine-tagged.

Kinetics Analysis of E. coli TGT with respect to PreQ$_1$ and Queuine

Similarly, the transglycosylase activity of the *E. coli* TGT (Figure III-3, lane 3) was measured via monitoring [^{3}H]-preQ$_1$ and [^{3}H]-queuine incorporation into *E. coli* tRNA^{Tyr} (fixed at 10 μM, K_M = 0.19 μM). The k_{cat} value for preQ$_1$ was determined to be 9.57 x 10^{-3} s^{-1}, slightly faster than that of the human enzyme

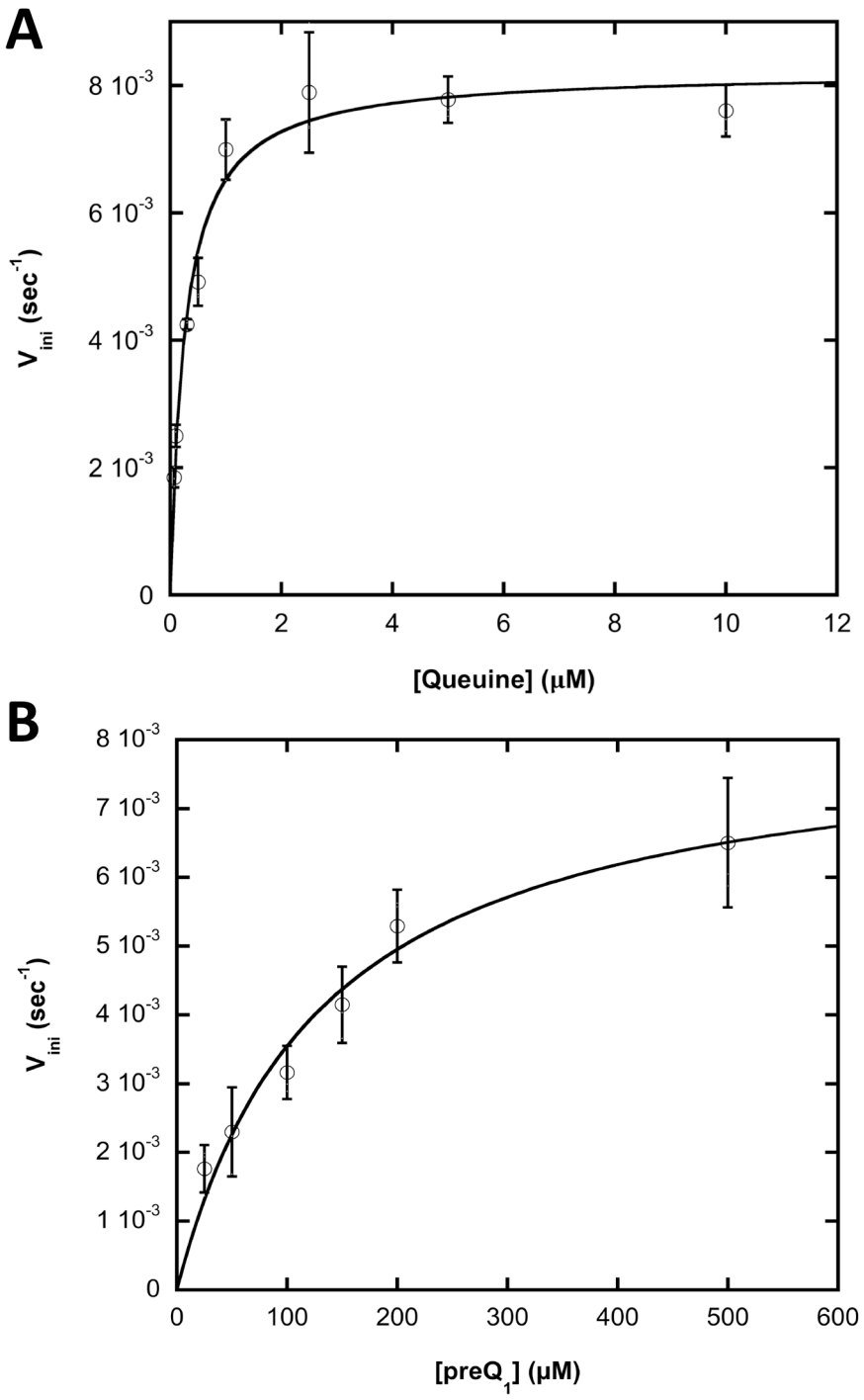

Figure III-4: Michaelis-Menten Fits of (A) Queuine and (B) $PreQ_1$ with Human TGT. Curves were obtained from the average of three independent determinations of initial velocity data. Error bars were generated from the standard deviation within each point.

(Figure III-5, Table III-1). In addition, the *E. coli* enzyme exhibits a low K_M (approximately 50 nM) for $preQ_1$, suggesting a high affinity in terms of substrate binding. Consistent with the previous report (22), the *E. coli* TGT does not seem to incorporate queuine as a substrate as no detectable transglycosylase activity was observed at queuine concentrations up to 50 μM (data not shown). A low amount of radioactivity (not linear with time) was captured on the filters at higher concentrations of queuine. However, control experiments conducted with no substrate RNA in the reaction mixtures confirm that the background radioactivity

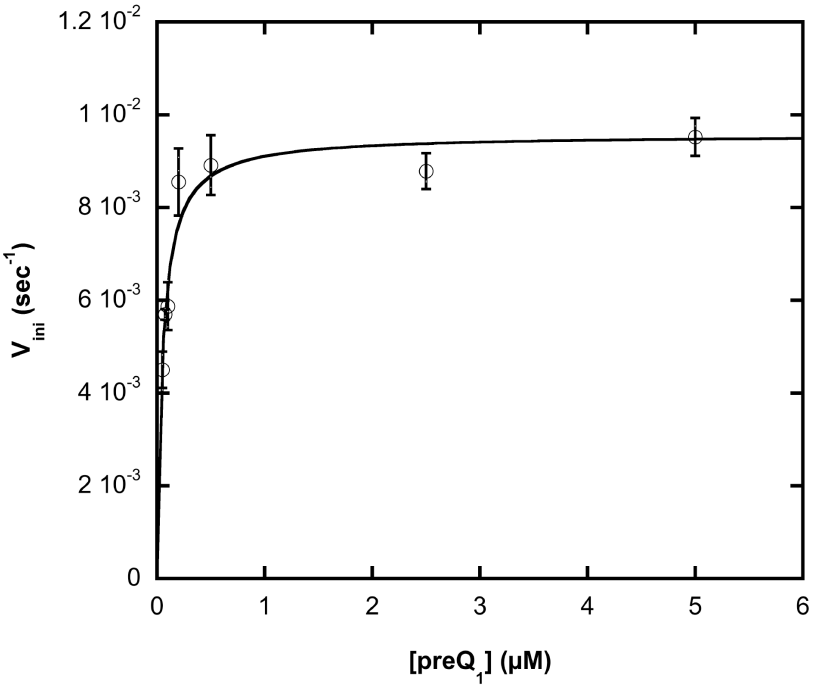

Figure III-5: Michaelis-Menten Fit of $PreQ_1$ with Wild-type *E. coli* TGT. Curves were obtained from the average of three independent determinations of initial velocity data. Error bars were generated from the standard deviation within each point.

most likely resulted from either non-specific binding of queuine to the filters (at the higher concentrations) or queuine approaching its limit of solubility, precipitating out of solution and being captured on the filters. Nevertheless, our kinetic data are consistent with the computational prediction that the side chain of queuine is most likely too sterically bulky to fit in the substrate-binding pocket of the *E. coli* TGT.

Table III-1: Kinetic Parameters for Human TGT and *E. coli* TGT with respect to Queuine and $PreQ_1$

	k_{cat} [a] (10^{-3}•s^{-1})	K_M [a] (μM)	k_{cat}/K_M [a, b] (10^{-3}•s^{-1}•μM^{-1})
Human TGT			
Guanine	5.86 (±0.10)	0.41 (±0.03)	14.2 (±0.9)
$PreQ_1$	8.23 (±0.71)	132 (±28)	0.062 (±0.014)
Queuine	8.22 (±0.20)	0.26 (±0.03)	31.6 (±3.4)
***E. coli* TGT**			
Guanine	6.29 (±0.12)[c]	0.35 (±0.03)[c]	18.0 (±1.6)[c]
$PreQ_1$	9.57 (±0.24)	0.05 (±0.01)	191 (±38.6)
Queuine	N.D.A[d]	N.D.A[d]	N.D.A[d]

[a]Standard errors are in parentheses.

[b]Derived from fit to the following equation: $v_i = \dfrac{\frac{k_{cat}}{K_M}[S]}{1+\frac{[S]}{K_M}}$

[c]From Goodenough-Lashua, D.M. (2002) Ph.D. Dissertation

[d]No detectable activity

Kinetics Analysis of E. coli TGT Cys145 mutants

The drastic decrease in recognition of $preQ_1$ versus queuine for the human TGT is somewhat intriguing as such reduction is not seen in the case of guanine. Other than the slight alteration from an N^7 to a C^7 on their pyrimidine-imidazole rings (i.e., $preQ_1$ and queuine are both 7-deazaguanine derivates), the major difference among these compounds is the size of their side chains. As a result, it is apparent that the aminomethyl side chain of $preQ_1$ must have a negative impact that is less favorable for binding to the human TGT. Previously, the pK_a of the aminomethyl side chain of $preQ_1$ was determined to be 9.8 in solution (23), which suggests that the molecule is protonated at physiological pH (also the pH that our assays were conducted). In addition, at the same pH, queuine appears to be neutral (at least partially) as the secondary amine on the side chain has a pK_a of 7.82 (predicted by MarvinSketch 3.5.1, ChemAxon®, kindly performed by Dr. Paul Kirchhoff, Appendix Figure III-2). Therefore, it is plausible to postulate that there may be an active site residue that is negatively charged during catalysis, allowing the enzyme to form an electrostatic interaction with $preQ_1$. Upon taking a closer look at the enzyme active site (Figure III-6), we hypothesized that the side chain of the *E. coli* TGT Cys145 might exist as a thiolate group, interacting with the protonated $preQ_1$ electrostatically.

To test our hypothesis, three mutants, Cys145Ala, Cys145Ser, Cys145Asp (Figure III-3, lanes 4-6) were generated to probe the heterocyclic substrate recognition using [^{3}H]-$preQ_1$. The kinetic parameters for $preQ_1$ exchange were determined while the concentration of tRNA was maintained at

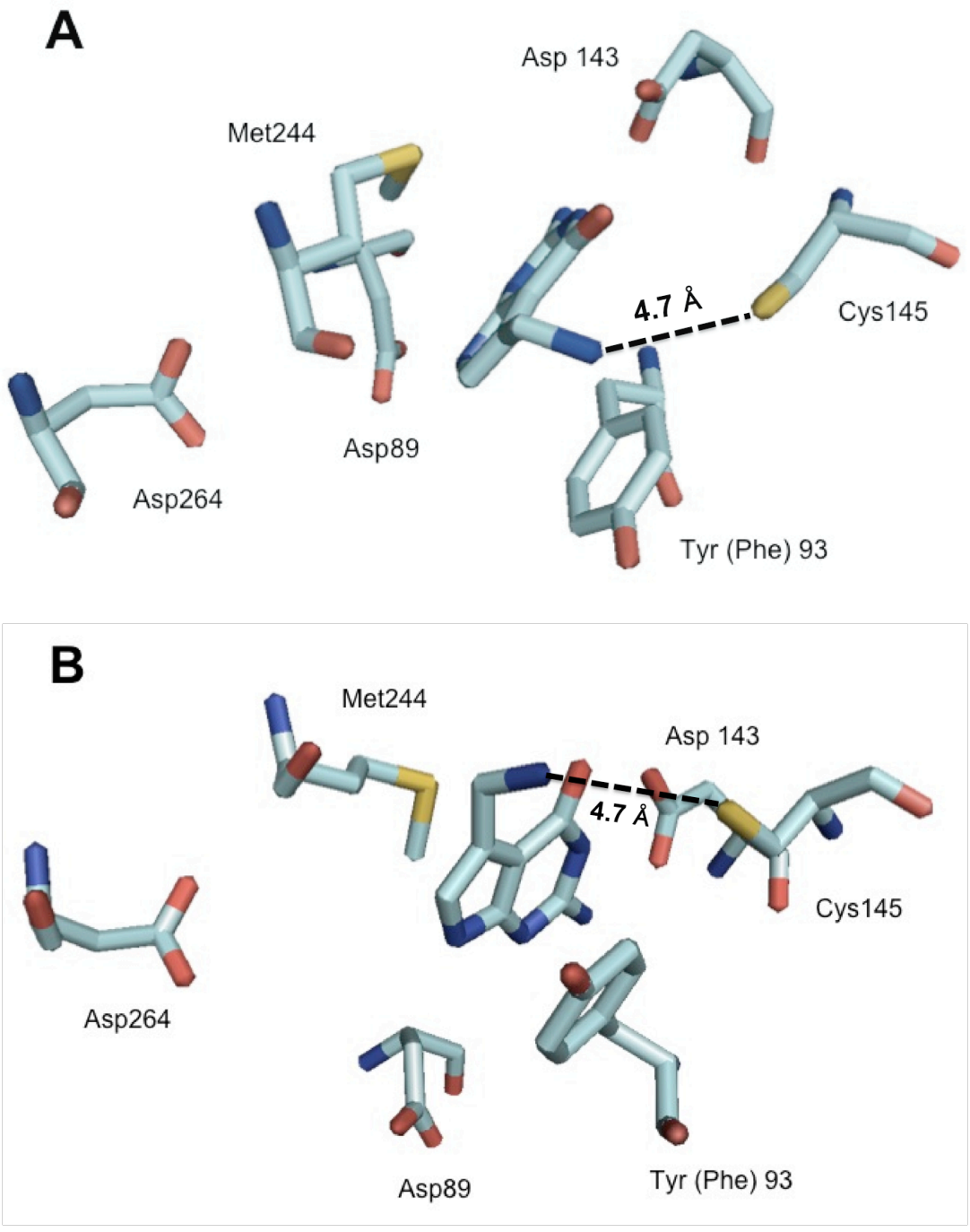

Figure III-6: Active Site of the $PreQ_1$-Bound *Z. mobilis* TGT (PDB accession code 1P0E). The images A and B (view from two different angles) were generated by PyMOL (The PyMOL Molecular Graphics System, Version 1.3, Schrödinger, LLC). To be consistent with the text, the amino acid residues were labeled based on the *E. coli* numbering. Atoms oxygen, nitrogen and sulfur are highlighted in red, blue and yellow, respectively. Note: Tyr 93 in the *Z. mobilis* TGT corresponds to Phe 93 in the *E. coli* enzyme.

saturating concentration (depending on the tRNA K_M for each individual mutant). It should be noted that the kinetic parameters for both the guanine and tRNA substrates with all of the three mutants were previously determined by Dr. DeeAnne M. Goodenough-Lashua (Tables III-2 & III-3). Shown in Figure III-7 and Table III-4, an increase in k_{cat} was observed for both the Cys145Ala and Cys145Ser mutants. The increases compared to the wild-type were 7.8- and 2.5-fold for Cys145Ala and Cys145Ser, respectively. The enzymatic function of Cys145Asp with respect to $preQ_1$ appears to be abrogated since no activity was found at $preQ_1$ concentrations up to 100 μM.

Table III-2: Guanine Kinetics for Wild-type and Cys145 Mutant *E. coli* TGTs.

Enzyme	k_{cat}[a,b] (10^{-3}•s^{-1})	K_M[a,b] (μM)	k_{cat}/K_M[a,b] (10^{-3}•s^{-1}•μM^{-1})
wild-type	6.29 (±0.12)	0.35 (±0.03)	18.0 (±1.6)
Cys145Ala	86.8 (±2.1)	2.34 (±0.23)	37.1 (±3.9)
Cys145Ser	28.0 (±0.7)	1.94 (±0.17)	14.4 (±1.3)
Cys145Asp	5.44 (±0.23)	68.1 (±7.8)	0.080 (±0.01)

[a]Standard errors are shown in parentheses. [b]Kinetic parameters were calculated from the average of three replicate determinations of initial velocity data. Note: Data adapted from Goodenough-Lashua, D.M. (2002) Ph.D. Dissertation, University of Michigan, Ann Arbor.

Table III-3: tRNA Kinetics for Wild-type and Cys145 Mutant *E. coli* TGTs.

Enzyme	k_{cat}[a,b] (10^{-3}•s^{-1})	K_M[a,b] (μM)	k_{cat}/K_M[a,b] (10^{-3}•s^{-1}•μM^{-1})
wild-type	5.19 (±0.29)	0.19 (±0.05)	27.3 (±7.3)
Cys145Ala	76.3 (±3.1)	1.11 (±0.22)	68.7 (±14.0)
Cys145Ser	28.2 (±1.0)	0.49 (±0.09)	58.0 (±10.5)
Cys145Asp	6.34 (±0.41)	3.30 (±0.79)	1.92 (±0.48)

[a]Standard Errors are shown in parentheses. [b]Kinetic parameters were calculated from the average of three replicate determinations of initial velocity data. Note: Data adapted from Goodenough-Lashua, D.M. (2002) Ph.D. Dissertation, University of Michigan, Ann Arbor.

Table III-4: $PreQ_1$ Kinetics for Wild-type and Cys145 Mutant *E. coli* TGTs.

Enzyme	k_{cat}[a,b] (10^{-3}•s^{-1})	K_M[a,b] (μM)	k_{cat}/K_M[a,b] (10^{-3}•s^{-1}•μM^{-1})
wild-type	9.57 (±0.24)	0.05 (±0.01)	191 (±38.6)
Cys145Ala	74.6 (±3.4)	43.4 (±5.0)	1.72 (±0.21)
Cys145Ser	23.7 (±1.0)	123 (±13.9)	0.19 (±0.02)
Cys145Asp	N.D.A.[c]	N.D.A.[c]	N.D.A.[c]

[a]Standard errors are shown in parentheses. [b]Kinetic parameters were calculated from the average of three replicate determinations of initial velocity data. [c]No detectable activity up to 100 μM $preQ_1$.

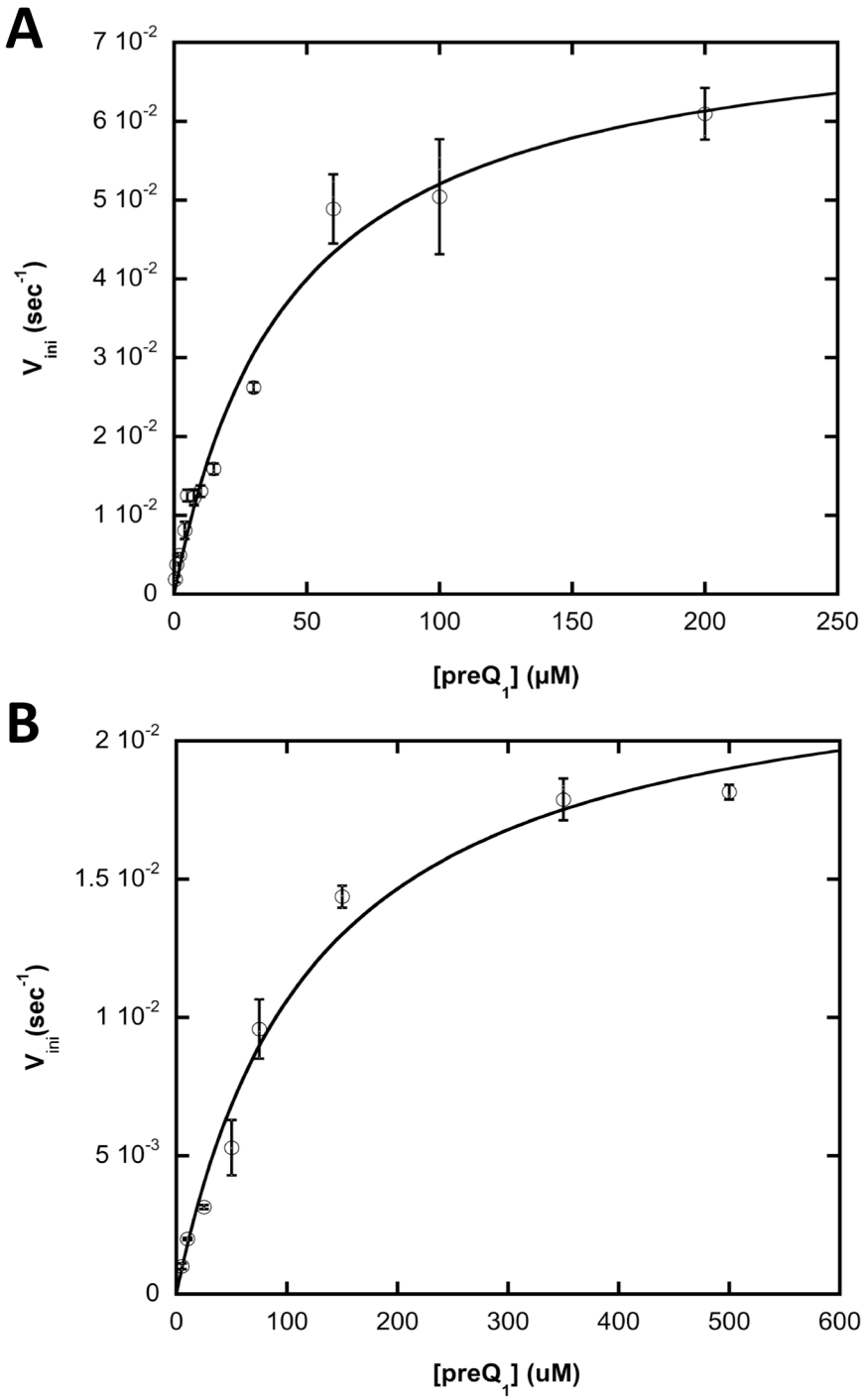

Figure III-7: Michaelis-Menten Fits of $PreQ_1$ with (A) *E. coli* TGT Cys145Ala Mutant and (B) *E. coli* TGT Cys145Ser Mutant. Curves were obtained from the average of three independent determinations of initial velocity data. Error bars were generated from the standard deviation within each point.

Interestingly, the greatest impact on the kinetics comes from the significant increase in K_M for preQ$_1$ with the Cys145Ala and Cys145Ser mutants as the values are approximately 800- and 2400-fold higher than that of the wild-type. Although a catalytic rate (k_{cat}) enhancement with these two mutants was also observed, the dramatic increases in K_M resulted in substantially greater catalytic efficiencies, indicating that these two mutants recognize preQ$_1$ much more poorly than the wild-type enzyme.

Biopterin Inhibition of the Human TGT

To assure the accuracy of our inhibition study, a serial dilution of biopterin samples (0.025-0.2 mM, pH 7.3) was first prepared and the absorbance of each dilution was determined at 354 nm. The extinction coefficient obtained (8.12 $mM^{-1}cm^{-1}$) appears to be very comparable with the reported value in the literature (6.3 $mM^{-1}cm^{-1}$, pH 7.6) (24), indicating the biopterin concentrations used in the assay are reliable. With respect to queuine, biopterin was found to be a competitive inhibitor of the human TGT according to intersecting lines in a Dixon plot (Figure III-8A), and parallel lines in a Cornish Bowden plot (Figure III-8B). Derived from the Dixon plot, the inhibition constant (K_i) of biopterin was determined to be 8.72 ± 0.62 μM, which is within two orders of magnitude of the K_M for queuine (0.26 ± 0.03 μM). This result suggests that biopterin is not a particularly potent inhibitor of the human TGT (25), consistent with the observation reported previously (7).

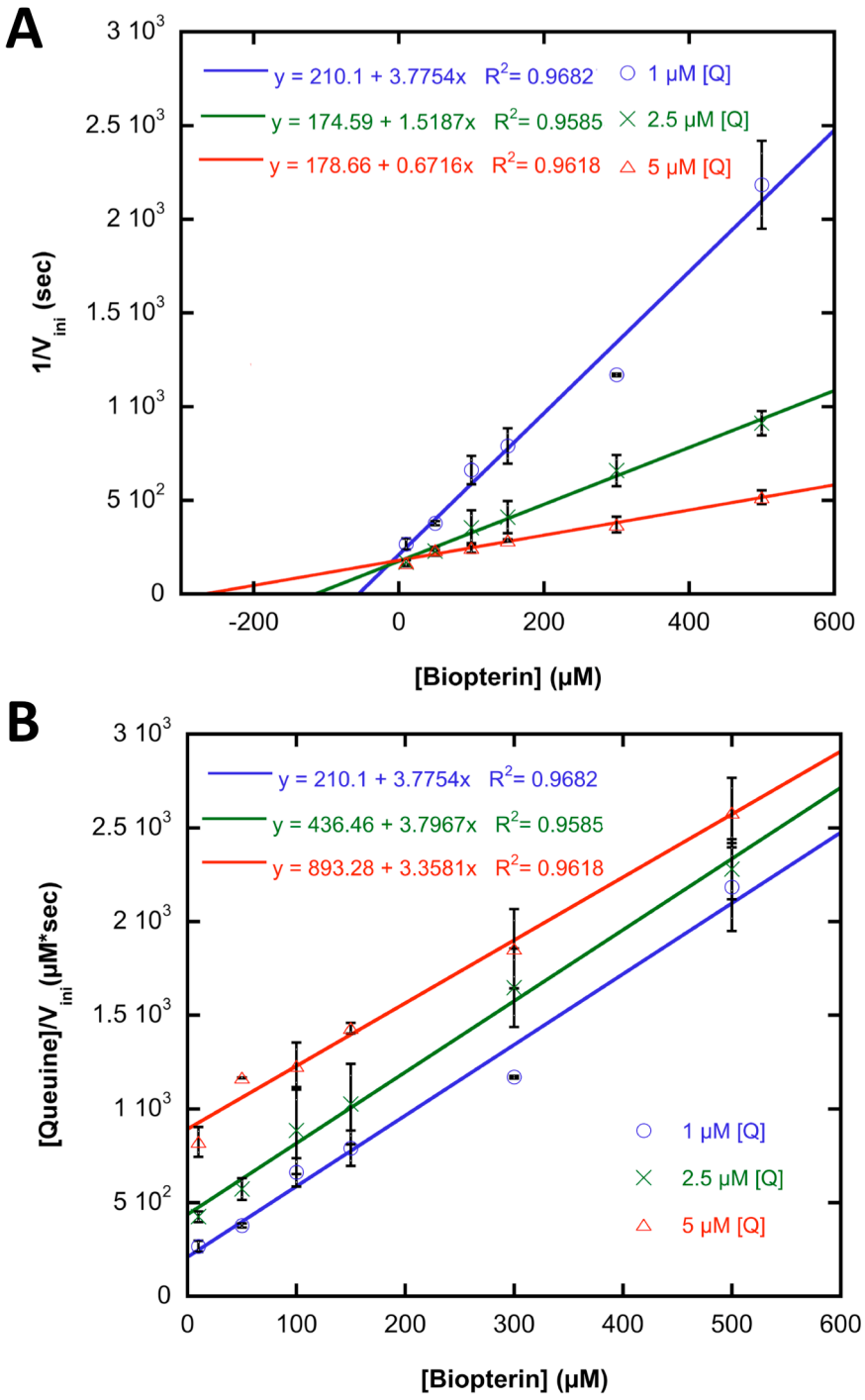

Figure III-8: Inhibition of Queuine Kinetics by Biopterin (A) Dixon and (B) Cornish-Bowden Plots. Curves were obtained from the average of two independent determinations of initial velocity data. Error bars were generated from the standard deviation within each point.

Discussion

Kinetic experiments using synthetic, tritiated queuine and $preQ_1$ were performed to investigate the heterocyclic substrate recognition of the human TGT. It is surprising that both k_{cat} and K_M with respect to queuine are not substantially different from those of guanine ($5.86 \pm 0.10 \times 10^{-3}$ s^{-1} and 0.41 ± 0.03 μM, (21)). Comparison of the catalytic efficiencies (k_{cat}/K_M) revealed that the human TGT appears to utilize queuine only 2-3 times more efficiently than guanine ($31.6 \pm 3.4 \times 10^{-3}$ $s^{-1}\mu M^{-1}$ vs. $14.2 \pm 0.9 \times 10^{-3}$ $s^{-1}\mu M^{-1}$). Given that queuine is the natural substrate for the human TGT and the fact the physiological concentrations are generally estimated to be in the low nM range in various eukaryal tissues (e.g., ca. 3.6 nM in human milk (26)), substantially lower K_M and significantly higher k_{cat}/K_M values would have been expected. However, the fact that queuine incorporation is irreversible (3) whereas guanine insertion simply regenerates the substrate tRNA (i.e., futile enzyme cycling) suggests that the human TGT may not experience significant selection pressure to improve the specificity for queuine over guanine. The slightly improved binding affinity (or catalytic efficiency) toward queuine is likely sufficient for organisms to efficiently generate Q-tRNA. Moreover, since product release is rate-limiting (27) during catalysis, a significant difference in k_{cat} would not be expected if the effect of queuine (e.g., Q-tRNA versus G-tRNA product) on the tRNA off-rate is minimal. Additionally, a recent report shows that the two subunits of the human TGT co-localize into mitochondria (28), suggesting that *in vivo* transglycosylase activity (and hence the differential activity with guanine versus queuine) might be

affected by an association with mitochondria which has yet to be studied.

It should be noted that the kinetic parameters reported here for the human TGT are different (Table III-5) than those previously reported by Shindo-Okada *et al.* (3) in 1980 for the TGT isolated from rat liver and from those reported by Howes & Farkas in 1978 for the TGT from rabbit erythrocytes (29). With all due respect, the methods used by the authors were much less precise in each of those cases and quite different from those reported here, largely due to the state of technology available at that time. For example, the "wash out" assay used by Shindo-Okada *et al*. is much less accurate than the direct incorporation assay conducted herein as mentioned previously. Also, the TGTs they studied are indeed not from human although we doubt the difference in species should lead to such significant variation. In addition, heterogenous tRNA was employed as a substrate by Shindo-Okada *et al*. and only 3 to 4 concentrations of the heterocyclic substrate were used to establish kinetic parameters. Furthermore, those assays employed single time points (2 h), with no assurance that the reaction was linear out to this endpoint. Finally, there is a considerable amount of error introduced by fitting the data to a linear, double reciprocal plot versus the non-linear fit directly to the Michaelis-Menten equation that was used in the present study.

The 500-fold higher k_{cat}/K_M for queuine relative to $preQ_1$ with the human TGT indicates that the enzyme preferentially utilizes queuine over $preQ_1$. The preferential heterocyclic substrate recognition appears to make perfect sense considering the incorporation of $preQ_1$ is irreversible and would not lead to the

generation of Q-tRNA in eukarya. This also indicates that eukarya have a protective mechanism to discriminate against $preQ_1$ and avoid the potential formation of the incompletely modified tRNA ($preQ_1$-tRNA in contrast to Q-tRNA). Additionally, this observation nicely matches the homology modeling results of the eukaryal TGT, as the two hydroxyls on the cyclopentenediol moiety are predicted to be capable of forming hydrogen bonds with the enzyme active site residues (6). If one assumes that changes in K_M correlate well with changes in

Table III-5: Kinetic Parameters for Eukaryal TGTs with Heterocyclic Substrates.

Enzyme	k_{cat}[a,b] (10^{-3}•s^{-1})	K_M[a,b] (μM)	k_{cat}/K_M[a,b] (10^{-3}•s^{-1}•μM^{-1})
Human			
Queuine	8.22 (±0.20)	0.26 (±0.03)	31.6 (±3.4)
$PreQ_1$	8.23 (±0.71)	132 (±28)	0.062 (±0.014)
Guanine[c]	5.86 (±0.10)	0.41 (±0.03)	14.2 (±0.9)
Rat Liver[d]			
Queuine	N.D.[f]	0.29[g]	N.D.
$PreQ_1$	N.D.	2.1[g]	N.D.
Guanine	N.D.	0.83[g]	N.D.
Rabbit Erythrocytes[e]			
Guanine	N.D.	0.15[g]	N.D.

[a]Standard errors are shown in parentheses. [b]Kinetic parameters were calculated from the average of three replicate determinations of initial velocity data. [c]Data from Chen et al. (2010) *RNA*, **16**, 958-968. [d]Data from Shindo-Okada et al. (1980) *Biochemistry*, **19**, 395-400. [e]Data from Howes & Farkas (1978) *Journal of Biological Chemistry*, **253**, 9082-9087. [f]Not Determined. [g]No errors reported.

K_D, a 500-fold increase in K_M in this case would represent close to 4 kcal/mol difference in binding free energy [as estimated by Δ(ΔG) = -RTΔ(lnK)]. This could reasonably account for the gain in binding free energy provided by additional hydrogen bonds. That being said, this interpretation cannot explain why there is only a 2.2-fold difference in k_{cat}/K_M between queuine and guanine. If the lack of additional hydrogen bonding led to the loss in binding free energy, one would anticipate that the human TGT would recognize $preQ_1$ somewhat better than guanine but poorer than queuine. Consequently, we conclude that the protonated side chain of $preQ_1$ (probably the most significant difference between $preQ_1$ and both guanine and queuine) should act as a negative element that results in poor recognition by the human enzyme. We should note that the side chain amine of queuine is predicted to be approximately 50% netural at physiological pH (Appendix Figure III-2).

To further examine the preferential heterocyclic substrate recognition that TGT exhibits, a series of *E. coli* TGT cysteine 145 mutants was generated to investigate the possible role of this residue. Although previous computational work has suggested a hydrophobic interaction between this residue and the 7-aminomethyl moiety of the base (5,6), there has been no kinetic evidence to support such interaction. To probe this, an alanine mutant at this position was generated and expected to display an attenuated hydrophobic effect due to the smaller side chain. In contrast, a serine mutant was designed to mimic a possible protonated cysteine (i.e., a thiol side chain), while a negatively charged aspartate (at physiological pH) substituent should imitate the effect of a

deprotonated cysteine (i.e., a thiolate side chain) and likely be involved in forming an electrostatic interaction.

A few significant observations arose from the kinetic characterization of the Cys145 mutants. First, the parallel increases in K_M values for both the guanine and tRNA substrates (Tables III-2 & III-3) suggest that similar interactions occur between this residue and guanine whether the base is free or integrated within the tRNA macromolecule, indicating that the enzyme recognizes its substrate tRNAs largely due to the presence of G_{34}. Second, comparing the k_{cat}/K_M values for the enzymes with respect to $preQ_1$ (Table III-4), the trend, wild-type > Cys145Ala > Cys145Ser > Cys145Asp (not actually detected) was observed, consistent with the crystallographic evidence that Cys145 interacts with the base via a hydrophobic interaction as either polar or charged amino acid substitutions lead to a decrease or even loss of substrate recognition. In the case of guanine, the trend in k_{cat}/K_M is slightly different (Cys145Ala > wild-type > Cys145Ser > Cys145Asp) and the reason for this difference is not obvious. The significant increase in k_{cat} for the alanine and serine mutants indicate that the off-rate for the product tRNA has increased and suggests that the substrate tRNA might exhibit a higher K_M. This is true for the alanine mutant, but not for the serine mutant. The serine mutant has a k_{cat}/K_M that is very similar to that for the wild-type. Both k_{cat} and K_M are increased by a factor of approximately 5, again consistent with faster off rates of product tRNA and substrate guanine; however, substrate tRNA exhibits a K_M only ~2.5-fold higher than that for the wild-type TGT. It is possible that there might be a water molecule mediating the

interactions between the side chain of Cys145Ser and guanine. In support of this hypothesis, Klebe and co-workers have found a crystallographically well-defined water molecule mediating a hydrogen bond between imidazole ligands (which they extrapolate to the N^7 of G_{34} of the substrate tRNA) and the peptide backbone in the active site (30).

The pK_a of the aminomethyl side chain of $preQ_1$ has been previously determined to be 9.8 in solution (23), which indicates that $preQ_1$ will be protonated at physiological pH, enabling it to participate in a possible electrostatic interaction with active site residues (Figure III-5). However, the severely reduced recognition of $preQ_1$ by the aspartate mutant appears to reject an electrostatic interaction with the residue at 145. Crystallographic evidence has shown that the amino group of the $preQ_1$ side chain forms a hydrogen bond with the carboxyl oxygen of Leu215 (*E. coli* numbering) (6). A hydrogen bond with the protonated $preQ_1$ side chain would provide a substantial contribution (greater than a simple, non-charged hydrogen bond) to the binding free energy. Another interesting fact is that both the serine and alanine mutants exhibited an increase in k_{cat}. The TGT-catalyzed reaction is extremely slow (~1 turnover every 2 minutes). Thus, the increases in activity exhibited by those two mutants are significant. However, this observation is not surprising considering product release is rate-limiting (27). Since Cys145 directly interacts with the base, removal of this interaction would enable faster product release.

Having both the human TGT and tritiated queuine allows us to directly examine whether pteridines inhibit the transglycosylase activity of the eukaryal

TGT, as reported previously. Originally, pterin was also chosen in the study as well as biopterin. However, the low water solubility of pterin limited our ability to obtain adequate concentrations for inhibition studies. Nevertheless, biopterin was confirmed to be a competitive inhibitor of the human TGT with a K_i value

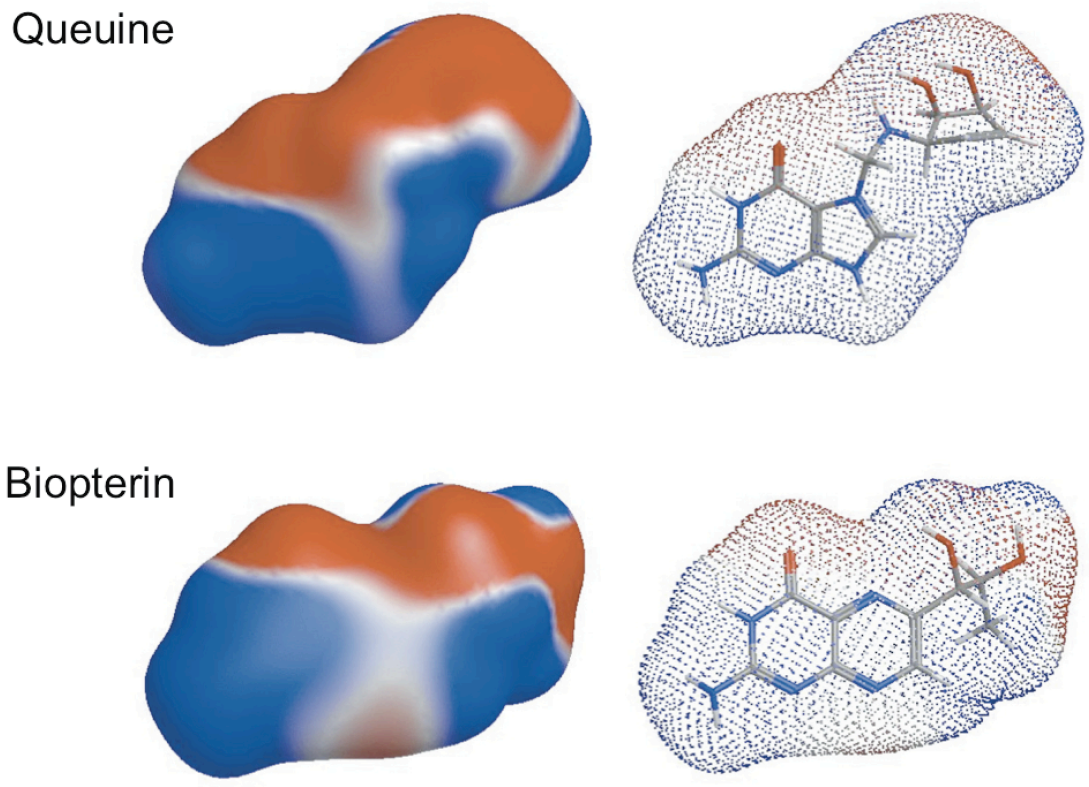

Figure III-9: Three-dimensional Electrostatic Models of Queuine and Biopterin. Molecules were generated in Molecular Operating Environment (MOE, Chemical Computing Group, Inc., Montreal, Canada) by Dr. Kate Abold, using the Molecular Builder. Electron density was estimated and the resulting surface was drawn while red and blue represent negative and positive charges, respectively. Note: Figure adapted from Thomas, C.E. (2004) Ph.D. Dissertation, University of Michigan, Ann Arbor.

within two orders of magnitude of the K_M for queuine. The inhibition observed by biopterin was expected, as the diol side chain of biopterin seems to be capable of partially substituting the interactions that the cyclopentenediol moiety of queuine provides. This postulate was established also based on 3D electrostatic models, performed by one of the former lab members, Dr. Kate Todorov (Abold), using Molecular Builder (Figure III-9), showing the similarity in electron density between biopterin and queuine. We should note that biopterin has been shown not to inhibit the *E. coli* TGT (31), indicating that the "queuine-like" side chain of bioptein is most likely sterically disallowed to fit in the active site of the *E. coli* enzyme. Additionally, our postulate agrees with the observation that pterin is a stronger eukaryal TGT inhibitor than biopterin with respect to guanine (8) as structurally pterin should be a more adequate substitute for guanine in the enzyme active site.

Our inhibition studies have provided new insight into how to directly investigate the physiological link between cellular pteridines and queuosine modification. Future directions for this part of the study are to examine the inhibition of the reduced forms of biopterin, such as dihydrobiopterin and tetrahydobiopterin. Both *in vivo* and *in vitro* experiments have suggested that tetrahydrobiopterin acts as a better inhibitor of the eukaryal TGT than biopterin does (7,8). Along with the concept that the reduced forms of "biopterins" are intracellularly predominating (32,33), it would be really interesting to elucidate the differences in inhibition among different oxidized states, as this may provide a mechanism for regulation of TGT activity *in vivo*.

Conclusions

In conclusion, the substrate specificity of the human TGT has been elucidated in this part of the study. To the best of our knowledge, this is the first report of the kinetics of the eukaryal TGT with respect to queuine and $preQ_1$ via direct incorporation assays. The unexpectedly high K_M value for $preQ_1$ led us to further investigate the role of Cys145 in the *E. coli* TGT active site. Although our results support previous computational predictions, indicating this residue forms hydrophobic rather than electrostatic interaction with $preQ_1$, information currently available does not fully explain the preferential heterocyclic substrate specificity of TGT. In addition, inhibition experiments indicate that the queuine analogue, biopterin, indeed inhibits the transglycosylase activity of the eukaryal TGT, and it is a competitive inhibitor with respect to queuine. It is apparent that the success in preparation of the human TGT and obtaining radiolabled queuine and $preQ_1$ has allowed a much more stringent approach for the characterization of the eukaryal TGT. Moreover, further inhibition studies using the reduced forms of biopterin will help address how different oxidized states of cellular biopterin may regulate Q-tRNA formation *in vivo*.

Notes to Chapter III

The majority of the work in this chapter has been published in, Yi-Chen Chen, Allen F. Brooks, DeeAnne M. Goodenough-Lashua, Jeffrey D. Kittendorf, H. D. Hollis Showalter and George A. Garcia, (2010) "Evolution of eukaryal tRNA-guanine transglycosylase: Insight gained from the heterocyclic substrate recognition by the wild-type and mutant human and *E. coli* tRNA-guanine transglycosylases", *Nucleic Acids Research*, In Press. In this study, syntheses of $preQ_1$ and queuine were designed and conducted by Allen F. Brooks and Prof. H. D. Hollis Showalter. We wish to thank them for their efforts for helping to complete this work. We also wish to acknowledge Moravek Biochemicals for conducting the tritiation for the [^{3}H]-$preQ_1$ and [^{3}H]-queuine syntheses.

Abbreviations used: Q, queuine; $preQ_1$, 7-aminomethyl-7-deazaguanine; $preQ_0$, 7-cyano-7-deazaguanine; TGT, tRNA-guanine transglycosylase; QTRT1, queuine tRNA-ribosyltransferase 1; QTRTD1, queuine tRNA-ribosyltransferase domain-containing 1; BH_4, tetrahydrobiopterin; THF, tetrahydrofolate; DTT, dithiothreitiol; IPTG, isopropyl β-D-thiogalactopyranoside; HEPES, hydroxyethylpiperazine-ethylsulfonate; Tris–HCl, tris(hydroxymethyl) aminomethane hydrochloride; SDS, sodium dodecyl sulfate; PAGE, polyacrylamide gel electrophoresis; TCA, trichloroacetic acid.

1. Garcia, G.A. and Kittendorf, J.D. (2005) Transglycosylation: A mechanism for RNA modification (and editing?). *Bioorganic Chemistry*, **33**, 229-251.

2. Okada, N. and Nishimura, S. (1979) Isolation and Characterization of a Guanine Insertion Enzyme, a Specific tRNA Transglycosylase, from *Escherichia coli*. *J. Biol. Chem.*, **254**, 3061-3066.

3. Shindo-Okada, N., Okada, N., Ohgi, T., Goto, T. and Nishimura, S. (1980) Transfer Ribonucleic Acid Guanine Transglycosylase Isolated from Rat Liver. *Biochemistry*, **19**, 395-400.

4. Watanabe, M., Matsuo, M., Tanaka, S., Akimoto, H., Asahi, S., Nishimura, S., Katze, J.R., Hashizume, T., Crain, P.F., McCloskey, J.A. *et al.* (1997) Biosynthesis of archaeosine, a novel derivative of 7-deazaguanosine specific to archaeal tRNA, proceeds *via* a pathway involving base replacement on the tRNA polynucleotide chain. *J. Biol. Chem.*, **272**, 20146-20151.

5. Romier, C., Reuter, K., Suck, D. and Ficner, R. (1996) Crystal structure of tRNA-guanine transglycosylase: RNA modification by base exchange. *EMBO Journal*, **15**, 2850-2857.

6. Romier, C., Meyer, J.E.W. and Suck, D. (1997) Slight sequence variations of a common fold explain the substrate specificities of tRNA-guanine transglycosylases from the three kingdoms. *FEBS Letters*, **416**, 93-98.

7. Farkas, W.R., Jacobson, K.B. and Katze, J.R. (1984) Substrate and Inhibitor Specificity of tRNA-Guanine Ribosyltransferase. *Biochimica et Biophysica Acta*, **781**, 64-75.

8. Jacobson, K.B., Farkas, W.R. and Katze, J.R. (1981) Presence of Queuine in *Drosophilia melanogaster*. Correlation of Free Pool with Queuosine Content of tRNA and Effect of Mutations in Pteridine Metabolism. *Nuc. Acids Res.*, **9**, 2351.

9. Parniak, M.A., Andrejchyshyn, S., Marx, S. and Kleiman, L. (1991) Alterations in cell tetrahydrobiopterin levels may regulate queuine hypomodification of tRNA during differentiation of murine erythroleukemia cells. *Experimental Cell Research*, **195**, 114-118.

10. Kuchino, Y., Kasai, H., Nihei, K. and Nishimura, S. (1976) Biosynthesis of the Modified Nucleoside Q in Transfer RNA. *Nucleic Acids Research*, **3**, 393-398.

11. Phillips, G., El Yacoubi, B., Lyons, B., Alvarez, S., Iwata-Reuyl, D. and de Crecy-Lagard, V. (2008) Biosynthesis of 7-Deazaguanosine-Modified tRNA Nucleosides: a New Role for GTP Cyclohydrolase I. *J. Bacteriol.*, **190**, 7876-7884.

12. McCarty, R.M. and Bandarian, V. (2008) Deciphering deazapurine biosynthesis: Pathway for pyrrolopyrimidine nucleosides toyocamycin and sangivamycin. *Chemistry & Biology*, **15**, 790-798.

13. Brooks, A.F., Garcia, G.A. and Showalter, H.D. (2010) A Short, Concise Synthesis of Queuine. *Tetrahedron Letters*, **51**, 4163-4165.

14. He, B., Rong, M.Q., Lyakhov, D., Gartenstein, H., Diaz, G., Castagna, R., McAllister, W.T. and Durbin, R.K. (1997) Rapid mutagenesis and purification of phage RNA polymerases. *Protein Expr. Purif.*, **9**, 142-151.

15. Michael, S.F. (1994) Mutagenesis by incorporation of a phosphorylated oligo during PCR amplification. *BioTechniques*, **16**, 410-412.

16. Chong, S. and Garcia, G.A. (1994) A Versatile and General Prokaryotic Expression Vector, pLACT7. *BioTechniques*, **17**, 686-691.

17. Kittendorf, J.D., Barcomb, L.M., Nonekowski, S.T. and Garcia, G.A. (2001) tRNA-guanine transglycosylase from *Escherichia coli*: Molecular mechanism and role of aspartate 89. *Biochemistry*, **40**, 14123-14133.

18. Studier, F.W. (2005) Protein production by auto-induction in high density shaking cultures. *Protein Expression and Purification*, **41**, 207-234.

19. Curnow, A.W. and Garcia, G.A. (1994) tRNA-Guanine Transglycosylase from *Escherichia coli*: Recognition of Dimeric, Unmodified $tRNA^{Tyr}$. *Biochimie*, **76**, 1183-1191.

20. Curnow, A.W., Kung, F.L., Koch, K.A. and Garcia, G.A. (1993) tRNA-Guanine Transglycosylase from *Escherichia coli*: Gross tRNA Structural Requirements for Recognition. *Biochemistry*, **32**, 5239-5246.

21. Chen, Y.C., Kelly, V.P., Stachura, S.V. and Garcia, G.A. (2010) Characterization of the human tRNA-guanine transglycosylase: Confirmation of the heterodimeric subunit structure. *RNA-a Publication of the RNA Society*, **16**, 958-968.

22. Okada, N., Noguchi, S., Nishimura, S., Ohgi, T., Goto, T., Crain, P.F. and McCloskey, J.A. (1978) Structure Determination of a Nucleoside Q Precursor Isolated from E. coli tRNA: 7-(Aminomethyl)-7-deazaguanine. *Nucleic Acids Research*, **5**, 2289-2296.

23. Hoops, G.C., Park, J., Garcia, G.A. and Townsend, L.B. (1996) The Synthesis and Determination of Acidic Ionization Constants of Certain 5-Substituted 2-Aminopyrrolo[2,3-d]pyrimidin-4-ones and Methylated Analogs. *Journal of Heterocyclic Chemistry*, **33**, 767-781.

24. Viscontini, M., Loeser, E. and Karrer, P. (1958) Fluoreszierende Stoffe aus Drosophila melanogaster .8. Isolierung und Eigenschaften des Pteridins HB2. *Helvetica Chimica Acta*, **41**, 440-446.

25. Rodrigues, A.D. and Lin, J.H. (2001) Screening of drug candidates for their drug-drug interaction potential. *Curr. Opin. Chem. Biol.*, **5**, 396-401.

26. Katze, J.R., Basile, B. and McClosky, J.A. (1982) Queuine, a Modified Base Incorporated Posttranscriptionally into Transfer RNA: Wide Distribution in Nature. *Science*, **216**, 55-56.

27. Garcia, G.A., Chervin, S.M. and Kittendorf, J.D. (2009) Identification of the Rate-Determining Step of tRNA-Guanine Transglycosylase from Escherichia coli. *Biochemistry*, **48**, 11243-11251.

28. Boland, C., Hayes, P., Santa-Maria, I., Nishimura, S. and Kelly, V.P. (2009) Queuosine Formation in Eukaryotic tRNA Occurs via a Mitochondria-localized Heteromeric Transglycosylase. *J. Biol. Chem.*, **284**, 18218-18227.

29. Howes, N.K. and Farkas, W.R. (1978) Studies with a Homogeneous Enzyme from Rabbit Erythrocytes Catalyzing the Insertion of Guanine into tRNA. *J. Biol. Chem.*, **253**, 9082-9087.

30. Stengl, B., Reuter, K. and Klebe, G. (2005) Mechanism and substrate specificity of tRNA-guanine transglycosylases (TGTs): tRNA-modifying enzymes from the three different kingdoms of life share a common catalytic mechanism. *Chembiochem*, **6**, 1926-1939.

31. Thomas, C.E. (2004) Ph.D. Dissertation, University of Michigan, Ann Arbor.

32. Gal, E.M., Hanson, G. and Sherman, A. (1976) Biopterin .1. Profile and Quantitation in Rat-Brain. *Neurochem. Res.*, **1**, 511-523.

33. Fukushima, T., Kobayashi, K.I., Eto, I. and Shiota, T. (1978) Differential Microdetermination for Various Forms of Biopterin. *Anal. Biochem.*, **89**, 71-79.

Appendix III

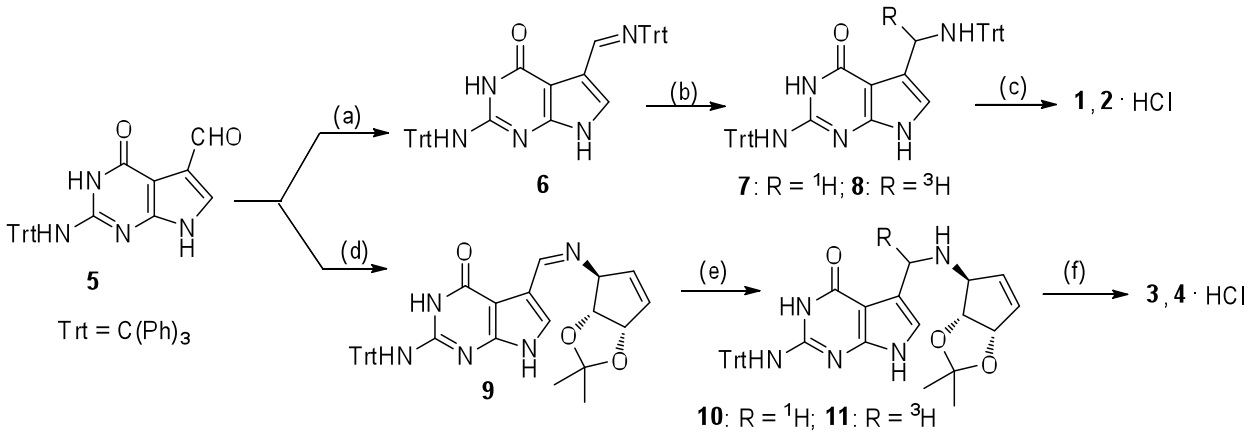

Appendix Figure III-1: Synthesis Schemes of [^{1}H]- and [^{3}H]-Labeled PreQ$_1$ and Queuine: (a) trityl amine, Na_2SO_4, anhydrous THF, reflux, 6 h; (b) 2eq. $NaBH_4$ or NaB^3H_4, THF, 0 - 25 °C, 3 h, 79% two steps; (c) 1.25 M methanolic HCl, reflux, 2 h, 89%; (d) (3*S*,4*R*,5*S*)-3-amino-4,5-isopropylidenedioxy-cyclopentene, Na_2SO_4, MeOH, 25 °C, 6 h (13); (e) 2eq. $NaBH_4$ or NaB^3H_4, MeOH, 0 - 25 °C, 4 h, 99% two steps (13); (f) 1.25 M methanolic HCl, 25 °C, 2.5 h, 87% (13).

Note: These syntheses were conducted by Allen Brooks and Prof. Hollis Showalter.

A

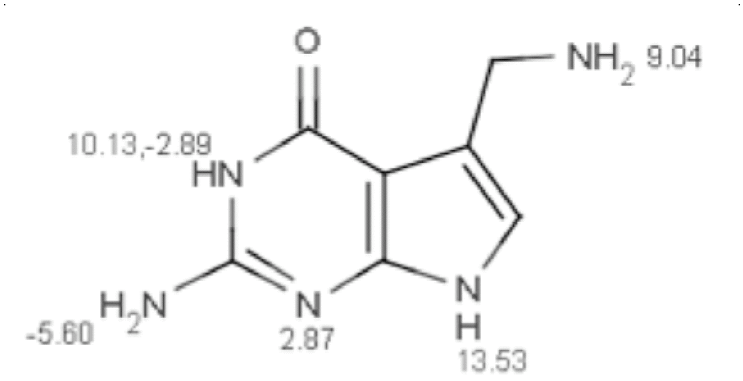

B

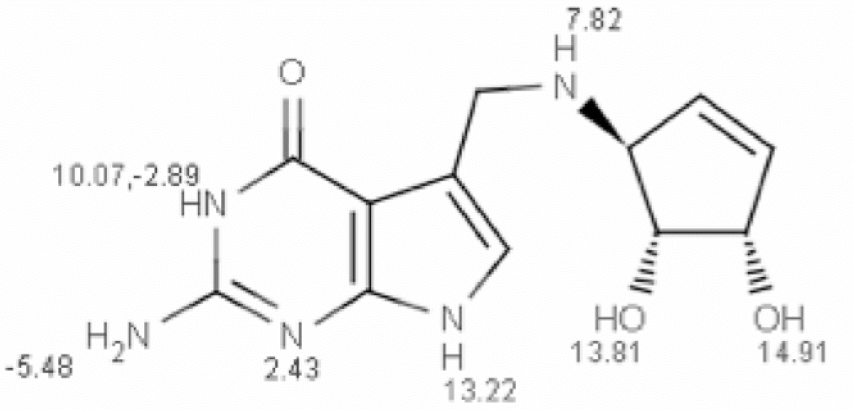

Appendix Figure III-2: Predicted pKa Values of (A) $PreQ_1$ and (B) Queuine. The prediction was kindly performed by Dr. Paul Kirchhoff using MarvinSketch 3.5.1, ChemAxon®.

CHAPTER IV

DIVERGENT EVOLUTION OF EUKARYAL TGT: INSIGHT GAINED FROM THE HETEROCYCLIC SUBSTRATE SPECIFICITY OF THE HUMAN AND *ESCHERICHIA COLI* tRNA-GUANINE TRANSGLYCOSYLASES

Abstract

The tRNA-modifying enzyme tRNA-guanine transglycosylase (TGT) is utilized across eukarya, eubacteria and archaea with differences in heterocyclic substrate and tRNA recognition. Based on the X-ray structural analyses, earlier studies (Stengl, et al. (2005) *Chembiochem*, **6**, 1926-1939) have made a compelling case for the divergent evolution of the eubacterial and archaeal TGTs. However, in the absence of an X-ray crystal structure, extension to the eukaryal TGT could only be inferred. To confirm the divergent evolution model for TGT and to extend it to eukarya, we performed sequence homology and phylogenetic analyses, the results of which are consistent with divergent evolution. Experimental studies with the wild type and mutant TGTs from human and *E. coli* also support the concept of the divergent evolution. Observations with the human TGT (QTRT1) Val161Cys and Val161Cys/ Gly232Val mutants (mutations made to their corresponding residues in the *E. coli* TGT) elucidated that amino acids in the human TGT active site evolved for increased

recognition of queuine and a concomitantly decreased recognition of $preQ_1$. Additionally, the $preQ_1$ kinetics of the *E. coli* TGT Cys145Val mutant are also consistent with the idea that the Cys145 evolved in eubacterial TGTs to recognize $preQ_1$ but not queuine. Both the phylogenetic and kinetic analyses support the conclusion that all TGTs have divergently evolved to specifically recognize their cognate heterocyclic substrates.

Introduction

Despite recognizing slightly different heterocyclic substrates, the TGT reaction across the three kingdoms shares a common mechanism through the replacement of a genetically encoded guanine. The transglycosylation occurs via a covalent TGT-RNA intermediate with ping-pong kinetics as elucidated by studies of the eubacterial TGT (1-3). Also, crystallographic evidence reveals that the N-terminal domains of eubacterial and archaeal TGTs fold into a $(\beta/\alpha)_8$ TIM barrel, while a characteristic zinc-binding motif is found in their C-terminal domains (4,5). Romier *et al.* observed a dimer interface when the structure of the *Zymomonas mobilis* TGT was determined (4). Later, co-crystallization of the enzyme with an anticodon stem loop confirmed a homodimer formation upon tRNA binding (6). The archaeal TGT has also been shown to contain two monomers per asymmetric unit and the two subunits were suggested to interact tightly through the zinc-binding domain (5). The most interesting subunit structure was found in eukarya. Although lacking a crystal structure, the eukaryal

TGT has been proposed for almost four decades to be a heterodimer (7) based upon biochemical and kinetic characterizations. Although there have been discrepancies regarding the reported size and composition of the subunits (7-10), it is now clear that the eukaryal TGT is composed of QTRT1 (queuine tRNA-ribosyltransferase 1) and QTRTD1 (queuine tRNA-ribosyltransferase domain-containing 1), which are homologous subunits of 44 and 46.7 kDa, respectively (11,12 and Chapter II). QTRTD1 has been proposed to be the queuine salvage enzyme that liberates free queuine from QMP (12).

Regarding the origin of TGT, an argument has been made that queuosine modification in eubacteria and eukarya may have resulted from convergent evolution based on the dramatic differences between their queuosine modification systems (e.g., eukarya do not synthesize queuine while eubacteria do and eukarya transport and salvage queuine while eubacteria do not) (13). At that time, the quaternary structure of the eukaryal TGT was thought to be different from that of the eubacterial TGT, as described earlier in Chapter I. Subsequently, based upon careful analyses of the X-ray crystal structures of eubacterial and archaeal TGTs, Klebe and co-workers have presented a compelling case for the divergent evolution of TGT (14). Their evidence includes the close overall structural homology and the absolute conservation of zinc-binding and key active site residues. They also present a cogent discussion of changes in key amino acids in the active site that are responsible for the differential heterocyclic substrate recognition between the eubacterial ($preQ_1$) and archaeal ($preQ_0$) TGTs. However, in the absence of an X-ray crystal

structure and any detailed biochemical evidence, extension of the divergent evolution concept to the eukaryal TGT could only be inferred from sequence homologies.

To confirm the divergent evolution model for TGT and to extend it to eukarya, we report further sequence homology and phylogenetic analyses, the results of which are consistent with divergent evolution. To provide experimental evidence for the divergent evolution of TGT in eukaryotes, $preQ_1$ incorporation studies were performed with mutant human and *E. coli* tRNA-guanine transglycosylases. Enzymological studies of mutants of Cys145 & Val217 (*E. coli* TGT) and the corresponding Val161 & Gly232 (human QTRT1) are consistent with the concept that these residues, in particular, have evolved to enhance recognition of $preQ_1$ in eubacteria and to decrease recognition of $preQ_1$, concomitant with increased recognition of queuine, in eukarya. These phylogenetic analyses and experimental results support the conclusion that all TGTs have divergently evolved to specifically recognize their cognate heterocyclic substrates, while minimizing recognition of non-cognate ones.

Materials and Methods

Reagents

Unless otherwise specified, all reagents were ordered from Sigma-Aldrich. DNA oligonucleotides, agarose, dithiothreitol (DTT), isopropyl β-D-thiogalactopyranoside (IPTG) and DNA ladders were ordered from Invitrogen. All restriction enzymes and Vent® DNA polymerase were ordered from New England Biolabs. The ribonucleic acid triphosphates (NTPs), pyrophosphatase and kanamycin sulfate were ordered from Roche Applied Sciences. The deoxyribonucleic acid triphosphates (dNTPs) were ordered from Promega. Scriptguard™ RNase Inhibitor was ordered from Epicentre. Epicurian coli® XL2-Blue ultracompetent cells were ordered from Stratagene. TG2 cells, K12 (DE3, Δ*tgt*) cells and K12 (DE3, Δ*tgt*)-pRIPL cells were from laboratory stocks. His•Bind resin and lysonase bioprocessing reagent were also purchased from Novagen. The QIAPrep® Spin Miniprep and Maxiprep Kits were ordered from Qiagen. Precast PhastGels and SDS buffer strips were from VWR. Bradford reagent was from Bio-Rad. Whatman GF/C Glass Microfibre Filters, Amicon Ultra Centrifugal Filter Devices, carbenicillin and all bacterial media components were ordered from Fisher. [8-^{14}C]-Guanine (46.4 mCi/mmol) was ordered from Moravek Biochemicals. [^{3}H]-PreQ$_1$ (4.9 Ci/mmol) was obtained as described in Chapter III. T7 RNA polymerase was isolated from *E. coli* BL21 (DE3) pLysS cells harboring the plasmid pRC9 via minor modifications of the procedure described in the literature (15). The human and *E. coli* tRNA^{Tyr} were generated as described in Chapter II and Chapter III (this dissertation), respectively.

Construction of Human TGT (QTRT1) Val161Cys and Val161Cys/Gly232Val Mutants

QuikChange™ site-directed mutagenesis (Stratagene) was used to introduce the Val161Cys and Val161Cys/Gly232Val mutations (in QTRT1) from the wild-type human TGT plasmid. The mutagenic primers for Val161Cys are: 5'-CATCATCATGCAGCTGGACGACTGTGTTAGCAGTACTGTGACTGGGCC-3' and 5'-GGCCCAGTCACAGTACTGCTAACACAGTCGTCCAGCTGCATGATGATG-3'. The Val161Cys/Gly232Val mutant plasmid was subsequently generated using the Val161Cys plasmid as a template and the following mutagenic primers: 5'-CTTCGCCATCGGGGGCCTGAGCGTGGGTGAGAGCAAGTCGCAGTTC-3' and 5'-GAACTGCGACTTGCTCTCACCCACGCTCAGGCCCCCGATGGCGAAG-3'. The conditions for site-directed mutagenesis were described previously in Chapter II (in this dissertation).

Construction of E. coli TGT Cys145Val and Cys145Val/Val217Gly Mutants

The expression plasmid for Cys145Val was generated using the plasmid for *E. coli* TGT Cys145Ala as a template and the following mutagenic primers: 5'-CAGTCAGCAGGATACGGCGTAACCTCATCAAAGATCATGACG-3' and 5'-CGTCATGATCTTTGATGAGGTTACGCCGTATCCTGCTGACTG-3'. Also, the expression plasmid for Cys145Val/Val217Gly was generated using the plasmid for *E. coli* TGT Cys145Val as a template and the following mutagenic primers: 5'-

CGCTGTCGGCGGTCTGGCTGGGGGTGAGCCGAAAGCAGATATG-3' and CATATCTGCTTTCGGCTCACCCCCAGCCAGACCGCCGACAGCG-3'. The conditions for site-directed mutagenesis were similar to general laboratory protocol for generating human TGT mutants with minor modifications. Briefly, 30 µL reactions containing 500 ng of template plasmid, 666 nmol of each of the respective mutagenic primers, Mg^{+2} (2 mM), dNTPs (0.25 mM each), ThermolPol buffer (1X) and 2 units of Vent DNA polymerase were subjected to 30 PCR cycles of the following temperature sequence: 94°C (1 min), 50°C (1 min), and 72°C (6.5 min). Following digestion with 20 units of Dpn I for 2 hours, 10 µL of the PCR product was transformed into 100 µL of Epicurian coli® XL2-Blue ultracompetent cells according to the vendor's protocol (Stratagene). Cells were grown overnight at 37°C on L-Agar plates containing 50 µg/mL kanamycin and 30 µg/mL chloramphenicol. Individual colonies were isolated, and 3 mL 2xTY (with 50 µg/mL kanamycin and 30 µg/mL chloramphenicol) liquid cultures were inoculated at 37°C with shaking. The plasmids were isolated via miniprep, and the *tgt* mutant genes were confirmed by DNA sequencing.

Expression and Purification of Human and E. coli TGT Mutants

The plasmids for the human and *E. coli* TGT mutants were transformed into *E. coli* K12 (DE3, Δ*tgt*)-pRIPL and *E. coli* K12 (DE3, Δ*tgt*) competent cells, respectively, for expression. The human TGT mutants were prepared in the same fashion as the wild-type enzyme, which was described previously in

Chapter II. The *E. coli* TGT mutants were prepared following an auto-induction procedure as described in Chapter III.

Activity Screen and Kinetic Analyses

To determine the kinetic parameters of human or *E. coli* TGT mutants, $preQ_1$ exchange assays were conducted by monitoring the incorporation of radiolabeled substrate, [^{3}H]-$preQ_1$, into their cognate tRNAs, as described in Chapter III (in this dissertation). To examine whether biopterin inhibits *E. coli* TGT mutants, the guanine exchange assays were performed under the following conditions: *E. coli* $tRNA^{Tyr}$ (15 μM), [8-^{14}C]-guanine (46.4 mCi/mmol, 25 μM), each *E. coli* TGT mutant (100 nM), biopterin (3 mM) and HEPES reaction buffer (100 mM HEPES, pH 7.3; 20 mM $MgCl_2$; 5 mM DTT) to a final volume of 400 μL. All reaction mixtures were incubated at 37°C for purposes of equilibration before initiating the reaction with the addition of TGT, and the studies were performed in triplicate. Aliquots (70 μL) were removed every 3 minutes throughout the 15-minute time course and immediately quenched in 2.5 mL of 5% trichloroacetic acid (TCA) for 1 hour before collection on glass-fiber filters. Each filter was washed with three volumes of 5% TCA and a final wash of ethanol to dry the filter. The samples were analyzed in a scintillation counter (Beckman) for radioactive decay, where counts were reported in DPM and later converted to picomoles [8-^{14}C] guanine as described previously.

tRNA Binding: Native PAGE

To access the binding of the *E. coli* $tRNA^{Tyr}$ to the *E. coli* TGT mutants, native PAGE band-shift assays were performed based on the method established previously (16) with minor modifications. Briefly, each TGT sample (25 μM) was incubated with a 4-fold excess of tRNA (100 μM) at 37°C for 1 hour. The reaction mixtures were then analyzed by native PAGE using 8-25% gradient polyacrylamide gels and native buffer strips (880 mM L-alanine, 250 mM Tris•HCl (pH 8.8) and 2% agarose). Aliquots of each reaction were loaded on the gel (approximately 4 μL) and run under the following conditions: 5°C, 400 V, 10 mA, 2.5 W, 200 AVH. After electrophoresis, the proteins were stained by Coomassie blue for visualization.

Covalent Complex Band-Shift Assay: Mildly Denaturing PAGE

To further examine whether the *E. coli* TGT mutants form covalent complexes with the *E. coli* $tRNA^{Tyr}$, mildly denaturing PAGE band-shift assays were conducted as follows. Each TGT sample (10 μM) was incubated with 40 μM of tRNA at 37°C for 1 hour. Subsequently, an equal volume of the mild SDS buffer (60 mM Tris•HCl (pH 6.8), 2% SDS, 10% glycerol and 0.01% bromophenol blue) was added to each reaction mixture and the incubation was carried at room temperature for an additional hour. The samples were then analyzed by denaturing PAGE using 8-25% gradient polyacrylamide gels and SDS buffer strips (8.9 mM tris base, 8.9 mM boric acid, 0.2 mM EDTA and 2% agarose). Aliquots of each reaction were loaded on the gel (approximately 4 μL) and run

under the following conditions: 15°C, 250 V, 10 mA, 3 W, 100 AVH. After electrophoresis, the proteins were stained by Coomassie blue for visualization.

Multiple Sequence Aligement of Representative TGTs Across the Three Kingdoms

The protein sequences of 15 TGTs (QTRT1 in eukarya), spanning the three phylogenic domains, were retrieved using the following accession numbers (*E. coli*, AAA24667; *Z. mobilis*, T46898; *S. flexneri*, NP_706294; *B. subtilis*, NP_390649; *A. aeolicus*, NP_213895; *M. acetivorans*, NP_619281; *M. mazei*, NP_633125; *H. volcanii*, BAB40327; *A. fulgidus*, NP_070314; *P. horikoshii*, NP_143020; *C. elegans*, NP_502268; *D. melanogaster*, NP_608585; *M. musculus*, NP_068688; *R. norvegicus*, NP_071586; *H. sapien*, AAG60033). Sequence alignment was performed using the PileUP alignment program found in the SeqWeb software package (Accelrys). Selected regions highlighting the conservation of aspartates 89, 143 & 264; cysteines 145, 302, 304 & 307; and histidine 333 (*E. coli* numbering) are shown in Figure IV-1.

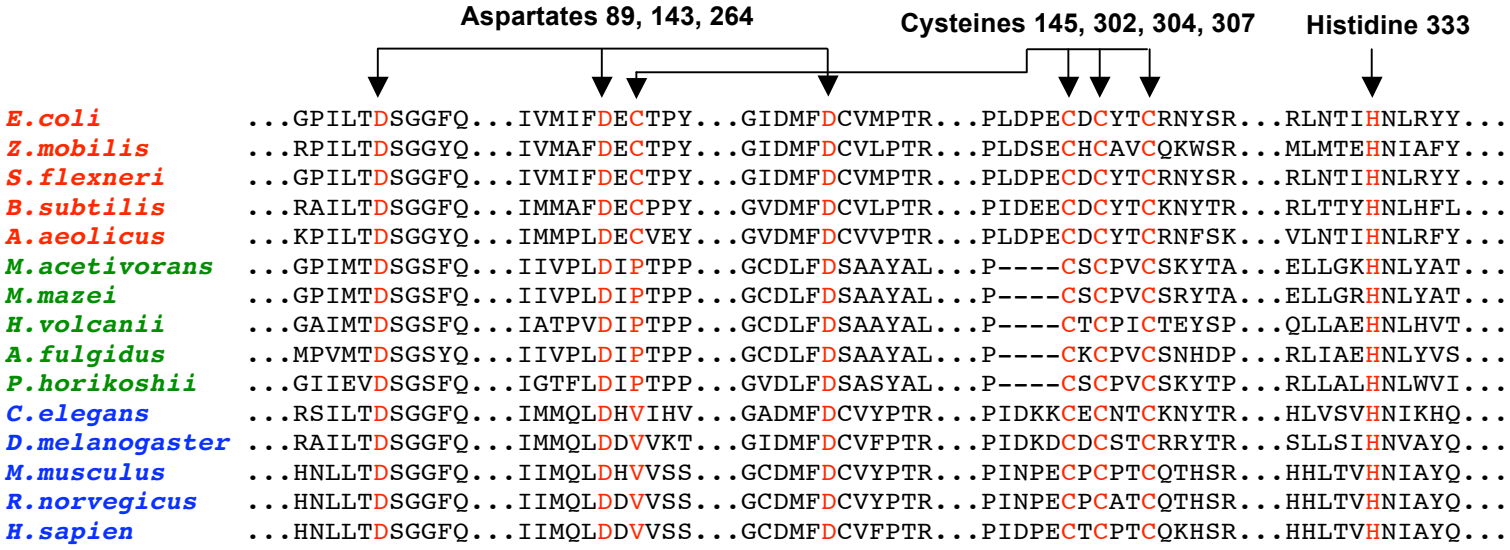

Figure IV-1: Selected Regions of a Sequence Homology Analysis of TGTs Across the Three Kingdoms of Life. A sequence alignment of representative TGTs from eubacteria, archaea, and eukarya (QTRT1) highlighting the conservation of aspartates 89, 143 & 264; cysteines 145, 302, 304 & 307; and histidine 333 (*E. coli* numbering). Dots (.) indicate regions intentionally deleted for this figure. Dashes (-) indicate gaps in the sequence alignment. The full alignment was generated by Dr. Jeffrey Kittendorf using PileUP in the SeqWeb software package (Accelerys). The conserved amino acids are colored-coded red.

Phylogenetic Tree for TGTs Across the Three Kingdoms

Amino acid sequences for eubacterial and archaeal TGT and eukaryal QTRT1 were manually extracted from the NCBI Protein sequence database. A very large number of sequences (~6000) were initially found. In the case of archaeal TGTs, these were sorted by phylogenetic tree and duplicates were discarded. Where a number of examples were present within each subgroup, only 1-2 were selected for inclusion in our study as we wanted the sample to be a diverse representation and not to be biased towards any one subgroup. A large number of protein sequences were annotated as "PUA domain containing"; however, only those clearly annotated as tRNA transglycosylase or ribosyltransferase (e.g., queuine, guanine, 7-cyano-preQ_1 or archaeosine) were included to avoid possible confusion with pseudouridine synthases and others. Due to the large number of subgroups for the eubacterial TGTs, the sequences were sorted by the highest level of identified organisms listed in the database; however, only one example per genus was chosen to minimize bias.

A multiple sequence alignment was then performed with Clustal W. A number of sequences (36) were found to be suspect. Reexamination of the NCBI database allowed us to correct 30 of these sequences. The six sequences that were deleted were found to not align with (or were missing) the conserved active site aspartates and zinc-binding ligands (see Figure IV-1) or were of lengths not consistent with the other sequences. This dataset contained ca. 100 eubacterial sequences. Our initial tree calculation suggested that the disproportionate number of eubacterial sequences might be biasing the analysis.

We therefore pared down the number of eubacterial sequences using the same criterion of maintaining phylogenetic diversity. This yielded 13 eukaryal QTRT1, 72 archaeal TGT and 59 eubacterial TGT sequences. A listing of these sequences can be found in Appendix Table IV-1.

The evolutionary history of the TGT enzymes was then inferred via Maximum Likelihood analysis using the MEGA4 software package (17,18). The Clustal W alignment was subjected to 500 bootstrap replicates resulting in the final consensus phylogenetic tree. Due to the number of sequences, a condensed version of the tree is shown in Figure IV-2. The full tree can be seen in Appendix Figure IV-1.

Results

Phylogenetic Tree for TGTs Across the Three Kingdoms

A complete search of the NCBI database for TGT sequences and subsequent paring down of some sequences yielded a representative number of sequences that were aligned via Clustal W. This alignment then was used for a phylogenetic tree analysis using MEGA4. The tree analysis (Figure IV-2) clearly demonstrates the relatedness of the TGT sequences. Consistent with the simple homology analysis, the archaeal sequences clearly group distinctly from the others and the eukaryal sequences group together, but closer to the eubacterial sequences.

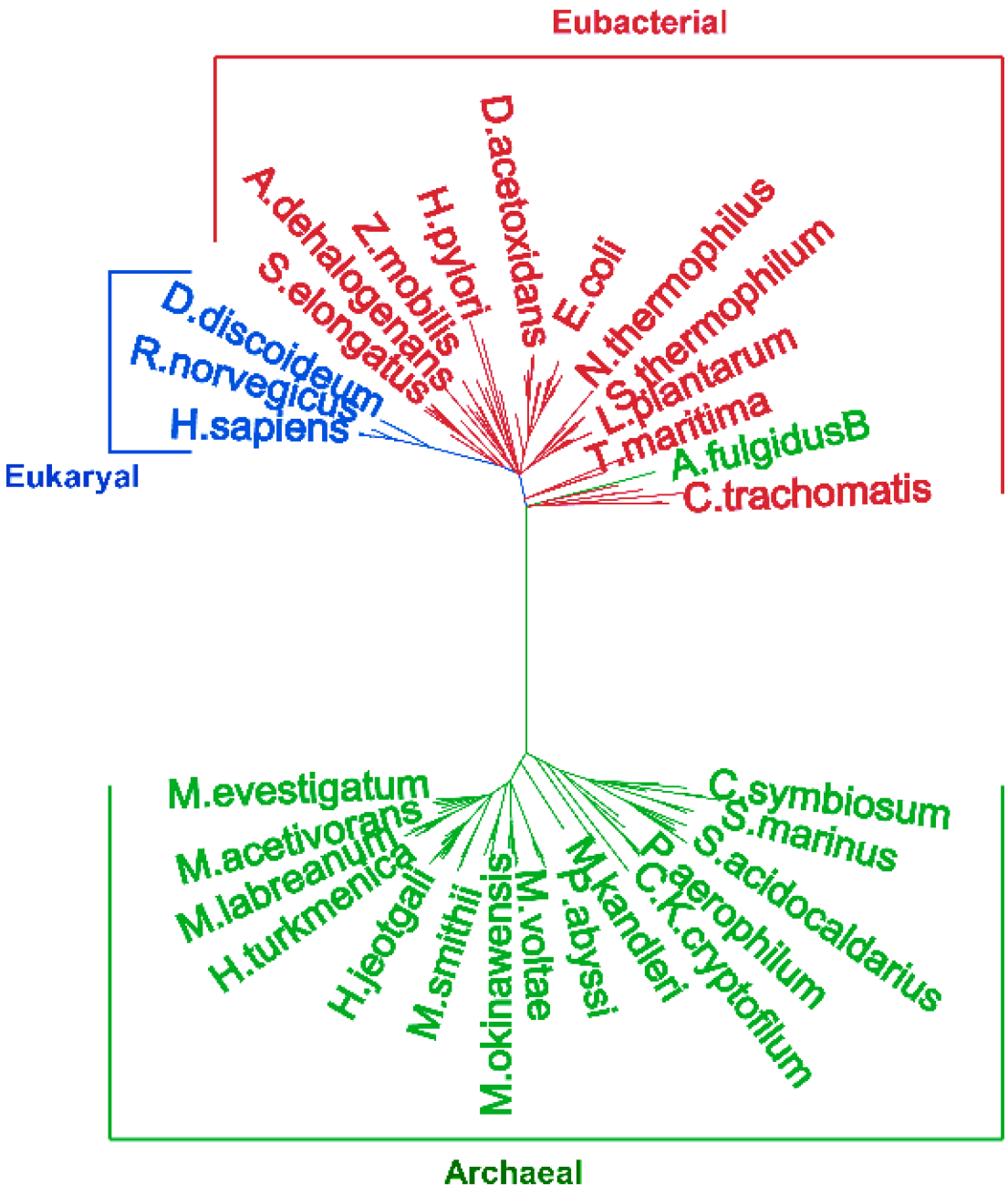

Figure IV-2: Phylogenetic Tree for TGTs Across the Three Kingdoms. The evolutionary history of the TGT enzymes was inferred via Maximum Likelihood analysis with the MEGA4 software package. Representative TGT sequences spanning the three domains of life (13 eukaryal (QTRT1), 59 eubacterial, 72 archaeal) were globally aligned using Clustal W. The alignment was subjected to 500 bootstrap replicates resulting in the final consensus phylogenetic tree. This is an unrooted tree and the branch lengths are proportional to the evolutionary distances between nodes. Due to the number of sequences, a condensed version of the tree is shown.

Kinetics Analysis of Human TGT Mutants with respect to PreQ$_1$

To provide experimental data to probe the divergent evolution of TGT, we sought to find amino acid alterations between the human and *E. coli* TGT active sites, which could account for differential heterocyclic substrate specificity. Two major differences that drew our attention are Cys145 (*E. coli* numbering, corresponding to Val161 in human QTRT1) and Val217 (*E. coli* numbering, corresponding to Gly232 in human QTRT1), as both of them are conserved and kingdom-specific. Assuming that the modern forms of TGT arose from divergent evolution, mutations of these residues in the human TGT to their counterparts in the *E. coli* enzyme should result in a better recognition for preQ$_1$. To verify our hypothesis, the human TGT (QTRT1) Val161Cys and Val161Cys/Gly232Val

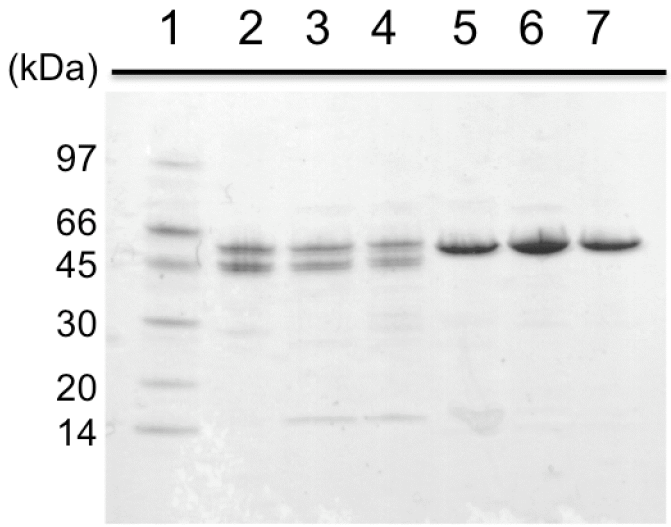

Figure IV-3: SDS-PAGE of Various Human and *E. coli* TGT Samples. 1. Low molecular weight standards (GE Healthcare), 2. Wild-type human TGT, 3. Human TGT (QTRT1) Val161Cys mutant, 4. Human TGT (QTRT1) Val161Cys/Gly232Val mutant, 5. Wild-type *E. coli* TGT, 6. *E. coli* TGT Cys145Val mutant, 7. *E. coli* TGT Cys145Val/Val217Gly mutant.

mutants were prepared (Figure IV-3, Lanes 3 and 4) and the transglycosylase activity of each mutant was examined via $preQ_1$ exchange assays. Shown in Figure IV-4 and Table IV-1, the K_M values the for the Val161Cys and Val161Cys/Gly232Val mutants were determined to be 22.32 ± 4.10 μM and 0.47 ± 0.82 μM, which are 6- and 282-fold lower than that of the wild-type human TGT, while the k_{cat} values also decrease (by approximately a factor of 2 and 5). Nevertheless, the substantial reduction in K_M leads to 3- and 60-fold greater k_{cat}/K_M for the mutants over the wild-type enzyme. It may be worth mentioning that compared to the *E. coli* TGT, the human TGT (QTRT1) Val161Cys/ Gly232Val mutant only shows a 50-fold decrease in k_{cat}/K_M, whereas the difference between the wild-type human and *E. coli* TGTs appears to be more than 3,000 fold.

Table IV-1: $PreQ_1$ Kinetics for Wild-type *E. coli* & Human TGT and Human TGT Mutants

Enzyme	k_{cat}[a,b] (10^{-3}•s^{-1})	K_M[a,b] (μM)	k_{cat}/K_M[a,b] (10^{-3}•s^{-1}•μM^{-1})
E. coli			
wild-type	9.57 (±0.24)	0.05 (±0.01)	191 (±38.6)
Human			
wild-type	8.23 (±0.71)	132 (±28)	0.062 (±0.014)
(QTRT1) Val161Cys	4.64 (±0.32)	22.3 (±4.1)	0.21 (±0.04)
(QTRT1) Val161Cys/Gly232Val	1.75 (±0.06)	0.47 (±0.08)	3.71 (±0.13)

[a]Standard errors are in parentheses. [b]Kinetic parameters were generally calculated from the average of three replicate determinations of initial velocity data.

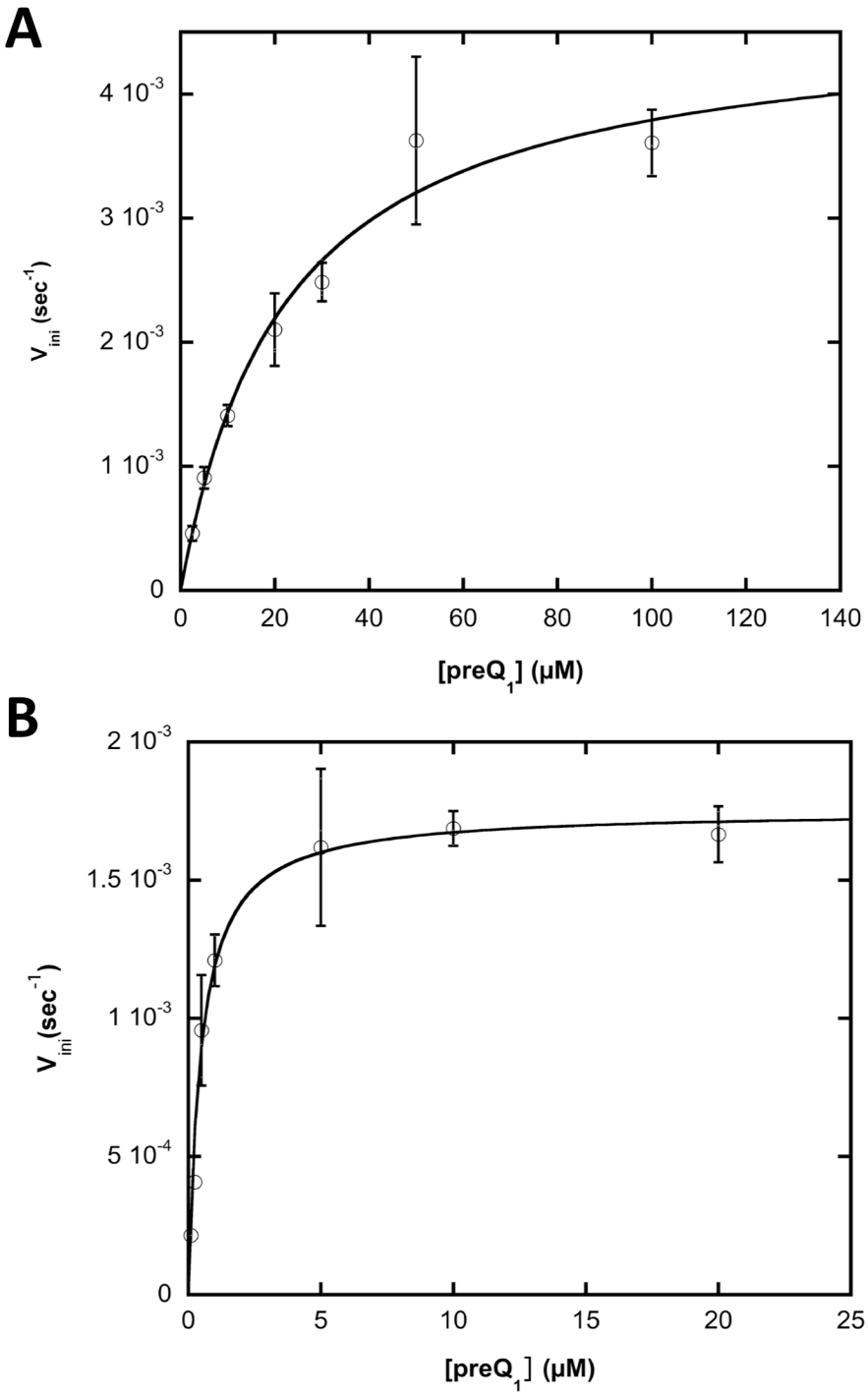

Figure IV-4: Michaelis-Menten Fit of $PreQ_1$ with (A) Human TGT (QTRT1) Val161Cys Mutant, and (B) Human TGT (QTRT1) Val161Cys/Gly232Val Mutant. Curves were generally obtained from the average of three independent determinations of initial velocity data. Error bars were generated from the standard deviation within each point.

Activity Screen, Kinetics Analysis and Physical Examination of E. coli TGT Mutants

It is encouraging that amino acid substitutions in the human TGT (QTRT1) active site (at least based on the homology model (19)) indeed enhance recognition of $preQ_1$. That also urged us to examine whether the corresponding alterations in the *E. coli* TGT active site would lead to the generation of an "artificial" human TGT (i.e., having the ability to recognize queuine). Therefore, the *E. coli* TGT Cys145Val and Cys145Val/Val217Gly mutants were prepared (Figure IV-3, Lanes 6 and 7). Unfortunately, preliminary studies using queuine exchange assays showed that neither of the mutants seem to recognize queuine. To assure that the undetectable activity was not due to any adverse effects during the process of protein preparation, the transglycosylase activity of each mutant was further verified by guanine exchange assays. The Cys145Val mutant clearly showed the ability to catalyze transglycosylase reaction (Figure IV-5A), whereas the Cys145Val/Val217Gly did not exhibit any incorporation of [^{14}C]-guanine into $tRNA^{Tyr}$. It may be worth mentioning that we also attempted to increase the substrate [^{14}C]-guanine up to 100 μM and extend the reaction to 2 hours; however, there was still no transglycosylase activity observed.

Compared to the other *E. coli* TGTs (wild-type or mutants) we have prepared, the preparation of the Cys145Val/Val217Gly mutant yields a comparable amount of soluble protein. Along with the fact that it does not show any apparent abnormalities on a SDS-PAGE gel led us to believe that the protein

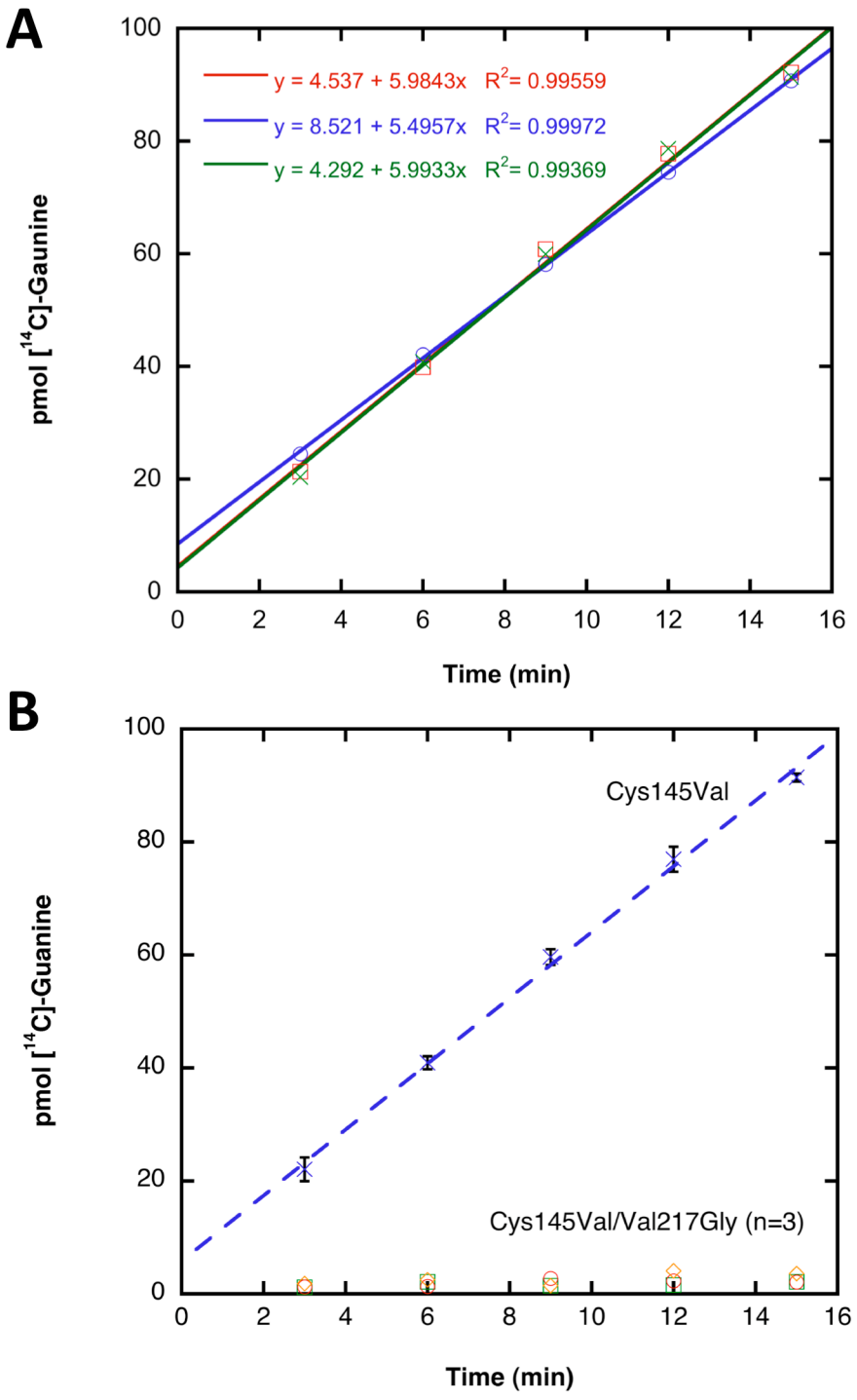

Figure IV-5: [^{14}C]-Guanine Incorporated over Time in *E. coli* tRNA^{Tyr} in the presence of (A) *E. coli* TGT Cys145Val Mutant, and (B) *E. coli* TGT Cys145Val/Val217Gly Mutant (Note: the [^{14}C]-Guanine incorporation averaged from A also shown in B for comparison purpose). The assays were performed in triplicate.

most likely did not encounter a global folding problem. In attempt to understand why this mutant loses its activity, the ability of tRNA binding was assessed via band-shift assays under both native and mildly denaturing conditions. When incubated with an excess amount of tRNA, the Cys145Val/Val217Gly mutant indeed binds to the substrate tRNA (Figure IV-6A), qualitatively similar to the wild-type and the Cys145Val mutant. Even more interestingly, the mutant also appears to be capable of forming a covalent complex with tRNA (Figure IV-6B), indicating the first half of the TGT reaction (i.e., the occurrence of a covalent TGT-RNA intermediate which is accompanied with guanine release) can be accomplished.

Although it does not utilize queuine as a substrate, the kinetic characterization of the *E. coli* TGT Cys145Val mutant with respect to $preQ_1$ (Figure IV-7) again supports the concept of divergent evolution and that this cysteine residue selectively recognizes $preQ_1$. Although the k_{cat} of this mutant is enhanced (relative to wild-type) by approximately 1.5-fold ($14.1 \pm 0.7 \times 10^{-3}$ s^{-1} vs. $9.57 \pm 0.24 \times 10^{-3}$ s^{-1}), a 55-fold increase in K_M (2.76 ± 0.51 μM vs. 0.05 ± 0.01 μM) clearly indicates that the *E. coli* TGT prefers a cysteine at this position rather than its human counterpart, valine. It should be noted that the $preQ_1$ kinetics for the Cys145Val mutant nicely fit into the trend we observed from the other Cys145 mutants (Chapter III in this dissertation). The substantial difference in $preQ_1$ recognition (a 37-fold decrease in k_{cat}/K_M for the mutant) also prompted us to examine the potential for biopterin inhibition of the Cys145Val mutant. Due to the limited amount of $preQ_1$, guanine exchange assays were performed in the

presence of biopterin (3 mM). The high concentrations of biopterin used in the assays were selected based on a previous observation that the *E. coli* TGT is not

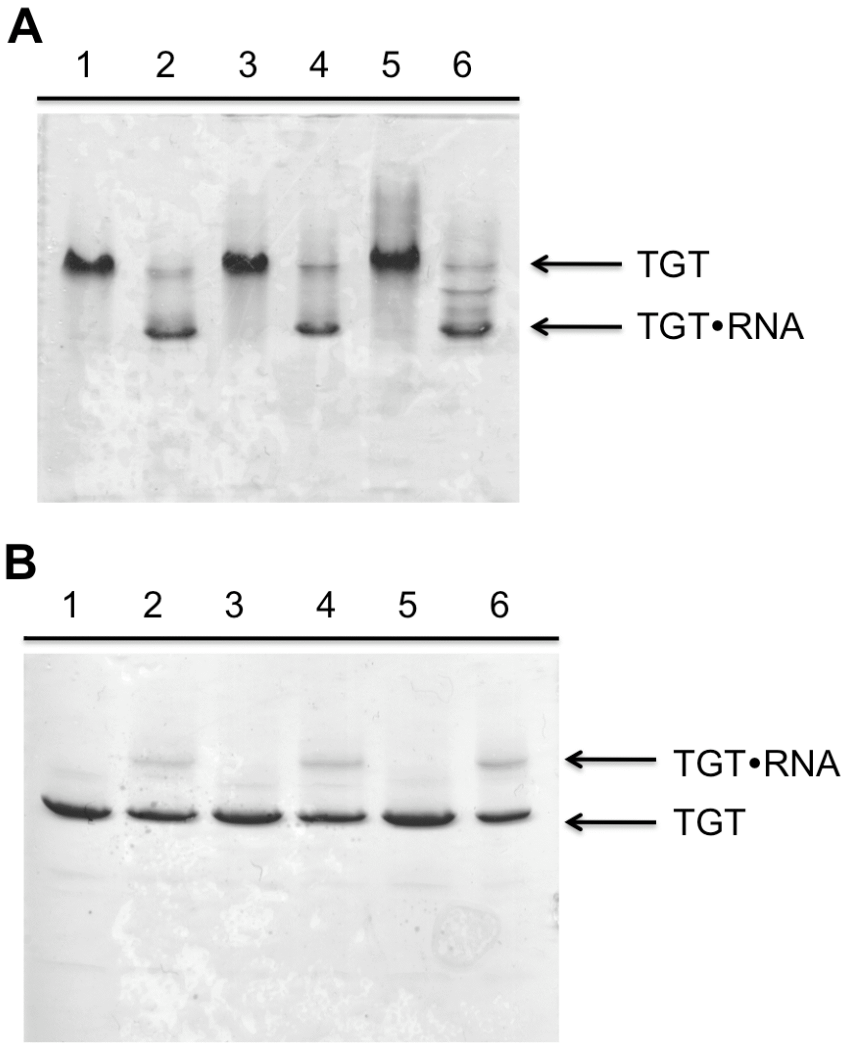

Figure IV-6: (A) Native PAGE and (B) Mildly SDS-PAGE of TGT and TGT•RNA. 1. Wild-type *E. coli* TGT, 2. Wild-type *E. coli* TGT + *E. coli* $tRNA^{Tyr}$, 3. *E. coli* TGT Cys145Val, 4. *E. coli* TGT Cys145Val + *E. coli* $tRNA^{Tyr}$, 5. *E. coli* TGT Cys145Val/Val217Gly, 6. *E. coli* TGT Cys145Val/Val217Gly+ *E. coli* $tRNA^{Tyr}$.

inhibited by such concentrations (Thomas and Garcia, unpublished data). As shown in Figure IV-8, there was no significant change in activity (presented as

the averaged initial velocity) observed between the experimental and control groups (statistical significance determined by Student's t-test, *p* value = 0.65), indicating biopterin does not inhibit the Cys145Val mutant at 3 mM. It is unfortunate that the Cys145Val/Val217Gly mutant is not kinetically active due to an unknown reason, and the consequences are that the $preQ_1$ kinetics and biopterin inhibition studies for the mutant cannot be conducted at this point.

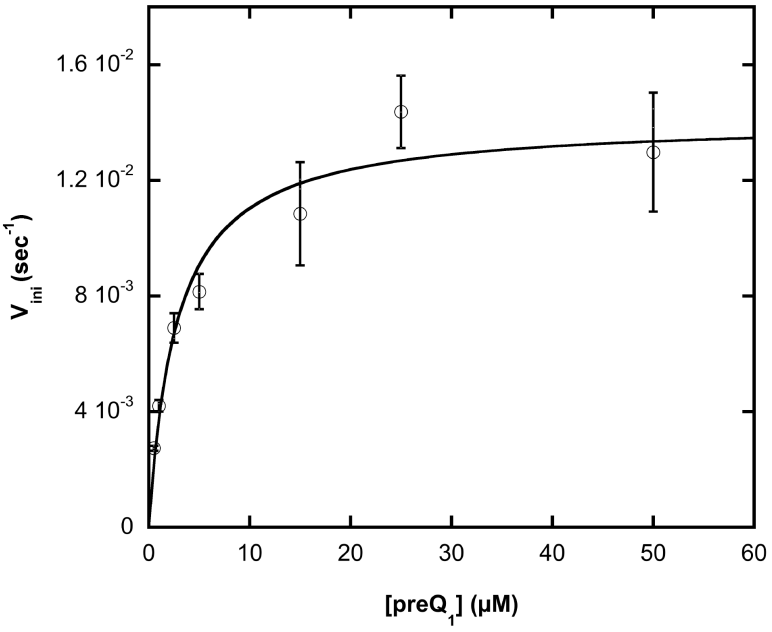

Figure IV-7: Michaelis-Menten Fit of $PreQ_1$ with *E. coli* TGT Cys145Val Mutant. Curves were obtained from the average of three independent determinations of initial velocity data. Error bars were generated from the standard deviation within each point.

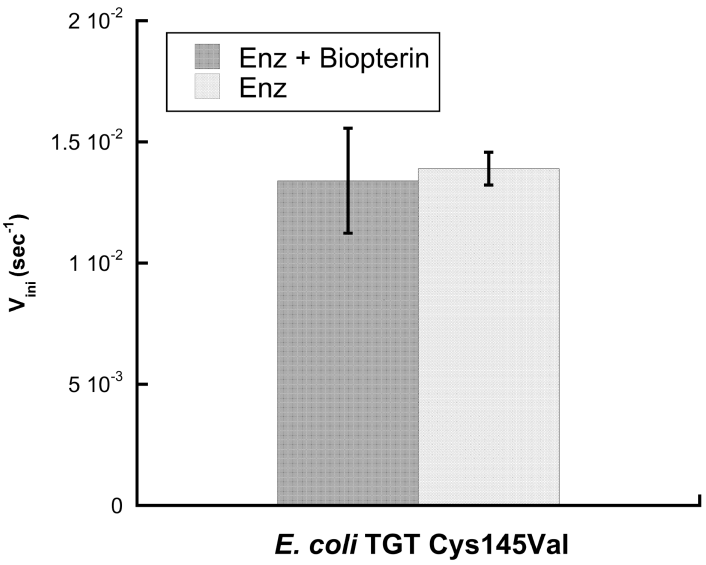

Figure IV-8: Activity of *E. coli* TGT Cys145Val Mutant. Dark grey represents the reactions pre-incubated with 3 mM biopterin while light grey serves as a control. Each column was depicted based on the average of three independent determinations of initial velocity data. Error bars were generated from the standard deviation within either group.

Discussion

It has been previously suggested that eubacterial and eukaryal TGTs arose via convergent evolution (13) due to real and perceived differences in the overall pathways for queuine incorporation. In eubacteria, it has been elucidated that the key intermediate of queuosine biosynthesis, $preQ_0$, is derived from GTP, where at least four enzymes, GTP cyclohydrolase I, QueC, QueD and QueE, have been shown to be involved in the conversion of GTP to $preQ_0$ (20-23). Subsequently, $preQ_0$ undergoes reduction to give $preQ_1$, catalyzed by an NADPH-dependent $preQ_0$ oxidoreductase, termed QueF (24). Then $preQ_1$ is subject to incorporation into tRNA by TGT followed by two additional steps to complete queuosine biosynthesis (25,26). On the other hand, eukarya lack a

queuosine biosynthetic pathway; necessarily acquiring queuine as a nutrient factor and directly incorporating queuine to generate Q-tRNA (27). Also, eukarya are capable of transporting and salvaging queuine (28,29), activities which have not been found in eubacteria.

More recently a divergent evolution model has been proposed which was based on careful analyses of the X-ray crystal structures of eubacterial and archaeal TGTs (14). The X-ray crystal structures of eubacterial and archaeal TGTs (4,5) reveal a common three-dimensional structure including absolute conservation of a structural zinc domain (19). Sequence homologies (Figure IV-1) in TGTs across the three kingdoms reveal the absolute conservation of the four zinc-binding ligands and three key catalytic aspartates in the active site. Eukaryotes also have a TGT-homologue (QTRTD1), which contains the zinc-binding domain and is homologous to the TGT family, but does not share the absolute conservation of the active-site aspartates. QTRTD1 has been proposed to be the salvage enzyme that hydrolyzes QMP to generate free queuine (30,31). It seems likely that the differences in active site amino acids may be due to the altered chemical reaction that the salvage enzyme catalyzes. All TGTs (QTRT1 in eukarya) across the three kingdoms are thought to share the same chemical and kinetic mechanism (32). Although there is a kingdom-based difference in TGT quaternary structure, a similar subunit structure of the enzyme has been identified, wherein eubacterial and archaeal TGTs form homodimers (4-6) and the eukaryal TGT is a heterodimer of two homologous subunits (11,12). The high degree of sequence conservation and similar dimeric subunit structures

suggest that the eukaryal TGTs will be found to share the same tertiary structure as the eubacterial and archaeal TGTs.

A simple multiple sequence alignment of representative TGTs (QTRT1 in eukarya) across the three kingdoms (Figure IV-1) reflects the absolute conservation of active-site and zinc-binding residues as well as significant additional sequence identity and homology. The phylogenetic tree analysis (Figure IV-2) clearly demonstrates the relatedness of the TGT sequences. The archaeal sequences group quite distinctly from the others, as might be expected, due to the presence of an additional domain in archaeal TGTs versus eukaryal QTRT1s and eubacterial TGTs. The eukaryal sequences also group together, but remain close to the eubacterial sequences. Their proximity to the eubacterial sequences may be due in part to the low number (13 vs. 59 and 72) of eukaryal sequences which may not be sufficient to reveal a larger separation between the eukaryal and eubacterial branches. The multiple sequence alignment and phylogenetic tree analysis both support divergent evolution of eubacterial and archaeal TGTs (14) and are clearly consistent with the extension of this concept to the eukaryal kingdom.

Our findings on differential heterocyclic substrate recognition of the human and *E. coli* TGTs (discussed in Chapter III in this dissertation) set up a foothold for us to experimentally examine the idea of divergent evolution of TGT. The fact that mutations in the QTRT1 subunit of the human TGT (both Val161Cys and Val161Cys/Gly232Val) recognize $preQ_1$ substantially better than the wild-type does indicates that the heterocyclic substrate specificity can indeed be altered by

subtle changes in the enzyme active site. Although the k_{cat}/K_M value for the Val161Cys/Gly232Val mutant with respect to $preQ_1$ is still approximately 50-fold lower than that of the wild-type *E. coli* TGT, the significant improvement in K_M implies that the mutation at position 232 to a valine most likely shrinks the substrate binding pocket, allowing better recognition for $preQ_1$. Our observation is also consistent with the reported computational prediction (19) that the corresponding residue (Val217) in *E. coli* TGT appears to form a ceiling in the active site, which prevents queuine from fitting in the binding site.

Similar efforts were attempted to examine a potential alteration in heterocyclic substrate specificity of the *E. coli* TGT mutants. It is not surprising that the Cys145Val mutant failed to recognize queuine and is not inhibited by biopterin, as an additional (and perhaps necessary) effect upon substrate recognition was expected to have come from a mutation at Val217. Unfortunately, the fact that the Cys145Val/Val217Gly mutant appears to be catalytically inactive is mysterious, considering it not only exhibits a similar physical appearance as the wild-type on a denaturing gel but also is capable of binding to the substrate RNA as well as forming a covalent complex. With that being said, it is important to note that the TGT•RNA complex evidently migrates faster than TGT (alone) does on a native PAGE gel (Figure IV-6A). It was previously thought that the presence of RNA causes TGT to dissociate from a trimeric quaternary structure (16); however, more recent studies have suggested that the functional TGT is most likely dimeric during catalysis (6,12). Therefore, we suspect that the faster migration of the TGT•RNA complex could simply be an

outcome of RNA binding (considering the negatively charged nature of RNA). Even so, it cannot be ruled out that the native form of the recombinant TGT in solution exhibits a multimeric (possibly tetrameric) quaternary structure that dissociates into a functional dimer upon substrate tRNA binding. Although no conclusion can be drawn whether mutations at positions 145 and 217 in the *E. coli* TGT would be sufficient enough to allow queuine recognition or biopterin inhibition at this point, all our kinetic data reported herein are consistent with the concept that the human and *E. coli* TGT have evolved the nature of the amino acid at key positions to optimize recognition of their cognate heterocyclic substrates.

The fact that the eubacterial and eukaryal TGTs selectively recognize their cognate heterocyclic substrates is evolutionarily significant. Unlike eubacteria, which biosynthesize queuine from its precursor preQ$_1$, eukarya lack a queuine biosynthesis pathway and are required to obtain queuine from diet as a nutrient factor (33) or through a salvage mechanism that is yet to be fully characterized (29). In addition, while absent in eubacteria, a specific transport system responsible for the cellular uptake of queuine was observed in human fibroblasts and the process appears to be modulated by protein kinase C (PKC) phosphorylation (28,34). We conclude that these differences are most likely due to an outcome of divergent evolution, in which eukarya somehow evolved to be capable of salvaging queuine so that a queuosine biosynthetic pathway is not required, which led to the direct incorporation of queuine by the eukaryal TGT. This postulate is consistent with our conclusion in Chapter II that the eukaryal

TGT has evolved into two homologues, where QTRT1 is in charge of queuine incorporation, and QTRTD1 not only assists in tRNA recognition but also generates free queuine for transglycosylation. It is also an interesting note that there is a 6-fold difference in k_{cat}/K_M between the human and *E. coli* TGTs with respect to their cognate substrates (Table IV-3). Considering eubacteria need to complete the queuosine biosynthesis pathway to obtain Q-tRNA while eukarya do not, the greater efficiency of the eubacterial TGT seems perfectly plausible.

Conclusions

In conclusion, we have performed sequence homology and phylogenetic analyses, the results of which are consistent with divergent evolution. Enzymological studies of the human and *E. coli* TGT mutants are also consistent with the concept that active site residues of TGT have evolved to enhance recognition of their cognate substrates. Future studies are planned in which we are attempting to confirm the postulate that QTRTD1 is the queuine salvage enzyme (see Chapter V). Consistent with the conclusions herein, it is intriguing to speculate that in eukaryotes, TGT evolved into the queuine-specific transglycosylase and into the salvage enzyme that helps to provide free queuine for the transglycosylase.

Notes to Chapter IV

Portions of the work in this chapter have been published in, Yi-Chen Chen, Allen F. Brooks, DeeAnne M. Goodenough-Lashua, Jeffrey D. Kittendorf, H. D. Hollis Showalter and George A. Garcia, (2010) "Evolution of eukaryal tRNA-guanine transglycosylase: Insight gained from the heterocyclic substrate recognition by the wild-type and mutant human and *E. coli* tRNA-guanine transglycosylases", *Nucleic Acids Research*, In Press. We wish to thank Dr. Jeffrey D. Kittendorf, who performed the phylogenetic tree analysis.

Abbreviations used: Q, queuine; $preQ_1$, 7-aminomethyl-7-deazaguanine; $preQ_0$, 7-cyano-7-deazaguanine; TGT, tRNA-guanine transglycosylase; QTRT1, queuine tRNA-ribosyltransferase 1; QTRTD1, queuine tRNA-ribosyltransferase domain-containing 1; DTT, dithiothreitiol; IPTG, isopropyl β-D-thiogalactopyranoside; HEPES, hydroxyethylpiperazine-ethylsulfonate; Tris–HCl, tris(hydroxymethyl) aminomethane hydrochloride; SDS, sodium dodecyl sulfate; PAGE, polyacrylamide gel electrophoresis; TCA, trichloroacetic acid; PKC, protein kinase C.

1. Garcia, G.A., Chervin, S.M. and Kittendorf, J.D. (2009) Identification of the Rate-Determining Step of tRNA-Guanine Transglycosylase from Escherichia coli. *Biochemistry*, **48**, 11243-11251.

2. Goodenough-Lashua, D.M. and Garcia, G.A. (2003) tRNA-Guanine Transglycosylase from *Escherichia coli*: a Ping-Pong Kinetic Mechanism is Consistent with Nucleophilic Catalysis. *Bioorganic Chemistry*, **31**, 331-344.

3. Xie, W., Liu, X.J. and Huang, R.H. (2003) Chemical trapping and crystal structure of a catalytic tRNA guanine transglycosylase covalent intermediate. *Nature Structural Biology*, **10**, 781-788.

4. Romier, C., Reuter, K., Suck, D. and Ficner, R. (1996) Crystal structure of tRNA-guanine transglycosylase: RNA modification by base exchange. *EMBO Journal*, **15**, 2850-2857.

5. Ishitani, R., Nureki, O., Fukai, S., Kijimoto, T., Nameki, N., Watanabe, M., Kondo, H., Sekine, M., Okada, N., Nishimura, S. *et al.* (2002) Crystal structure of archaeosine tRNA-guanine transglycosylase. *Journal of Molecular Biology*, **318**, 665-677.

6. Stengl, B., Meyer, E.A., Heine, A., Brenk, R., Diederich, F. and Klebe, G. (2007) Crystal structures of tRNA-guanine transglycosylase (TGT) in complex with novel and potent inhibitors unravel pronounced induced-fit adaptations and suggest dimer formation upon substrate binding. *Journal of Molecular Biology*, **370**, 492-511.

7. Howes, N.K. and Farkas, W.R. (1978) Studies with a Homogeneous Enzyme from Rabbit Erythrocytes Catalyzing the Insertion of Guanine into tRNA. *Journal of Biological Chemistry*, **253**, 9082-9087.

8. Walden, J., T. L. , Howes, N. and Farkas, W.R. (1982) Purification and properties of guanine, queuine-tRNA transglycosylase from wheat germ. *Journal of Biological Chemistry*, **257**, 13218-13222.

9. Morris, R.C., Brooks, B.J., Eriotou, P., Kelly, D.F., Sagar, S., Hart, K.L. and Elliott, M.S. (1995) Activation of transfer RNA-guanine ribosyltransferase by protein kinase C. *Nucleic Acids Res*, **23**, 2492-2498.

10. Slany, R.K. and Mueller, S.O. (1995) tRNA-guanine transglycosylase from bovine liver - Purification of the enzyme to homogeneity and biochemical characterization. *Eur J Biochem*, **230**, 221-228.

11. Boland, C., Hayes, P., Santa-Maria, I., Nishimura, S. and Kelly, V.P. (2009) Queuosine Formation in Eukaryotic tRNA Occurs via a Mitochondria-localized Heteromeric Transglycosylase. *Journal of Biological Chemistry*, **284**, 18218-18227.

12. Chen, Y.C., Kelly, V.P., Stachura, S.V. and Garcia, G.A. (2010) Characterization of the human tRNA-guanine transglycosylase: Confirmation of the heterodimeric subunit structure. *RNA-a Publication of the RNA Society*, **16**, 958-968.

13. Morris, R.C. and Elliott, M.S. (2001) Queuosine modification of tRNA: a case for convergent evolution. *Molecular Genetics & Metabolism*, **74**, 147-159.

14. Stengl, B., Reuter, K. and Klebe, G. (2005) Mechanism and substrate specificity of tRNA-guanine transglycosylases (TGTs): tRNA-modifying enzymes from the three different kingdoms of life share a common catalytic mechanism. *Chembiochem*, **6**, 1926-1939.

15. He, B., Rong, M.Q., Lyakhov, D., Gartenstein, H., Diaz, G., Castagna, R., McAllister, W.T. and Durbin, R.K. (1997) Rapid mutagenesis and purification of phage RNA polymerases. *Protein Expr. Purif.*, **9**, 142-151.

16. Curnow, A.W. and Garcia, G.A. (1994) tRNA-Guanine Transglycosylase from *Escherichia coli*: Recognition of Dimeric, Unmodified $tRNA^{Tyr}$. *Biochimie*, **76**, 1183-1191.

17. Kumar, S., Nei, M., Dudley, J. and Tamura, K. (2008) MEGA: A Biologist-centric Software for Evolutuonary Analysis of DNA and Protein Sequences. *Briefings in Bioinformatics*, **9**, 299-306.

18. Tamura, K., Dudley, J., Nei, M. and Kumar, S. (2007) MEGA4: Molecular Evolutionary Genetics Analysis (MEGA) software version 4.0. *Molecular Biology and Evolution*, **24**, 1596-1599.

19. Romier, C., Meyer, J.E.W. and Suck, D. (1997) Slight sequence variations of a common fold explain the substrate specificities of tRNA-guanine transglycosylases from the three kingdoms. *FEBS Letters*, **416**, 93-98.

20. McCarty, R.M. and Bandarian, V. (2008) Deciphering deazapurine biosynthesis: Pathway for pyrrolopyrimidine nucleosides toyocamycin and sangivamycin. *Chemistry & Biology*, **15**, 790-798.

21. Phillips, G., El Yacoubi, B., Lyons, B., Alvarez, S., Iwata-Reuyl, D. and de Crecy-Lagard, V. (2008) Biosynthesis of 7-Deazaguanosine-Modified tRNA Nucleosides: a New Role for GTP Cyclohydrolase I. *J. Bacteriol.*, **190**, 7876-7884.

22. Gaur, R. and Varshney, U. (2005) Genetic analysis identifies a function for the queC (ybaX) gene product at an initial step in the queuosine Biosynthetic pathway in Escherichia coli. *Journal Of Bacteriology*, **187**, 6893-6901.

23. Reader, J.S., Metzgar, D., Schimmel, P. and de Crecy-Lagard, V. (2004) Identification of four genes necessary for biosynthesis of the modified nucleoside queuosine. *Journal of Biological Chemistry*, **279**, 6280-6285.

24. Lee, B.W.K., Van Lanen, S.G. and Iwata-Reuyl, D. (2007) Mechanistic studies of bacillus subtilis QueF, the nitrile oxidoreductase involved in queuosine biosynthesis. *Biochemistry*, **46**, 12844.

25. Frey, B., McCloskey, J., Kersten, W. and Kersten, H. (1988) New Function of Vitamin B_{12}: Cobamide-Dependent Reduction of Epoxyqueuosine to Queuosine in tRNAs of *Escherichia coli* and *Salmonella typhimurium*. *Journal of Bacteriology*, **170**, 2078-2082.

26. Kinzie, S.D., Thern, B. and Iwata-Reuyl, D. (2000) Mechanistic studies of the tRNA-modifying enzyme QueA: A chemical imperative for the use of AdoMet as a "ribosyl" donor. *Organic Letters*, **2**, 1307-1310.

27. Shindo-Okada, N., Okada, N., Ohgi, T., Goto, T. and Nishimura, S. (1980) Transfer Ribonucleic Acid Guanine Transglycosylase Isolated from Rat Liver. *Biochemistry*, **19**, 395-400

.

28. Elliott, M.S., Katze, J.R. and Trewyn, R.W. (1984) Relationship between a tumor promoter-induced decrease in queuine modification of transfer RNA in normal human cells and the expression of an altered cell phenotype. *Cancer Res*, **44**, 3215-3219.

29. Reyniers, J.P., Pleasants, J.R., Wostmann, B.S., Katze, J.R. and Farkas, W.R. (1981) Administration of Exogenous Queuine Is Essential for the Biosynthesis of the Queuosine-containing Trnasfer RNAs in the Mouse. *Journal of Biological Chemistry*, **206**, 11591-11594.

30. Gunduz, U. and Katze, J.R. (1984) Queuine Salvage In Mammalian-Cells - Evidence That Queuine Is Generated From Queuosine 5'-Phosphate. *Journal Of Biological Chemistry*, **259**, 1110.

31. Kirtland, G.M., Morris, T.D., Moore, P.H., O'Brian, J.J., Edmonds, C.G., McCloskey, J.A. and Katze, J.R. (1988) Novel Salvage of Queuine from Queuosine and Absence of Queuine Synthesis in *Chlorella pyrenoidosa* and *Chlamydomonas reinhardii*. *J. Bacteriol.*, **170**, 5633.

32. Garcia, G.A. and Kittendorf, J.D. (2005) Transglycosylation: A mechanism for RNA modification (and editing?). *Bioorganic Chemistry*, **33**, 229-251.

33. Farkas, W.R. (1980) Effect of diet on the queuosine family of tRNAs of germ-free mice. *Journal of Biological Chemistry*, **255**, 6832-6835.

34. Morris, R.C., Brooks, B.J., Hart, K.L. and Elliott, M.S. (1996) Modulation of queuine uptake and incorporation into tRNA by protein kinase C and protein phosphatase. *Biochimica et Biophysica Acta*, **1311**, 124-132.

Appendix IV

Appendix Table IV-1: Protein Sequences Used for Phylogenetic Tree Analysis.

Kingdom	*Accession Code*	*Organism*
Eukarya – QTRT1	ref|NP_112486.1	human
	gb|AAH54695.1	zebrafish
	gb|DAA27968.1	bovine
	gb|AAH44811.1	mouse
	ref|NP_001089529.1	frog (Xenopus laevis)
	gb|AAH97321.1	rat
	ref|XP_629936.1	slime mold (Dictyostelium discoideum)
	ref|XP_002761781.1	marmoset
	ref|XP_001490992.2	horse
	XP_002828715.1|	orangutan
	Q28HC6.2	frog (Xenopus tropicalis)
	XP_002921441.1	giant panda
	EFA85809.1	slime mold (Polysphondylium pallidum)
	XP_512381.1	chimpanzee
	XP_001514262.1	platypus
Archaea – TGT	gb|ACX72045.1	*Methanocaldococcus vulcanius*
	ref|YP_003128298.1	*Methanocaldococcus fervens*
	ref|YP_003616492.1	*Methanocaldococcus infernus*
	ref|YP_003707434.1	*Methanococcus voltae*
	sp|A6UVD8.1	*Methanococcus aeolicus*
	sp|A6USA4.1	*Methanococcus vannielii*
	sp|A9A6B5.1	*Methanococcus maripaludis*
	ZP_07331496.1	*Methanothermococcus okinawensis*
	ref|NP_248016.1	*Methanocaldococcus jannaschii*
	ref|ZP_03999086.1	*Halogeometricum borinquense*
	ref|YP_003480803.1	*Natrialba magadii*
	ref|YP_003402284.1	*Haloterrigena turkmenica*
	ref|YP_002566807.1	*Halorubrum lacusprofundi*
	gb|ACV47555.1	*Halomicrobium mukohataei*
	ref|YP_003131077.1	*Halorhabdus utahensis*
	gb|ADJ14326.1	*Halalkalicoccus jeotgali*
	emb|CAI49344.1	*Natronomonas pharaonis*
	emb|CAP14435.1	*Halobacterium salinarum*
	sp|Q9C4M3.2	*Haloferax volcanii*
	ref|YP_137663.1	*Haloarcula marismortui*
	ref|YP_002307001.1	*Thermococcus onnurineus*

	ref|YP_002993510.1	*Thermococcus sibiricus*
	ref|YP_183173.1	*Thermococcus kodakarensis*
	ref|ZP_04877589.1	*Thermococcus barophilus*
	ref|NP_126796.1	*Pyrococcus abyssi*
	pdb|1IQ8	*Pyrococcus Horikoshii*
	ref|YP_002959507.1	*Thermococcus gammatolerans*
	ref|NP_578775.1	*Pyrococcus furiosus*
	ref|YP_003849537.1	*Methanothermobacter marburgensis*
	gb|ADC47362.1	*Methanobrevibacter ruminantium*
	ref|NP_275319.1	*Methanothermobacter thermautotrophicus*
	ref|YP_447562.1	*Methanosphaera stadtmanae*
	ref|YP_001274130.1	*Methanobrevibacter smithii*
	gb|ABK15426.1	*Methanosaeta thermophila*
	ref|YP_566411.1	*Methanococcoides burtonii*
	ref|YP_304508.1	*Methanosarcina barkeri*
	ref|YP_003725763.1	*Methanohalobium evestigatum*
	ref|YP_003543091.1	*Methanohalophilus mahii*
	gb|AAM07966.1	*Methanosarcina acetivorans*
	sp|Q8PXW5.1	*Methanosarcina mazei*
	gb|ACL17137.1	*Methanosphaerula palustris*
	ref|YP_502588.1	*Methanospirillum hungatei*
	ref|YP_001030643.1	*Methanocorpusculum labreanum*
	ref|YP_001404474.1	*Candidatus Methanoregula boonei*
	ref|YP_001047199.1	*Methanoculleus marisnigri*
	ref|YP_003482943.1	*Aciduliprofundum boonei*
	ref|NP_111588.1	*Thermoplasma volcanium*
	emb|CAC12611.1	*Thermoplasma acidophilum*
	gb|AAT43039.1	*Picrophilus torridus*
	ref|ZP_05570642.1	*Ferroplasma acidarmanus*
	gb|AAB90652.1	*Archaeoglobus fulgidus* TGT-A
	gb|AAB89762.1	*Archaeoglobus fulgidus* TGT-B
	gb|ADB58867.1	*Archaeoglobus profundus*
	ref|YP_003436229.1	*Ferroglobus placidus*
	ref|NP_613475.1	*Methanopyrus kandleri*
	ref|YP_003356571.1	*Methanocella paludicola*
	ref|YP_001192334.1	*Metallosphaera sedula*
	ref|NP_341823.1	*Sulfolobus solfataricus*
	ref|YP_255336.1	*Sulfolobus acidocaldarius*
	ref|NP_376195.1	*Sulfolobus tokodaii*
	ref|YP_003420109.1	*Sulfolobus islandicus*
	ref|YP_001057030.1	*Pyrobaculum calidifontis*
	ref|NP_558839.1	*Pyrobaculum aerophilum*
	ref|YP_001152302.1	*Pyrobaculum arsenaticum*
	ref|YP_001539868.1	*Caldivirga maquilingensis*
	ref|YP_919768.1	*Thermofilum pendens*
	ref|YP_001435068.1	*Ignicoccus hospitalis*

	ref|YP_001040918.1	*Staphylothermus marinus*
	ref|NP_148325.1	*Aeropyrum pernix*
	ref|YP_003650498.1	*Thermosphaera aggregans*
	ref|YP_002428951.1	*Desulfurococcus kamchatkensis*
	gb|ADM26950.1	*Ignisphaera aggregans*
	ref|YP_001012678.1	*Hyperthermus butylicus*
	ref|YP_003815746.1	*Acidilobus saccharovorans*
	ref|NP_963418.1	*Nanoarchaeum equitans*
	sp|B1L6M8.1	*Candidatus Korarchaeum cryptofilum*
	ref|YP_876568.1	*Cenarchaeum symbiosum*
	ref|YP_001582870.1	*Nitrosopumilus maritimus*
	ref|YP_002335509.1	*Thermosipho africanus*
	ref|NP_229361.1	*Thermotoga maritima*
Eubacteria – TGT	emb|CAQ30875.1	*Escherichia coli*
	ref|ZP_07354458.1	*Streptococcus pneumoniae*
	emb|CAD08861.1	*Salmonella enterica*
	ref|YP_162098.2	*Zymomonas mobilis*
	ref|ZP_04960423.1	*Vibrio cholerae*
	emb|CAL21786.1	*Yersinia pestis*
	ref|YP_002758238.1	*Listeria monocytogenes*
	gb|AAX87304.1	*Haemophilus influenzae*
	emb|CAA72784.1	*Helicobacter pylori*
	gb|ABQ43125.1	*Borrelia burgdorferi*
	ref|NP_895689.1	*Prochlorococcus marinus*
	ref|YP_001482523.1	*Campylobacter jejuni*
	gb|ADI51881.1	*Chlamydia trachomatis*
	ref|NP_539807.1	*Brucella melitensis*
	ref|ZP_06877136.1	*Pseudomonas aeruginosa*
	ref|YP_143572.1	*Thermus thermophilus*
	ref|YP_003867029.1	*Bacillus subtilis*
	emb|CBJ50159.1	*Ralstonia solanacearum*
	ref|YP_687948.1	*Shigella flexneri*
	ref|YP_002240127.1	*Klebsiella pneumoniae*
	ref|ZP_05635188.1	*Buchnera aphidicola*
	ref|NP_300278.1	*Chlamydophila pneumoniae*
	ref|YP_201123.1	*Xanthomonas oryzae*
	ref|NP_785768.1	*Lactobacillus plantarum*
	ref|NP_229361.1	*Thermotoga maritime*
	YP_000978.1	*Leptospira interrogans*
	ref|YP_001431768.1	*Roseiflexus castenholzii*
	ref|YP_001037385.1	*Clostridium thermocellum*
	ref|YP_002517032.1	*Caulobacter crescentus*
	ref|YP_001601158.1	*Gluconacetobacter diazotrophicus*
	ref|YP_399474.1	*Synechococcus elongates*
	ref|ZP_05027266.1	*Microcoleus chthonoplastes*

	ref|YP_001945074.1	*Burkholderia multivorans*
	ref|YP_267863.1	*Colwellia psychrerythraea*
	ref|ZP_01127895.1	*Nitrococcus mobilis*
	ref|YP_197480.1	*Ehrlichia ruminantium*
	ref|YP_003449280.1	*Azospirillum sp.*
	ref|ZP_01871172.1	*Caminibacter mediatlanticus*
	ref|YP_632753.1	*Myxococcus Xanthus*
	ref|YP_465749.1	*Anaeromyxobacter dehalogenans*
	ref|ZP_01286906.1	*delta proteobacterium*
	ref|ZP_01312044.1	*Desulfuromonas acetoxidans*
	gb|EDP75112.1	*Hydrogenivirga sp.*
	ref|YP_001955297.1	*Bifidobacterium longum*
	ref|YP_001637299.1	*Chloroflexus aurantiacus*
	ref|YP_074995.1	*Symbiobacterium thermophilum*
	ref|YP_001211582.1	*Pelotomaculum thermopropionicum*
	ref|YP_002930214.1	*Eubacterium eligens*
	ref|YP_001332575.1	*Staphylococcus aureus*
	ref|NP_442693.1	*Synechocystis sp.*
	ref|NP_923748.1	*Gloeobacter violaceus*
	ref|YP_585086.1	*Cupriavidus metallidurans*
	ref|YP_995397.1	*Verminephrobacter eiseniae*
	ref|YP_547328.1	*Polaromonas sp.*
	ref|YP_001022921.1	*Methylibium petroleiphilum*
	ref|NP_273761.1	*Neisseria meningitidis*

[a]Protein sequences were extracted from the NCBI Protein Sequence database as described in Methods.

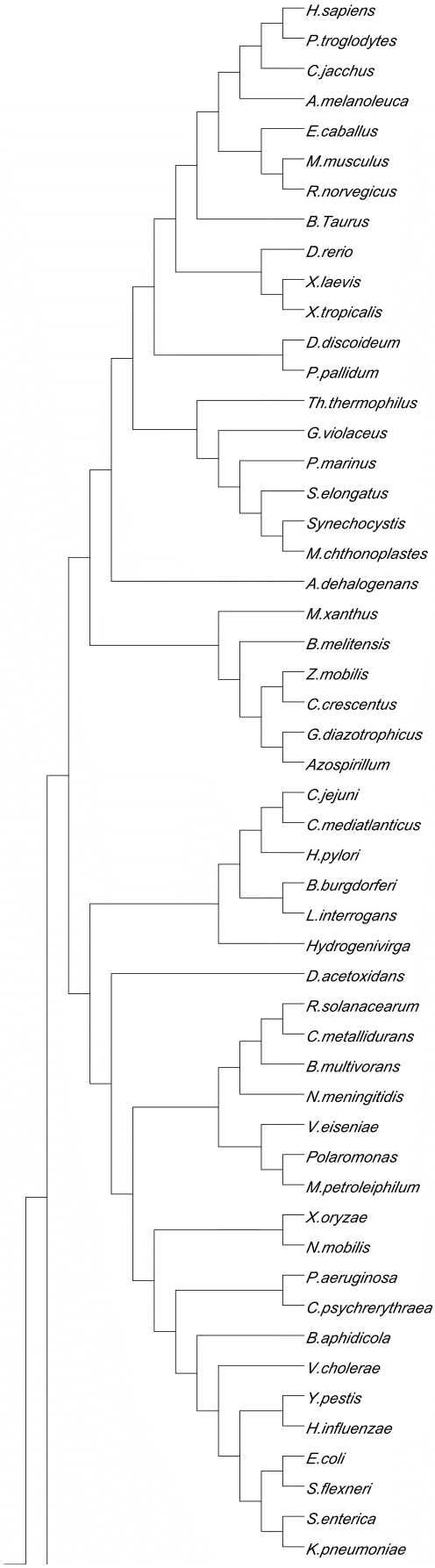
H.sapiens
P.troglodytes
C.jacchus
A.melanoleuca
E.caballus
M.musculus
R.norvegicus
B.Taurus
D.rerio
X.laevis
X.tropicalis
D.discoideum
P.pallidum
Th.thermophilus
G.violaceus
P.marinus
S.elongatus
Synechocystis
M.chthonoplastes
A.dehalogenans
M.xanthus
B.melitensis
Z.mobilis
C.crescentus
G.diazotrophicus
Azospirillum
C.jejuni
C.mediatlanticus
H.pylori
B.burgdorferi
L.interrogans
Hydrogenivirga
D.acetoxidans
R.solanacearum
C.metallidurans
B.multivorans
N.meningitidis
V.eiseniae
Polaromonas
M.petroleiphilum
X.oryzae
N.mobilis
P.aeruginosa
C.psychrerythraea
B.aphidicola
V.cholerae
Y.pestis
H.influenzae
E.coli
S.flexneri
S.enterica
K.pneumoniae

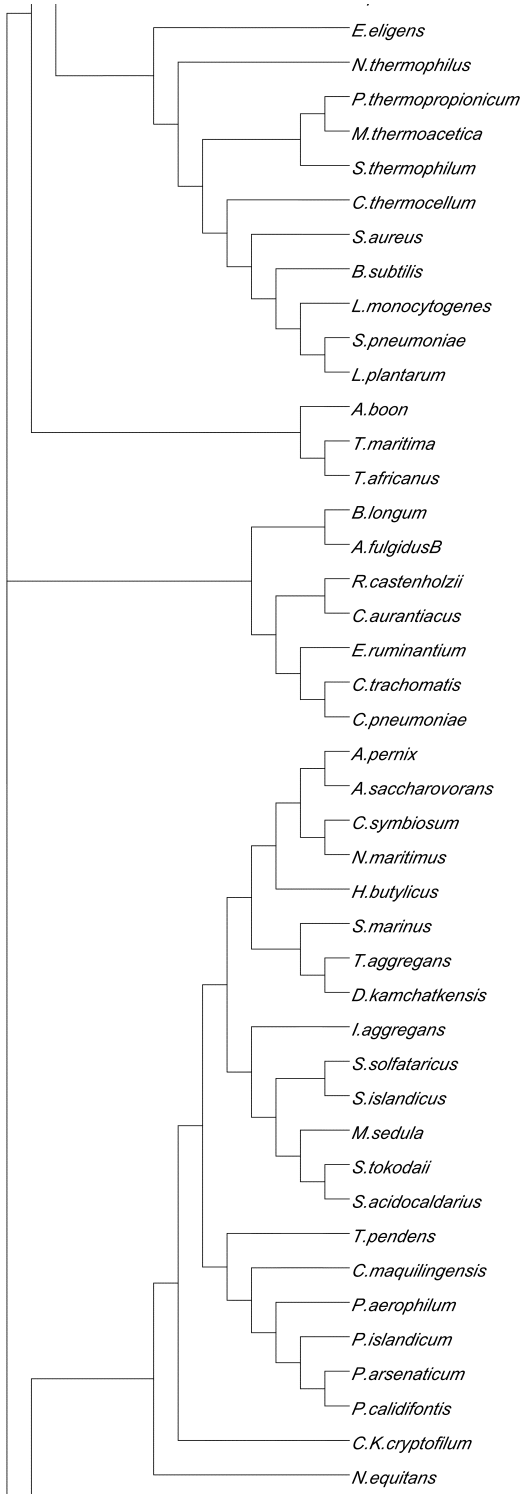
E.eligens
N.thermophilus
P.thermopropionicum
M.thermoacetica
S.thermophilum
C.thermocellum
S.aureus
B.subtilis
L.monocytogenes
S.pneumoniae
L.plantarum
A.boon
T.maritima
T.africanus
B.longum
A.fulgidusB
R.castenholzii
C.aurantiacus
E.ruminantium
C.trachomatis
C.pneumoniae
A.pernix
A.saccharovorans
C.symbiosum
N.maritimus
H.butylicus
S.marinus
T.aggregans
D.kamchatkensis
I.aggregans
S.solfataricus
S.islandicus
M.sedula
S.tokodaii
S.acidocaldarius
T.pendens
C.maquilingensis
P.aerophilum
P.islandicum
P.arsenaticum
P.calidifontis
C.K.cryptofilum
N.equitans

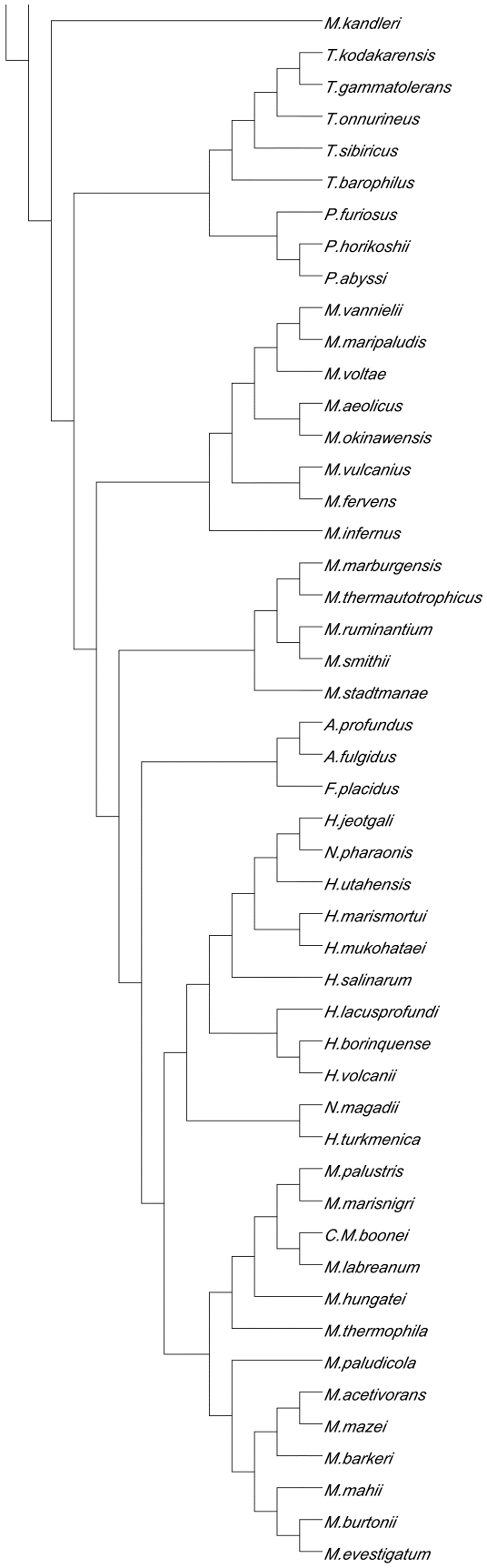
M.kandleri
T.kodakarensis
T.gammatolerans
T.onnurineus
T.sibiricus
T.barophilus
P.furiosus
P.horikoshii
P.abyssi
M.vannielii
M.maripaludis
M.voltae
M.aeolicus
M.okinawensis
M.vulcanius
M.fervens
M.infernus
M.marburgensis
M.thermautotrophicus
M.ruminantium
M.smithii
M.stadtmanae
A.profundus
A.fulgidus
F.placidus
H.jeotgali
N.pharaonis
H.utahensis
H.marismortui
H.mukohataei
H.salinarum
H.lacusprofundi
H.borinquense
H.volcanii
N.magadii
H.turkmenica
M.palustris
M.marisnigri
C.M.boonei
M.labreanum
M.hungatei
M.thermophila
M.paludicola
M.acetivorans
M.mazei
M.barkeri
M.mahii
M.burtonii
M.evestigatum

Appendix Figure IV-1: Full Phylogenetic Tree Analysis. The evolutionary history of the TGT enzymes was inferred via Maximum Likelihood analysis with the MEGA4 software package. Representative TGT sequences spanning the three domains of life (13 eukaryal, 59 eubacterial, 72 archaeal) were globally aligned using Clustal W. The alignment was subjected to 500 bootstrap replicates resulting in the final consensus phylogenetic tree. This is an unrooted tree and the branch lengths are proportional to the evolutionary distances between nodes.

CHAPTER V

CONCLUSIONS

Although the presence of the queuosine modification in eukarya has been known for almost 40 years (1), the characteristics of the key enzyme, tRNA-guanine transglycosylase (TGT), had been very poorly understood, and in fact the a previously proposed subunit structure (2,3) has now been proven to be incorrect (4,5). Described in Chapter II, we utilized molecular biology strategies to construct and co-express recombinant human QTRT1 (hQTRT1) and QTRTD1 (hQTRTD1) in a *tgt* (-) *E. coli* strain. Physical evidence via co-purification through two chromatographies, mass spectrometry and chemical cross-linking experiments all indicate the formation of a 1:1 heterodimeric hQTRT1•hQTRTD1 complex. More importantly, only the hQTRT1•hQTRTD1 complex, not the individual subunits, exhibits guanine exchange ability via *in vitro* studies while hQTRT1 evidently catalyzes the transglycosylase reaction. All of the evidence we obtained supports the conclusion that the human TGT is a heterodimer of hQTRT1 and hQTRTD1.

Considering that hQTRT1 and hQTRTD1 are protein homologues, the dimeric subunit structure of eukaryal TGT is similar to those of eubacterial and archaeal TGTs that have both been shown to be homodimeric based on X-ray

crystal structures. The results of our studies with the human TGT along with insights gained from studies of the eubacterial TGT, are all consistent with the conclusion that hQTRT1 is responsible for the replacement of the heterocyclic substrate; whereas, hQTRTD1 only assists in maintaining the proper orientation of the bound substrate tRNA during the transglycosylase reaction. In collaboration with the Klebe group (University of Marburg, Germany), we are seeking to obtain further crystallographic evidence (X-ray structure of the human TGT) to support our postulate. It is worth mentioning that although no evidence was found for the involvement of USP14 in our studies, the possibility of USP14 regulation of the human TGT (6) *in vivo* cannot be entirely excluded. Since the molecular weights of QTRT1 and QTRTD1 are only slightly different (44 and 46.7 kDa), it is possible that these two proteins were not well resolved on SDS-PAGE gels in previous work with isolated eukaryal TGTs. As a result, it is remotely possible that USP14 could act as a regulatory subunit, modulating the activity of the QTRT1•QTRTD1 heterodimer.

The conclusion that the eukaryal TGT evolved into two homologous subunits is evolutionarily intriguing and implies undefined function(s) of QTRT1 in addition to solely serving as a member of the "supporting cast" for transglycosylation. The sequence analysis of QTRTD1 exhibits a high homology to QTRT1 despite alterations of key catalytic residues. Also, it is well known that eukarya do not synthesize queuine and are capable of recycling the free base through a salvage system (7,8). All of these findings, including our observations in Chapter II, have led us to propose a new paradigm for the eukaryal TGT

(Figure V-1). We hypothesize that the main function of QTRTD1 is to hydolyze QMP (degraded from Q-tRNA) to produce queuine where QTRT1 can then easily utilize the free base so generated for transglycosylation.

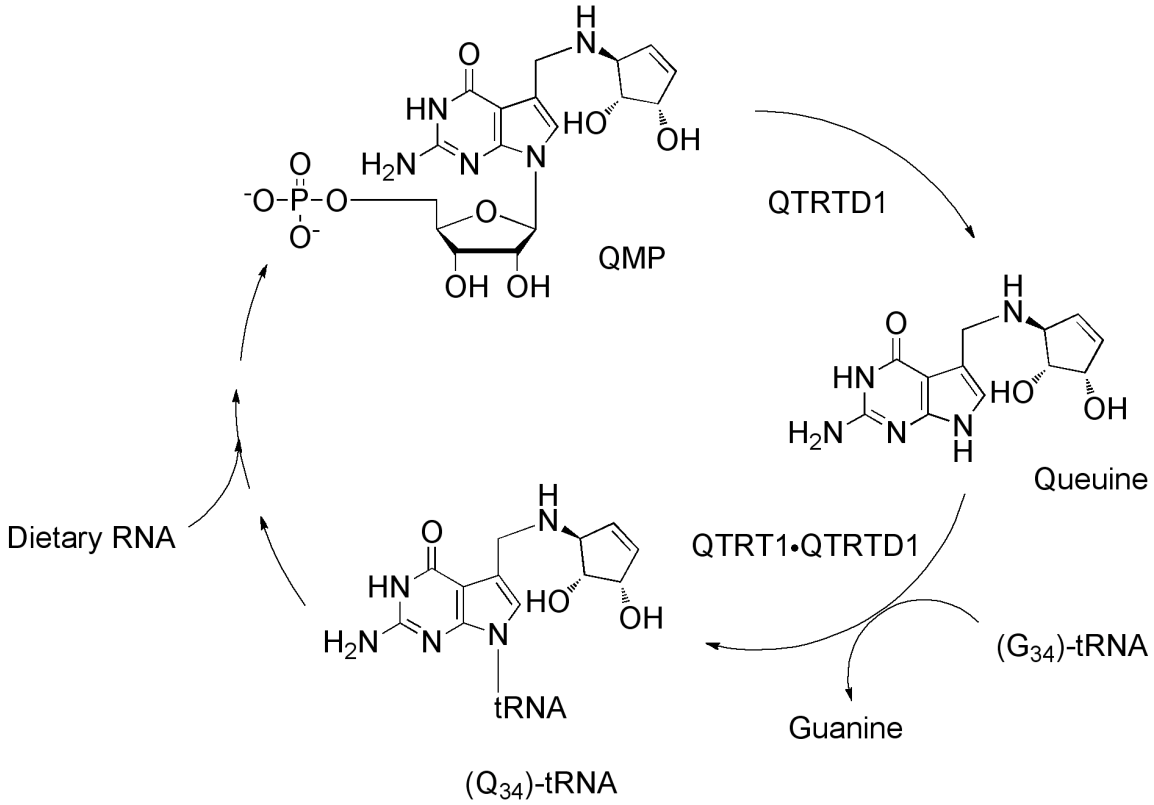

Figure V-1: Proposed Queuine Utilization in Eukarya. Instead of biosynthesizing queuosine, eukarya salvage the free base, queuine, from degraded tRNA.

Prior to the study described in Chapter III, not much was known regarding the heterocyclic substrate specificity of the eukaryal TGT. The success in obtaining radiolabeled queuine and $preQ_1$ allowed us to directly investigate the substrate recognition of the human TGT. The major advantage of our approach is that a direct replacement assay provides much more reliable and efficient

kinetic determinations. Our results revealed a novel finding that the human TGT preferentially recognizes queuine over $preQ_1$ by a factor of approximately 500, which was not observed previously (9). Although our additional kinetic studies do not completely elucidate the underlined reason, the protonated aminomethyl side chain of $preQ_1$ at physiological pH seems most likely to account for this preferential recognition. Moreover, the establishment of biopterin inhibition studies has provided a new approach to examine how cellular pteridines may regulate Q-tRNA formation, which may also help understand the biological significance of the queuosine modification in eukarya.

The unanticipated observations from the substrate specificity study of the eukaryal TGT further inspired us to probe its origin. Despite one previous suggestion that modern TGTs arose as an outcome of convergent evolution (10), TGTs across all three kingdoms of life appear to have arisen divergently based on crystallographic and kinetic evidence regarding eubacterial and archaeal TGTs (11) (also described previously in Chapter IV). To extend the divergent evolution model to eukarya, we first performed sequence homology and phylogenetic analyses, which are both consistent with the concept of divergent evolution. Subsequently, the enzymological studies where we mutated two active site residues in both human and *E. coli* TGT indicate that those residues have divergently evolved to enhance recognition for their cognate heterocyclic substrates.

In summary, the work presented in this dissertation has not only elucidated the intriguing evolutionary scenario of the eukaryal TGT (the enzyme

evolved into two homologous subunits and the active site residues evolved to specifically recognize queuine), but also built a foundation for gaining a full understanding of the eukaryal TGT, which may ultimately help identify TGT as a potential drug target for the biological disorders that are associated with the hypomodification of queuosine in tRNA.

Notes to Chapter V

1. White, B.N., Tener, G.M., Holden, J. and Suzuku, D.T. (1973) Activity of a transfer RNA modifying enzyme during the development of Drosophila and its relationship to the su(s) locus. *Journal of Molecular Biology*, **74**, 635-651.

2. Deshpande, K.L. and Katze, J.R. (2001) Characterization of cDNA encoding the human tRNA-guanine transglycosylase (TGT) catalytic subunit. *Gene*, **265**, 205-212.

3. Deshpande, K.L., Seubert, P.H., Tillman, D.M., Farkas, W.R. and Katze, J.R. (1996) Cloning and characterization of cDNA encoding the rabbit tRNA-guanine transglycosylase 60-kilodalton subunit. *Arch Biochem Biophys*, **326**, 1-7.

4. Boland, C., Hayes, P., Santa-Maria, I., Nishimura, S. and Kelly, V.P. (2009) Queuosine Formation in Eukaryotic tRNA Occurs via a Mitochondria-localized Heteromeric Transglycosylase. *J. Biol. Chem.*, **284**, 18218-18227.

5. Chen, Y.C., Kelly, V.P., Stachura, S.V. and Garcia, G.A. (2010) Characterization of the human tRNA-guanine transglycosylase: Confirmation of the heterodimeric subunit structure. *RNA-a Publication of the RNA Society*, **16**, 958-968.

6. Morris, R.C., Brooks, B.J., Eriotou, P., Kelly, D.F., Sagar, S., Hart, K.L. and Elliott, M.S. (1995) Activation of transfer RNA-guanine ribosyltransferase by protein kinase C. *Nucleic Acids Res*, **23**, 2492-2498.

7. Gunduz, U. and Katze, J.R. (1982) Salvage of the nucleic acid base queuine from queuine-containing tRNA by animal cells. *Biochem Biophys Res Commun*, **109**, 159-167.

8. Kirtland, G.M., Morris, T.D., Moore, P.H., O'Brian, J.J., Edmonds, C.G., McCloskey, J.A. and Katze, J.R. (1988) Novel Salvage of Queuine from Queuosine and Absence of Queuine Synthesis in *Chlorella pyrenoidosa* and *Chlamydomonas reinhardii*. *J. Bacteriol.*, **170**, 5633.

9. Shindo-Okada, N., Okada, N., Ohgi, T., Goto, T. and Nishimura, S. (1980) Transfer Ribonucleic Acid Guanine Transglycosylase Isolated from Rat Liver. *Biochemistry*, **19**, 395-400.

10. Morris, R.C. and Elliott, M.S. (2001) Queuosine modification of tRNA: a case for convergent evolution. *Molecular Genetics & Metabolism*, **74**, 147-159.

11. Stengl, B., Reuter, K. and Klebe, G. (2005) Mechanism and substrate specificity of tRNA-guanine transglycosylases (TGTs): tRNA-modifying enzymes from the three different kingdoms of life share a common catalytic mechanism. *Chembiochem*, **6**, 1926-1939.